



## Diploma thesis

# A systematic study on self-reinforcing thermoplastic urethane/urea elastomers

ausgeführt zum Zwecke der Erlangung des akademischen Grades  
eines Diplom-Ingenieurs

unter Anleitung von

Univ.Prof. Dipl.-Ing. Dr.techn. Robert **Liska**

Univ.Ass. Dipl.-Ing. Dr.techn. Stefan **Baudis**

Univ.Ass. Dr. techn. Katharina **Ehrmann**, MSc

am Institut für Angewandte Synthesechemie (IAS)  
der Technischen Universität Wien

von

Markus **Fitzka**, BSc

01329069



---

Markus Fitzka, BSc



Die approbierte gedruckte Originalversion dieser Diplomarbeit ist an der TU Wien Bibliothek verfügbar  
The approved original version of this thesis is available in print at TU Wien Bibliothek.

# Danksagung

Beginnen möchte ich meinen Dank bei **Prof. Dr. Robert Liska** für die Betreuung meiner Diplomarbeit und die Möglichkeit diese in seiner Arbeitsgruppe zu absolvieren. Du hast stets ein Auge für eine positive Arbeitsatmosphäre in deiner Arbeitsgruppe und schaffst es so gute wissenschaftliche Arbeit und gleichzeitige Freude daran zu verbinden.

Auch Frau **Prof. Dr. Simone Knaus** gilt mein Dank. Obwohl aufgrund der COVID-Pandemie die Zusammentreffen doch sehr beschränkt waren, ist ihre Präsenz und schützende Hand zum Wohle der Arbeitsgruppe in schwierigen Situationen immer spürbar.

Herrn **Dr. Stefan Baudis** gilt ein besonderer Dank. Als direkter Betreuer meines Forschungsthemas ermöglichtest du mir, an einer interessanten Arbeit die auch schon in meiner Bachelorarbeit begann, weiterzuarbeiten und mein Wissen in diesem Bereich deutlich zu vertiefen. Danke auch für deinen Überblick und Weitsicht dieser Arbeit von Beginn an eine runde Form zu geben.

Ein sehr großer Dank gilt besonders Frau **Dr. Katharina Ehrmann**. Schon als Betreuerin meiner Bachelorarbeit wusstest du zu fordern ohne zu überfordern und gleichzeitig immer eine angenehme Arbeitsatmosphäre zu schaffen. Danke auch für die Mitbetreuung dieser Diplomarbeit und vielen nützlichen Tipps die mir die praktische Arbeit oft erleichtert haben.

Vielen Dank auch Herrn **Dr. Thomas Koch**, der immer eine hervorragende Hilfe bei der Umsetzung aller mechanischen und thermischen Tests war. Danke für deinen unermüdlichen Einsatz beim Bereitstellen von Unterstützung, egal ob die Nutzung deiner Geräte als auch beim Messen einiger Proben, „dass du ja locker nebenbei mitmachen kannst“.

Meinen **Arbeitskolleginnen und Arbeitskollegen** möchte ich für die wunderbare gemeinsame Zeit im Labor und auch außerhalb danken. Sowohl der alten Partie, die Neuankömmlinge immer mit offenen Armen aufnahm, als auch meinen jetzigen Kollegen, Tina, Lukas, Alex, Roli, Antonella, Klaus, Carola, Anna, Stephan, Ralle, Babsi, AD, Jan, David, Jakob, Anna Z., Oskar, Lisa und Sarah. Ein besonderer Dank soll dabei sowohl meinen H35-Laborkollegen Larissa, Elise, Yazgan, Flo und Philip gelten, die immer für eine unterhaltsame Zeit im Labor sorgten, als auch Pontus, Florian, Michi, Dani und Viola, die besonders zu erwähnen sind.

Ein ganz besonderer Dank gilt auch meiner Familie. Meinem Bruder **Stefan**, der mich immer in allen Lebenslagen unterstützt. Meinen Eltern **Marianne und Alois**, welche mir von Beginn alles ermöglicht haben und meine größten Förderer waren. Ich danke euch, dass ich mich immer auf auch verlassen konnte und kann.



Die approbierte gedruckte Originalversion dieser Diplomarbeit ist an der TU Wien Bibliothek verfügbar  
The approved original version of this thesis is available in print at TU Wien Bibliothek.



# Table of contents

<b>Abstract</b>		<b>i</b>
<b>Kurzfassung</b>		<b>ii</b>
<b>Introduction</b>		<b>1</b>
1. The cardiovascular system – functions, diseases and treatments		1
2. Tissue engineering		4
2.1 Scaffold materials for vascular tissue engineering		6
3. Thermoplastic poly(urethane/urea) elastomers		10
3.1 General aspects		10
3.2 Synthesis route and synthesis requirements		12
4. Hindered urea bonds		14
<b>Objective</b>		<b>16</b>
<b>State of the art</b>		<b>17</b>
<b>Results and discussion</b>	<b>R&amp;D</b>	<b>Exp.</b>
1. Synthesis	25	88
1.1 Chain extenders	26	88
1.2 Polymers	28	89
1.2.1 Prerequisites for polymer synthesis	28	89
1.2.1.1 Analysis of macrodiols	29	89
1.2.1.2 Purification of diisocyanates	34	91
1.2.1.3 Purification of chain extenders	34	91
1.2.2 General polymer synthesis procedure	37	92
2. Polymer analysis	40	106
2.1 Chemical constitution and polymer composition	40	106
2.2 Molecular weight via GPC	41	106
2.3 Thermal properties	46	107
2.3.1 Glass transition temperatures and melting behavior <i>via</i> DSC	46	
2.3.2 Thermal stability <i>via</i> TGA	50	

2.4 Mechanical properties	54	108
2.4.1 Preparation of films for tensile testing	54	
2.4.2 Tensile tests	55	
2.5 Degradation behavior	80	114
<b>Summary</b>		<b>82</b>
<b>Materials and Methods</b>		<b>116</b>
<b>Abbreviations</b>		<b>121</b>
<b>References</b>		<b>121</b>
<b>Appendix</b>		<b>130</b>
DSC measurement curves		130
Film reproducibility		135
Additional tensile tests		137



Die approbierte gedruckte Originalversion dieser Diplomarbeit ist an der TU Wien Bibliothek verfügbar  
The approved original version of this thesis is available in print at TU Wien Bibliothek.

## Abstract

Cardiovascular diseases are the primary concern of healthcare professionals as they are the leading cause of death worldwide. With aging societies, the impact of unhealthy lifestyles increases and the already strong influence of these diseases on public health will rise to even higher levels. For many of these diseases, significant achievements have been made, however for diseases of blood vessels with small diameters, the treatment options are still fairly limited. To combat this, the field of tissue engineering could offer new possibilities and hopes to achieve a solution with broad and easy applicability to tailor to each patient's individual needs. The final goal is the achievement of *in situ* tissue engineering. By supplying the body with a suitable and readily available scaffold, the function of the diseased blood vessel tissue is maintained during the natural healing process of the damaged organ and in the last step, regenerated native tissue again takes over its natural function.

The first steps towards such an ambitious goal were already achieved in previous works, which showed promising results using thermoplastic poly(urethane/urea) elastomers. Their typical hard- and soft-block structure combines the mechanical needs of high tensile strength while still being flexible and, through their thermoplastic nature, allow the processing through electrospinning to form the needed architecture. As a multicomponent system, high flexibility with the substitution of monomers and variation of monomer ratios is possible and the behavior of the final materials can be (fine) tuned to specific needs. Also, an introduction of biodegradable cleavage sites was already previously accomplished and shown to be easily possible to allow for the wanted replacement of the tissue-engineered interim solution with native tissue in the long term.

The newest achievements showed even more possibilities in the potential properties of such materials with the introduction of hindered urea bonds. This form of urea bonds shows dynamic behavior under mild conditions through the destabilization with sterically demanding nitrogen substituents, allowing the mechanical properties to change even in the final solid form. This was determined by previous findings, which showed that such materials could increase their tensile strength after self-reinforcement triggered by moisture under mild conditions. In this work, the scope of such materials was expanded: through the mentioned broad exchangeability of singular monomers in the thermoplastic poly(urethane/urea) elastomers and the incorporation of monomers forming hindered urea bonds, a wide range of new polymers were synthesized and characterized using different analysis methods and mechanical tests.

## Kurzfassung

Kardiovaskuläre Erkrankungen sind als weltweit führende Todesursache ein Hauptanliegen des Gesundheitswesens. Durch das steigende Durchschnittsalter der Bevölkerung schlägt sich der Einfluss eines ungesunden Lebensstils stärker nieder und die bereits jetzt große Bedeutung dieser Erkrankungen auf das Gesundheitswesen wird auf ein noch höheres Level ansteigen. Bei vielen Erkrankungen wurden große Fortschritte in der Behandlung erzielt, allerdings sind die Behandlungsmöglichkeiten der Erkrankungen von kleinen Blutgefäßen noch stark limitiert. Als eine Antwort wird Tissue Engineering gesehen, welches neue Behandlungsmöglichkeiten bieten könnte und die Hoffnung auf einfache und individuelle Lösungen eröffnet. Das Endziel wäre hierbei *in situ* Tissue Engineering: durch das Bereitstellen einer passenden und jederzeit verfügbaren, durch Tissue Engineering hergestellten Blutgefäßprothese wird die Funktion des geschädigten Gewebes während des natürlichen Heilungsprozesses aufrechterhalten und letztendlich durch körpereigenes Gewebe wieder übernommen.

Erste Schritte in Richtung dieses Ziels wurden bereits durch die vielversprechenden Ergebnisse früherer Arbeiten mit thermoplastischen Poly(urethan/urea) Elastomeren erreicht. Aufgrund deren typischer Hart- und Softblock Struktur werden die mechanischen Anforderungen an hohe Reißfestigkeit bei gleichzeitiger Elastizität erfüllt. Außerdem wird durch die Thermoplastizität des Materials die Möglichkeit zur Verarbeitung zu benötigter Architektur mittels Electrospinning gewährleistet. Als Multikomponentensystem ist eine hohe Flexibilität in der Monomersubstitution und der Variation der Monomerverhältnisse möglich um das Endmaterial an benötigte Anforderungen anzupassen. Auch eine Inkorporation von biologisch abbaubaren Spaltungsstellen ist beschrieben, um die als Übergangslösung konzipierten Prothesen langfristig durch körpereigenes Gewebe zu ersetzen.

Die neuesten Ergebnisse zeigten noch weitere Möglichkeiten für Materialeigenschaften auf: Durch die Einführung von sterisch gehinderten Ureabindungen („hindered urea bonds/HUB“) wird ein dynamisches Verhalten auch unter milden Bedingungen zugänglich, da sich durch die Destabilisierung der Ureabindung durch sterisch anspruchsvolle Stickstoffsubstituenten die mechanischen Eigenschaften auch noch in fester Form verändern können. Diese Veränderung wurde erstmals in einer früheren Arbeit in der Erhöhung der Zugfestigkeit nach Auslösen einer Selbstverstärkung durch Feuchtigkeit aufgezeigt. In dieser Arbeit wird der Umfang solcher Materialien erweitert: die bereits erwähnte breite Austauschbarkeit einzelner Monomere und Einführung von Monomeren, welche sterisch gehinderte Ureabindungen erzeugen wird genutzt, um neue Materialien zu synthetisieren und mit verschiedenen Analysemethoden und mechanischen Tests zu analysieren.



Die approbierte gedruckte Originalversion dieser Diplomarbeit ist an der TU Wien Bibliothek verfügbar  
The approved original version of this thesis is available in print at TU Wien Bibliothek.

# Introduction

## 1. The cardiovascular system – functions, diseases and treatments

The cardiovascular system is the main circulatory system in the human body, with its function of delivering oxygen and nutrients being of utmost importance in keeping the human alive. This system incorporates all vessels transporting blood and is divided into two connected circuits, which meet at the four-chambered heart acting as a blood pump, which moves blood through rhythmic contractions.<sup>1</sup> The first, smaller circuit called the pulmonary circuit is a circular system from the heart's right side to the lung. In this subsystem, the oxygen-depleted and carbon dioxide-rich blood undergoes an exchange of dissolved gases. In the small vessels of the lung, carbon dioxide is extracted from the blood while parallel enrichment with oxygen occurs. After this exchange of gases, the now oxygen-rich blood circulates back to the left side of the heart through the two pulmonary veins. From the heart, following the aorta, the blood can then find its way to deliver oxygen and nutrients to all cells of the body using systemic circulation.

The blood vessels of both systems are again divided into two groups, depending on their function. Arteries, which normally carry oxygen-rich blood (except the pulmonary artery), show blood flow starting at the heart and spreading outwards to all body systems. These blood vessels typically have bigger diameters than their counterparts, the veins. As the antagonists of arteries, veins function in the opposite direction. After delivering oxygen to different parts of the body through arteries, the now oxygen-depleted blood uses veins as paths to travel back to the heart before undergoing the gas exchange in the pulmonary system again.

Independent from the function and size, all blood vessels show a similar composition with three major layers,<sup>2,3</sup> which can be seen in Figure 1.<sup>1</sup> The lumen, the open tube-shaped space in which the blood flows, is first enclosed by the innermost layer, the tunica intima. This first layer is comprised of endothelial cells and connective tissue. Surrounding this layer, smooth muscle cells form the second layer, called the tunica media. This layer is then protected from external sources by the last layer called tunica externa/ tunica adventitia, which again consists of connective tissue similar to the tunica intima. The main difference between arteries and veins is in the different proportions of these layers in the final blood vessel, which is adapted to the blood pressure. Also, since the blood pressure is generally lower in veins, these have additional valves to prevent backflow.

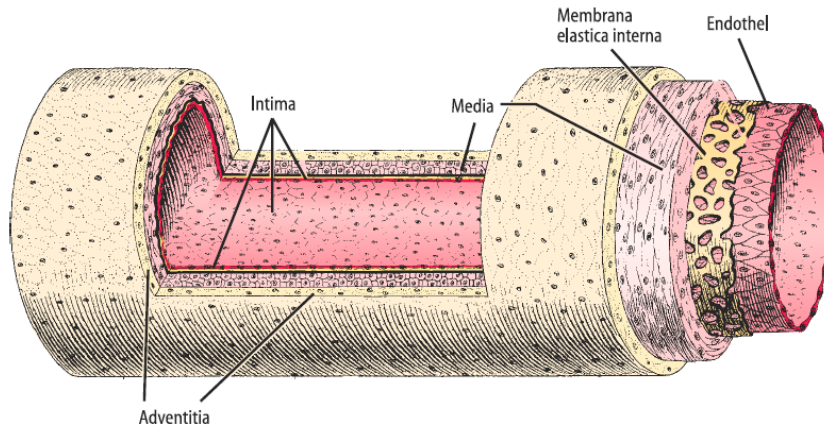
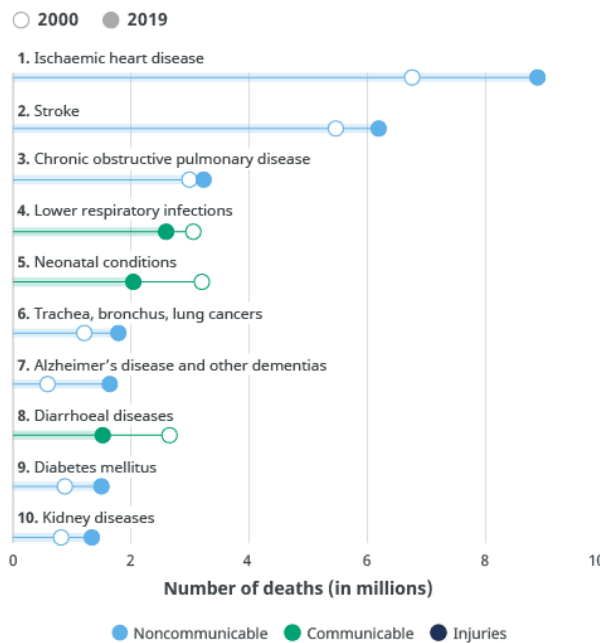


Figure 1: General three-layer structure of a blood vessel

With the high importance of the cardiovascular system in the human body, its diseases are a global health concern, with several of them leading the causes of death globally. Especially in developed nations, their share in the causes of death is high and steadily increasing, as reports from the WHO show (as shown in Figures 2 and 3, taken from official WHO websites<sup>1</sup>).

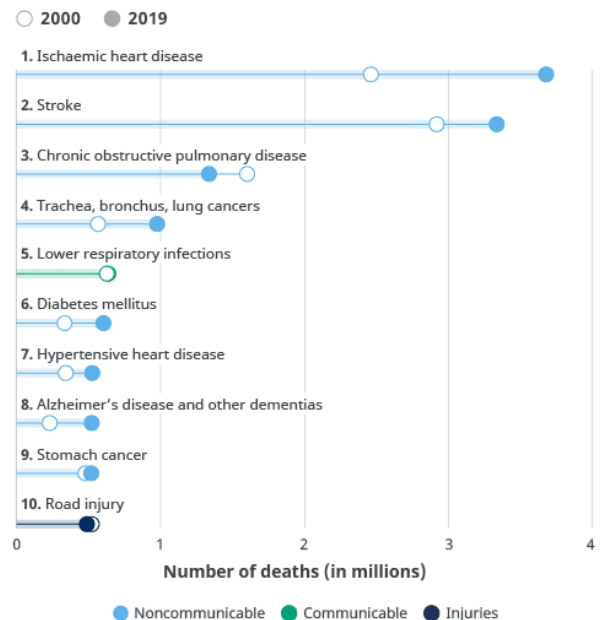
### Leading causes of death globally



Source: WHO Global Health Estimates.

Figure 2: Leading causes of death globally

### Leading causes of death in upper-middle-income countries



Source: WHO Global Health Estimates. Note: World Bank 2020 income classification.

Figure 3: Leading causes of death in upper-middle-income countries

<sup>1</sup> <https://www.who.int/news-room/fact-sheets/detail/the-top-10-causes-of-death> (date of access: 1.4.2021)



Many cardiovascular diseases can be traced back to unhealthy choices in the lifestyle of the patients.<sup>4</sup> Unhealthy diets, sedentary lifestyles lacking physical activity both in the working atmosphere and free time and smoking often cause cardiovascular diseases in the long term.<sup>5</sup> Therefore, even though cardiovascular diseases already play an essential role in the medical field today, they will do even more so with aging societies and increasingly stronger influences of diseases caused by long-term risks. This also means that the causes for these diseases can also be the first target to prevent future illness or worsening of already present diseases. However, not all health problems stemming from cardiovascular diseases can be undone by later lifestyle changes. Irreversible problems often demand therapies, which, depending on the severity of the case, can span a wide variety of possibilities.<sup>6</sup>

Apart from anti-thrombotic drug therapies,<sup>7,8</sup> standard treatments for non-severe diseases caused by plaque deposition often start with a minimally invasive procedure called percutaneous coronary intervention (PCI). In the most commonly used and long-established procedure of these surgical interventions called balloon angioplasty (first scientific publication 1979<sup>9</sup>), a catheter with a balloon is inserted into the blocked blood vessel. After reaching the thrombus, the balloon is inflated with gas and mechanically destroys the blockage. After subsequent deflation of the balloon, both catheter and balloon are again removed from the blood vessel and the blood flow is restored. In order to prevent future blockage of the artery, balloon angioplasty is often combined with the insertion of a stent. This small device with a metal mesh structure remains indefinitely at the previous blockage site. It supports the site mechanically to reduce the chances of restenosis, which is often also aided by parallel drug delivery through the stent.<sup>10-12</sup>

If percutaneous coronary intervention is not sufficient to target the problem, the next procedure of choice often comes with coronary-artery bypass grafting (CABG, first employed by DeBakey in 1964).<sup>13</sup> The idea of all such procedures is to reroute the blood flow away from the blocked blood vessels to suitable alternative vessels, avoiding the blockage but keeping its following blood vessels supplied with oxygen and nutrients. Such replacement vessels can be autologous or heterologous depending on their source (patient or donor).<sup>14</sup> For autologous replacements, the veins used for bypassing usually are the saphenous vein from the leg or the internal thoracic artery. In these auto transplantation procedures, the transplanted blood vessel is harvested from the patient in a separate surgery before being used as a bypass graft. However, this method can be limited by the number of suitable native vessels the patient has<sup>15</sup> and, due to the separate harvesting procedure of the transplanted blood vessel, is problematic for diseases needing intermediate intervention. As an alternative, donations of the needed blood vessels from donors are possible. However, these show different problems as they carry the risk of immune responses of the body rejecting foreign tissue and the possibly difficult

search for compatible donors. With such limitations to the standard medical procedures of autologous and heterologous transplantations, easier and more broadly applicable alternatives for such cases are in high demand. One such alternative can come from tissue engineering.

## 2. Tissue engineering

*„Tissue Engineering is an interdisciplinary field that applies the principles of engineering and life sciences toward the development of biological substitutes that restore, maintain or improve function or a whole organ. “*

*Langer, Vacanti (1993)<sup>16</sup>*

As described by one of its most commonly used definitions following Langer and Vacanti, tissue engineering is an interdisciplinary field and a major part of regenerative medicine. Embracing many different sciences and methods, the goal of restoring organ function is fulfilled through all possible means. For the replacement of damaged native tissue, potential methods can either be *in vivo* or *in vitro*. Also, the biocompatible material can either be made from artificial cellular tissue or non-cellular tissue with mechanical properties comparable to the native tissue, which it should restore or replace. Disregarding the choice of material, many tissue engineering applications rely on the three main pillars<sup>17</sup> – cells, scaffolds and signals/growth factors. This can be seen in Figure 4.

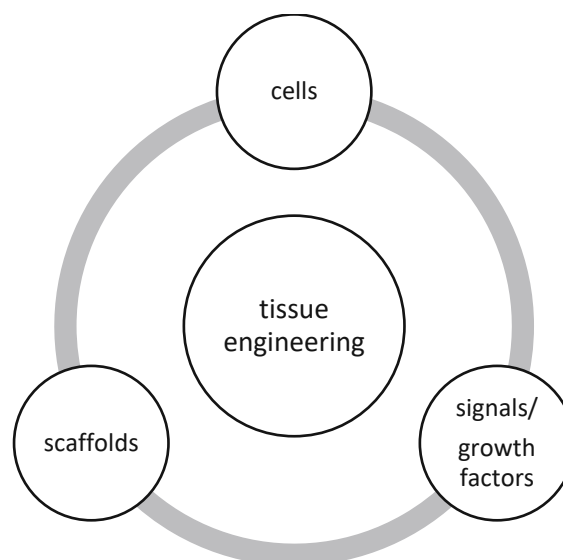


Figure 4: the triangle of tissue engineering

The area “cells” incorporates all aspects regarding the choice of cells used and the cultivation in different media and is often tightly linked with the signals/growth factors. Although the two areas, “cells” and “signals/growth factors” play the most important roles in many different applications in the vast field of regenerative medicine, the main focus in the development of blood vessel substitutes lies within the area of “scaffolds”. This part of tissue engineering involves all possible aspects of scaffolds that form the matrices in which the cells are cultivated and, therefore, shape the regenerated tissue's final form. These scaffolds can be materials of biological or synthetic origin or hybrids in between.<sup>18</sup> Based on its use, several criteria must be met for a synthetic material to be employable in the desired tissue engineering application.

Starting with the demands on the **mechanical properties** of the final regenerated tissue, a first material selection has to be made. Depending on the application, many different materials can be used. While ceramics and different thermoplastic natural or synthetic polymers are a good choice for hard tissue substitution like bone and teeth, for the usage in soft tissue, the selection is already limited to natural or synthetic polymers,<sup>18</sup> which should mimic the mechanical attributes of human blood vessels with high tensile strength and elasticity to avoid complications.<sup>19,20</sup> Also, mechanical stability in long-term applications can be a huge issue.<sup>21</sup>

Another important aspect is the demands for **biocompatibility** (and in some cases biodegradability) of the monomers, the final material, and possible degradation products. Although the mechanical properties needed for certain tissue functions can be achieved by substituting the native tissue with various materials, two main limiting factors often come into play, reducing the possible choices drastically. Since the tissue produced via tissue engineering has to be integrated into the whole functional organ system, immune responses to the foreign material must be prohibited. Limitations stemming from the interface between native tissue and replaced tissue can also be a great difficulty.<sup>22</sup> Mechanical failures or immune responses at these sites can lead to severe complications, ranging from simply hindering the function of the tissue to new diseases or death in the worst-case scenarios. Also, biodegradability is a critical factor in long-term treatments: As non-native materials often show worse mechanical properties after longer use,<sup>23</sup> the main focus should lie in providing an interim solution with engineered tissue aiding the formerly damaged native tissue and allowing the regrowth of native tissue.

**Processability** of the replacement material is often also a significant challenge. Since native tissue and organs often have high complexity in their structure, special shaping techniques have to be applied in most cases to allow mimicry of their function. For example, in bone or other soft tissue replacements, newer developments often follow 3D printing techniques<sup>24-26</sup> to be able to tailor the final form needed for each individual patient. Depending on the used method, the shaping process is often only possible after the synthesis step; therefore, in such

cases, the final product of the synthesis must still be shapeable, which can introduce new limitations on the material. For blood vessel substitutes, the final implantable device should be comparable to small blood vessels in shape and function<sup>27</sup> – this means hollow tubes with uniform mechanical properties along the whole tube. Additionally, the tube has to be penetrable by cells to allow cell growth and regrowth of native tissue while also preventing leakage of fluids/blood. One method of choice for such demands is electrospinning.<sup>28,29</sup>

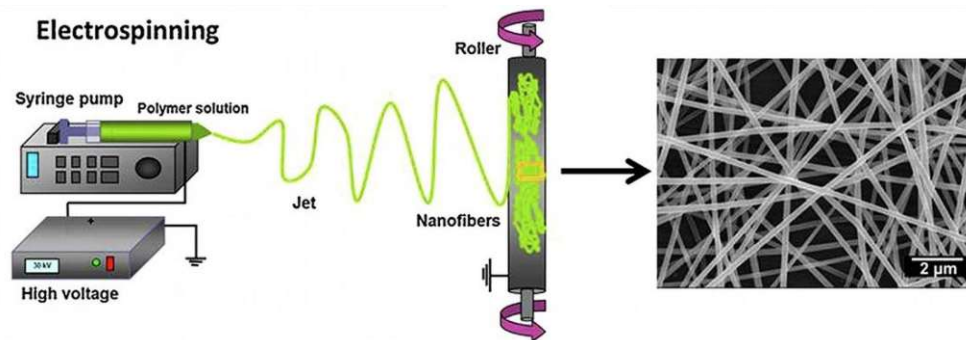


Figure 5: The electrospinning process to fabricate hollow tubes for vascular tissue engineering

In this technique (as depicted in Figure 5<sup>30</sup>), the thermoplastic polymer is dissolved in a volatile solvent to prepare a polymer solution. Through a setup containing a syringe with a blunt needle, this solution is then ejected into an electric field with high voltage forming a fine polymer jet which is randomly woven onto a collecting target. This target determines the final shape of the graft and, in the case of vascular tissue engineering, is a rotating mandrel, around which the polymer strands are collected. After drying and removal of the remaining volatile solvent the final polymer graft can then be collected. In this method, several parameters like the solvent, polymer concentration in the solution, injection speed and voltage can be tuned to achieve a final graft which is mechanically comparable to native blood vessels.

## 2.1 Scaffold materials for vascular tissue engineering

In scaffold-based vascular tissue engineering, the scaffold materials can be either natural, synthetic or hybrid biomaterials.<sup>18,31</sup> For **natural biomaterials**, the choice is between two groups which are either protein- or polysaccharide-based.

For **protein-based biomaterials**, the most researched ones are collagen,<sup>32,33</sup> and its denatured derivative gelatin,<sup>34</sup> elastin<sup>33</sup> and fibrin and newer research is going towards silk-

fibroin.<sup>35-39</sup> Although the first three are all of high interest as they naturally occur in the body, their insufficient mechanical properties can be significant for stand-alone applications.

**Type-I-collagen**, the major protein of the extracellular matrix, and **elastin**, a natural part of blood vessel tissue, are interesting as they are widely available and easily harvestable, but both show bad mechanical performance. This can be overcome by introducing crosslinking or reinforcing with mechanically strong polymers like poly(ethylene terephthalate) (commercial product Dacron) for Type-I-collagen<sup>40-42</sup> or being part of a polymer blend biodegradable synthetic polymers for elastin.<sup>38,43,44</sup> However, using both of these natural materials in combination with synthetic materials contradicts the idea of using only natural biomaterials. In the case of elastin, its primary function is not mechanical support but instead in improving biocompatibility and having a role in regulating cell growth.<sup>45</sup>

Another promising protein-based biomaterial is **fibrin**, which can be harvested from the patient's blood as it is a naturally occurring component for blood coagulation. This biopolymer has been used as a scaffold in tissue regeneration on its own,<sup>46</sup> in blends<sup>47-49</sup> or to coat other materials and improve biocompatibility.<sup>50,51</sup>

**Silk-fibroin** has attracted interest in a wide range of different tissue engineering applications in recent years<sup>52</sup> (bone, cartilage, nervous system, vascular system etc.). As a natural protein-based biopolymer produced by silkworms, it shows good biocompatibility if the second component of silk sericin is removed properly.<sup>53</sup> This material was used also in combination with Type-I-collagen<sup>54</sup> and poly(lactide).<sup>55,56</sup> Also, long-term patency studies of small-diameter grafts showed better results compared to PTFE grafts,<sup>57</sup> making it an interesting material for vascular tissue engineering of small-diameter blood vessels.

For **polysaccharide-based biomaterials**, most research was conducted towards the usability of chitosan,<sup>58</sup> hyaluronic acid and alginate.

**Chitosan** is a derivative of chitin mainly found in fungi and the exoskeletons of crustaceans and insects, with additional favorable properties of being hemostatic and antimicrobial.<sup>59</sup> However, its application is again limited, as it also shows weak mechanical properties. Therefore, its primary use is in coating tissue grafts<sup>60,61</sup> or combination with other mechanically stronger polymers.

**Hyaluronic acid** is mainly known for its use in the cosmetics industry but has been successfully used as a biomaterial in cartilage tissue engineering.<sup>62</sup>

**Alginate** is not part of the human body but instead harvested from seaweed, in which it is the central part of cell walls. This component shows high biocompatibility and low toxicity with good gelation properties, making it an exciting candidate for biomedicine. It is mainly used for

coating<sup>63</sup> or as a matrix material for encapsulation<sup>64-66</sup> and substance delivery<sup>67</sup> in different tissue engineering applications.

Parallel to the previously mentioned use of natural biomaterials, the second approach is done with synthetic materials with their main problem of lackluster mechanical strength. First concepts of such synthetic polymers for vascular tissue engineering applications were meant as permanent replacements, with the use of synthetic polymers like expanded **poly(tetrafluoro ethylene) (ePTFE)**<sup>68</sup> (commercial product “Gore-Tex”) or **poly(ethylene terephthalate) (PET)**,<sup>69</sup> often with additional surface modification,<sup>69-73</sup> having mechanical properties comparable to native blood vessel tissue (Figure 6).



Figure 6: Repeating units of ePTFE (left) and PET (right) used as non-degradable scaffold materials

However, this approach can only be used successfully in grafts for large diameter blood vessels,<sup>74,75</sup> as the problem of thrombosis is a limiting factor for small diameter grafts.<sup>76</sup> Also, the longevity of such transplants has been an issue, with worsening of the mechanical properties over time. Therefore, newer developments go towards biodegradable solutions with *in-situ* tissue engineering.<sup>77-79</sup> The implanted scaffolds act as an interim solution upholding the needed mechanical properties of the diseased blood vessel.<sup>31,80-83</sup> At the same time, native tissue can regenerate into the matrix provided by the polymer graft. Using such an *in-situ* approach, the natural degradation of the implants in the body is turned from a problem to a feature. After the natural degradation process, with appropriate design, the regenerated native tissue should already have taken over the tissue function and therefore show no problem with long-term stability.

For **biodegradable synthetic polymers**, different polymer classes can be used. Biocompatible polyester-based materials are among the most promising and the most used for incorporating ester moieties in their chain, allowing hydrolytic degradation. Examples of such polymers can be seen in Figure 7.

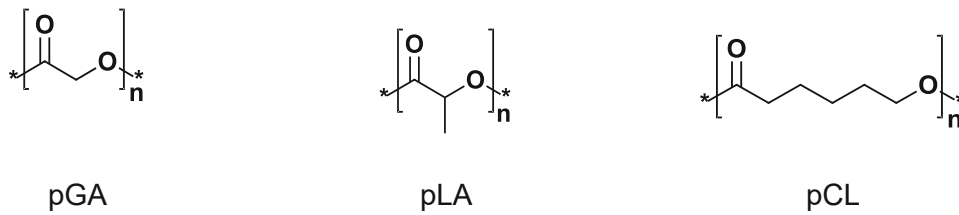


Figure 7: Repeating units of the polyester biomaterials pGA, pLA, pCL

**Poly(glycolic acid) (PGA)** is a thermoplastic material with high crystallinity synthesized using a ring-opening polymerization of glycolide. While the results of its degradation are promising as the degradation product glycolic acid is a natural human metabolite, its fast degradation under aqueous conditions<sup>84,85</sup> can be a problem for *in-situ* tissue engineering: the high speed of degradation can weaken the structural integrity of the implant before the native issue can take over this function leading to mechanical failure.<sup>86</sup> Also, its high reactivity with water can be a problem in processing and storage if not considered.

**Poly(lactic acid) (PLA)** is structurally very similar to PGA, with an additional methyl group in its chain introducing chiral properties. The main application of this material is made with the L-isomer (PLLA), which has an advantage over the D-isomer (PDLA) with better metabolization processes. Both isomers are semi-crystalline solids, whereas the third possible racemic isomer leads to an amorphous solid with the alignment of its chains being hindered. Compared to PGA, the slight change in the polymer backbone with the methyl group impacts the hydrophilicity of PLA and slows down the degradation process.<sup>87,88</sup>

**Poly(caprolactone) (PCL)** is synthesized in a ring-opening polymerization of caprolactone. In its structure, the longer aliphatic chain leads to hydrophobicity, which manifests in an even slower degradation process. This polymer shows good mechanical properties<sup>89</sup> and the possibility to copolymerize with other lactones<sup>90,91</sup> or forming composite materials<sup>36,92</sup> makes it promising as a VTE material. However, the main limitation is its slow degradation process, which can hinder the idea of an *in-situ* approach with fast replacement back to native tissue.

In order to exploit the advantages of each of these different biopolymers, they are often combined in polymer blends<sup>34,36</sup> (like in multi-layer grafts) or used as copolymers prepared by ring-opening polymerization reactions with different monomers in the same reaction.<sup>71</sup>

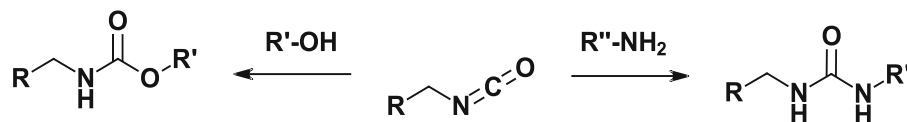
Another possibility is the incorporation of these polymers as smaller subunits into other biodegradable polymers. This can be done by using them as starting points in the synthesis of thermoplastic poly(urethane/urea) elastomers in the form of diol derivatives with smaller molecular weights, which are another class of polymers used in vascular tissue engineering given their good mechanical properties.<sup>93-96</sup>



### 3. Thermoplastic poly(urethane/urea) elastomers

#### 3.1 General aspects

Thermoplastic poly(urethane/urea) elastomers (TPUU) are a subclass of poly(urethane/urea) polymers and are commonly used in tissue engineering applications of soft tissue as they can fulfill all previously mentioned demands on materials for blood vessel substitutes.<sup>97</sup> This polymer class is defined by the urethane and urea groups in its polymer chain, derived from the addition reactions of isocyanate groups with the functional groups of alcohols and amines coming from the second monomer depicted in Scheme 1.



*Scheme 1: Reaction to form urethane or urea groups: Isocyanates react with alcohols to form urethane and amines to form ureas in an addition reaction*

Depending on the number of functional groups per monomer, the final polymer is either purely linear (using only difunctional monomers) or crosslinked (polyfunctional monomers). In the case of only difunctional monomers, the linear chains of the final product result in a thermoplastic material and therefore remains soluble and meltable. The elastomeric properties derive from the capability of the urethane and urea groups to form strong hydrogen bonds, which physically crosslink the chains.<sup>98</sup> This difference in behavior between the non-crosslinked chain segments and physical crosslinks through hydrogen bonds leads to a typical block copolymer structure, in which chain segments are referred to as hard and soft blocks. As the names suggest, hard and soft blocks show very different mechanical properties.<sup>99</sup>

Soft blocks in the material derive from the flexible macrodiol and therefore import flexibility; hard blocks are often short segments in which urethane and urea bonds and the small chain extenders come together. In these areas, the physical crosslinking via hydrogen bonding between urethanes and ureas can often happen.<sup>100</sup> Also, with chain extenders containing aromatic rings pi-stacking or with esters or carbonates, additional hydrogen bonding can happen. Depending on the ratio of hard to soft blocks<sup>101</sup> and the amount and strength of physical crosslinks in the hard block, the mechanical properties of the final material can be changed significantly<sup>102</sup> and tailored to the specific needs of the application.<sup>98,103</sup>



For tissue engineering applications to achieve blood vessel substitutes, the processability and the elasticity of thermoplastic elastomers with high ultimate tensile strength are crucial. While the most common uses of polyurethanes in PU foams rely on a simple synthetic route with just combining the polyisocyanates and polydiols in one step – the so-called “one-pot route” – the final results of such a route are often fairly limited to structurally straightforward polymers. However, this also means that the more complicated “prepolymer method” must be used as a synthesis route. Otherwise, it is impossible to achieve the desired more complex tertiary structure of the thermoplastic poly(urethane/urea) elastomer containing hard and soft blocks in a controlled sequence.<sup>98</sup>

In the prepolymer method (often also called the “two-shot method”), the synthesis process is subdivided into two parts: In the first step, moderately large prepolymers are built up as a starting point from various macrodiols with the addition of diisocyanates forming macrodiisocyanates. Subsequently, these macrodiisocyanates are then connected with the addition of small diols or diamines. These building blocks linking the previously built macromers are referred to as “chain-extenders” and offer an additional and more accessible possibility to introduce many different functionalities in the final polymer. Chain extenders are purely difunctional and lead to linear chains and thermoplastic polymers. Another possible choice as monomers to form networks are cross-linkers. With functionalities higher than two, they react with multiple chains and become a junction of these polymer strands. With cross-linkers, the final polymer loses its thermoplastic nature and becomes insoluble. Therefore, the use of cross-linkers is prohibited by the shaping demands in the usage as blood vessel substitutes with electrospinning. The simplest synthesis procedure following the prepolymer method for thermoplastic polyurethane elastomers with one single chain extender is shown in Figure 8.

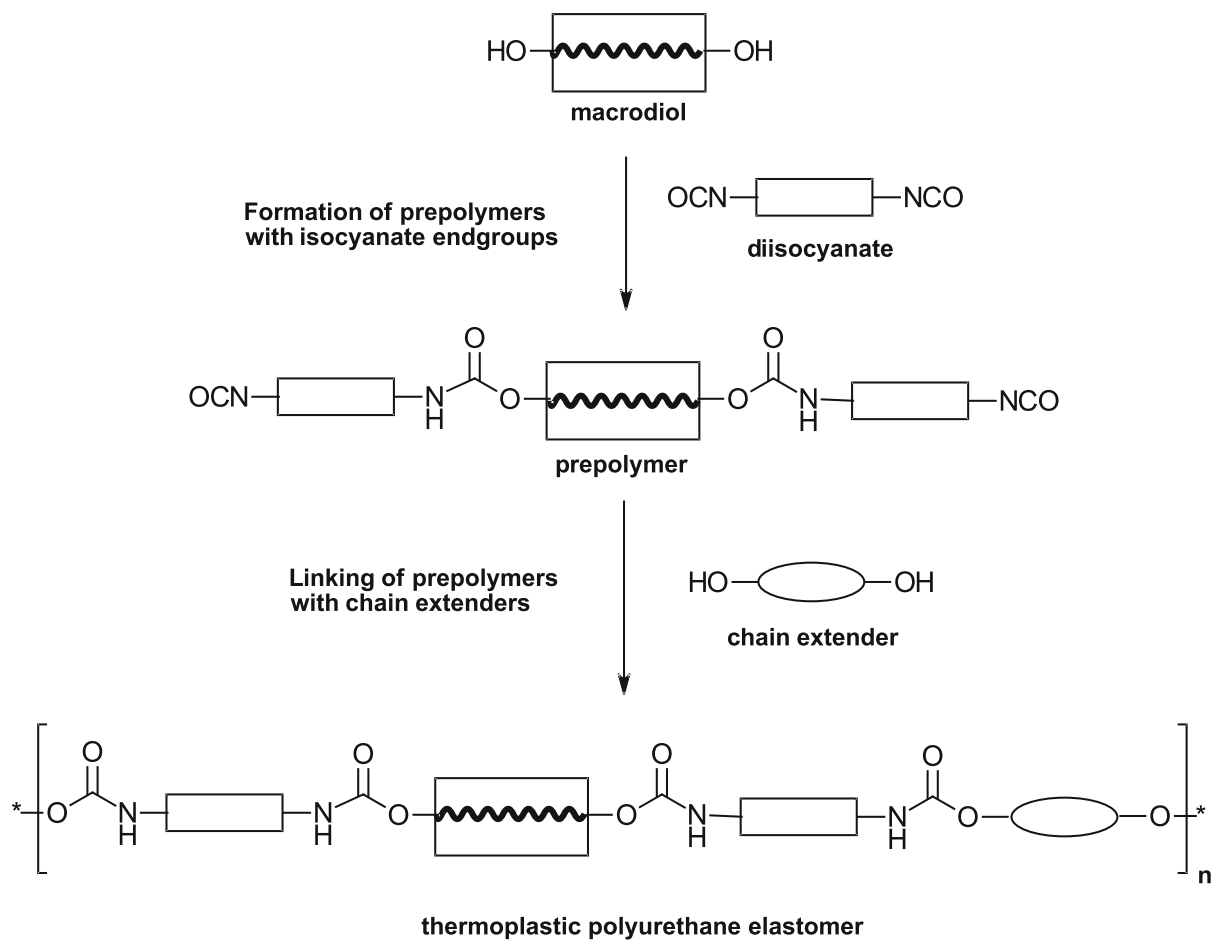


Figure 8: General procedure of the prepolymer method to synthesize thermoplastic polyurethane elastomers using one chain extender in its simplest form

Following this synthesis procedure, many different variations of the final polyurethane with new monomers and different stoichiometric ratios can be employed, allowing significant changes in mechanical or degradation properties. An example would be incorporating monomers with ester or carbonate functionalities, which act as cleavage sites even under mild conditions.

### 3.2 Synthesis route and synthesis requirements

All different synthesis routes of polyurethanes and polyureas rely on the polyaddition reaction of polyisocyanates with polyalcohols and polyamines. Therefore, as with all step-growth reactions, Carother's equation can be applied to predict the degree of polymerization and molecular weights depending on the conversion. For a polyurethane/urea system consisting of macrodiols, diisocyanates and small diols/diamines as chain extenders, the AA/BB model is used with AA monomers being monomers carrying alcohol and amine functionalities

(combination of macrodiols and chain extenders) and BB monomers having isocyanate functionalities (diisocyanates).

In this model, the degree of polymerization depends on two parameters: the ratio  $r$  of AA/BB monomers and the conversion  $p$ .

$$r = \frac{AA}{BB} \quad (r \leq 1) \qquad 0 \leq p \leq 1$$

While the ratio  $r$  is defined by the fraction of monomers and, per definition, smaller than one, the conversion ranges from zero (no reaction) to one (full conversion). The final Carother's equation combines these parameters to calculate the degree of polymerization (Equation 1). For a perfect stoichiometric ratio ( $r = 1$ ), the equation can be simplified (Equation 2). In the simplified version, it can easily be seen that the degree of polymerization  $X_n$  only depends on the conversion and ranges from the starting point of having only unreacted monomers ( $X_n = 1$  with  $p = 0$ ) at the beginning of the reaction to the theoretical value of infinite with full conversion ( $p = 1$ ).

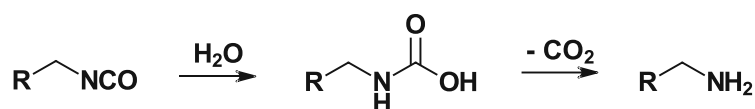
$$X_n = \frac{1+r}{1+r-2pr} \quad (1)$$

*Carother's equation for non-ideal AA/BB systems  
( $r \neq 1$ )*

$$X_n = \frac{1}{1-p} \quad (2)$$

*Simplified Carother's equation for A/B systems and  
ideal AA/BB systems ( $r = 1$ )*

In non-ideal AA/BB systems, the ratio of monomers  $r$  always shows slight deviations from the value of one. This can be either be traced back to impurities of the monomers, (minor) differences in the weigh-ins or side reactions. While impurities of the monomers can be dealt with by using suitable purification methods and differences in weigh-ins can often be minimized with good laboratory practice and routine of the handler, side reactions are more difficult to avoid. The most important side reaction is the unwanted reaction of isocyanates with even traces of water in the system. Here, through an unstable carbamic acid intermediate, the isocyanates degrade to amines, which can also react with isocyanates to form urea bonds shifting the stoichiometric ratios even more. The reaction path for this can be seen in Scheme 2.



*Scheme 2: Hydrolytic degradation of isocyanates to form amines and  $\text{CO}_2$*

To combat this undesired side reaction, the water contents of all reactants must be lowered before usage with different drying procedures.

## 4. Hindered urea bonds

Common urea bonds normally are formed by the reaction of isocyanates with amines and provide bonds, which are stable under normal conditions. One variation of these bonds are hindered urea bonds (HUB), which are a form of urea bonds synthesized through the reaction of isocyanates with secondary amines with bulky substituents at the nitrogen atom. One application of these bonds, also referred to as blocked isocyanates in this context, has been known for a long time to introduce cleavable sites in thermosets for recycling by breaking the bonds irreversibly higher temperatures.<sup>104</sup> Recent research focused on the inherent reversibility of these bonds at mild conditions, allowing recycling, self-healing effects<sup>105,106</sup> or an improved malleability of the final thermoset material.<sup>107</sup> The variety of possible substituents to achieve the destabilization of the urea bond is quite diverse, ranging from linear aliphatic substituents like methyl and ethyl groups to branched aliphatic substituents like *tert*-butyl or isopropyl substituents to even more complex substituents.<sup>108,109</sup> While this behavior is already known for several years now and has gained more and more interest in the last years, a combination of the results in this field and vascular tissue engineering was only recently done by the first work of Ehrmann,<sup>110</sup> who used the monomer *N,N'*-Di-*tert*-butylethylenediamine (TBEDA) as a chain extender in the synthesis of a thermoplastic poly(urethane/urea) elastomer. In this work, the focus was laid on branched substituents like in the already mentioned monomer *N,N'*-Di-*tert*-butylethylenediamine (TBEDA) or *tert*-butyl amino ethanol (TBAE) and *N,N'*-Di-isopropylethylenediamine (IPEDA). The sterically demanding substituents of these monomers change the properties of the otherwise stable urea bond drastically by transforming it to a dynamic bond with low activation energy: With the destabilization of the bond, a reverse bond-formation/cleavage reaction can take place even under mild conditions.<sup>108,111</sup> In this reaction, the reactive isocyanate and the amine groups can be freed into the open form of the hindered urea bonds (Figure 9).

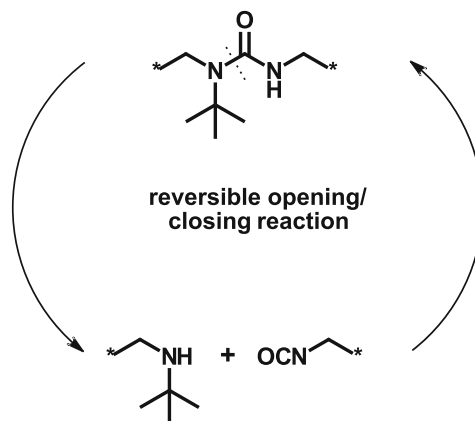


Figure 9: Reversible opening/closing reaction of hindered urea bonds incorporated into the polymer chain, allowing the switch between open and closed form under mild conditions

The now free isocyanate groups can then either react with the secondary amine again, closing the former broken hindered urea bond resulting in self-healing effects<sup>106</sup> or react with other present monomers containing alcohols to form urethane bonds or amines to form stable urea bonds. The alcohols or amines reacting with the isocyanate can already be present in the polymer as end groups of other polymer strands extending the chains. Under the influence of water, the freed isocyanate group from the hindered urea bond can also undergo a degradation reaction with water to form an amine and CO<sub>2</sub>. With harsh reaction conditions, this reaction is uncontrolled. The end result is a chain cleavage with two amine endgroups, which cannot close the chain again. However, contrary to the negative effects of this reaction during the initial synthesis, the described reaction path can also show beneficial outcomes and applicability under certain circumstances: Under mild conditions, a newly formed amine coming from one hydrolyzed hindered urea bond can react with the isocyanate of another polymer strand and also perform a linkage between the chains.<sup>112</sup> This means that the former hindered urea bond is replaced with a stable urea bond. Therefore, the steric hindrance negatively impacting the hard block formation is reduced as hydrogen bonding is improved, strengthening the material.

## Objective

Thermoplastic poly(urethane/urea) elastomers are a promising polymer class in the area of tissue engineering. With their flexibility in the choice of monomers, the mechanical properties can be adjusted easily and span from elastic as needed in scaffolds for vascular blood vessel substitutes to hard and inflexible, fulfilling the requirements of many different uses.

Based on previous research results in our research group in applying these polymers, the versatility of the underlying system of thermoplastic poly(urethane/urea) elastomers in materials comprised of soft-blocks from various macrodiols and hard-blocks from diisocyanates combined with single chain extenders was already shown. In recent findings, the already highly tunable material properties were again expanded by introducing hindered urea bonds. This form of dynamic bond is formed by destabilizing the urea bond with sterically demanding substituents at one nitrogen atom. The material gains new reversible reaction paths under mild conditions, allowing the mechanical properties to be altered in the solid polymer after the synthesis reaction, strengthening the material through storage in wet conditions.

This work aims to expand knowledge of this behavior and the scope of such thermoplastic poly(urethane/urea) elastomers with a systematic study. Therefore, the goals can be defined as such:

- reproduce previous findings on the first such dynamic material
- increase the range of polymers, which include these special dynamic bonds with slight alterations in the composition between polymers
- test the (mechanical) properties of each new polymer before/after preconditioning in deionized water to see changes in (mechanical) behavior
- judge new polymers afterwards for their possible suitability in tissue engineering applications regarding their mechanical properties

To evaluate the (dis)advantages of each monomer substitution, polymers are then also compared to each other. On the search for the best materials, the influence of every single substitution can also be evaluated simultaneously and act as a key to identify the influence of each parameter and aid future decisions in the choice of monomers.

## State of the art

Thermoplastic poly(urethane)s (TPUs) and thermoplastic poly(urethane/urea)s have been widely used in different biomedical applications.<sup>21,113</sup> The broad applicability of this polymer class is quite apparent, as it shows suitable mechanical properties for many different uses in hard and soft tissue engineering, with the possibility of it being easily tailored to adjust in steps towards the perfect material in each individual case.<sup>21,113</sup> The mechanical needs are also very different depending on the application: replacement of bone tissue demands for tough and hard materials,<sup>114</sup> soft tissue (cartilage, blood vessels) need low Young's moduli and high elongations,<sup>21,115</sup> which can all be achieved by suitable choice of monomers.

Now in order to change the final material to the requirements in mechanical performance and biodegradability, the polymer can be changed either one of the typical hard and soft segments by exchanging monomers (macrodiols for soft block variation,<sup>101,116-118</sup> diisocyanate and chain extenders for hard block variation)<sup>96,119,120</sup> or by varying the monomer ratio,<sup>116,117,121-123</sup> which then, in turn, alters the proportions of these segments. For such material adaptations, several criteria in the selection are crucial:

The final TPU(U) must show the capability to form **strong interactions** between chains **in its hard block**, with the most used such interaction being hydrogen bonding.<sup>99,124</sup> These physical crosslinks strengthen the material as a whole and can be improved by using monomers that allow good interaction between chains or increasing the hard block content.<sup>98,125</sup> Also, it has been shown that chain extenders with branched structure can hinder the formation of hydrogen bonds and worsen the mechanical properties.

The synthesized polymer should have **high molecular weights**, as it was shown that increasing the molecular weight of the TPU has positive effects on the mechanical properties.<sup>126</sup>

The wanted **biodegradability** for in-situ tissue engineering is not an inherent property and must be introduced with appropriate biocompatible and biodegradable monomers. Cleavage sites can be integrated both into monomers of the soft-block and hard-block of the final material.<sup>119,127-131</sup>

As such cleaving sites, incorporating ester or carbonate moieties in the macrodiol is a promising and, therefore, often employed idea.<sup>120,126,132</sup> In the typical hard- and soft block structure of TPUs, ester and carbonate cleavage sites can be part of either.<sup>118,120</sup> For a soft-block integration of esters, using poly(caprolactone)diol as a macrodiol in the starting point in the TPU synthesis can be done.<sup>119,133,134</sup> Even though poly(caprolactone) (pCL) is one of the most commonly used polymers in tissue engineering applications on its own, using it to create

the soft-blocks of TPUU can lead to difficulties. The esters in the soft-block chains coming from pCL can limit their function of introducing the flexible properties into the final polymer, with a possible and unwanted formation of semicrystalline soft-blocks.<sup>124</sup> On the other hand, crystallinity is very much wanted in the hard-block and in order to get esters into this part of the chain, many different possibilities are viable. With small molecules containing ester motifs as chain extenders, a wide variety of commercially available compounds could be used or new ones synthesized using established transesterification synthesis routes. Both possibilities are reported in literature.<sup>130,135-137</sup> However, ester degradation can lead to acidic degradation products, which are undesired in the body and accelerating further degradation.<sup>129,138,139</sup> Therefore, similar carbonate groups are often preferred, as they do not lead to such acidic degradation products and usually are more stable under the same conditions.

Alternative possible cleavage sites can be peptides or disulfides, which are mainly cleaved by enzymes<sup>96,140,141</sup> and normally introduced in chain extenders.

The macrodiols used in TPUU synthesis can contain different functionalities: pTHF is one of the simplest and often used macrodiols in TPU(U). Its structure contains only ether groups and alcohol end groups, making the soft-block made with its chemical structure stable under normal application conditions. Using poly(hexamethylene carbonate)diol (pHMC) introduces carbonate functionalities, while using poly(caprolactone)diol introduces ester functionalities into the soft-block, which therefore allow hydrolytic cleavage in the soft-block. Both are again used with two hydroxyl end groups.

Table 1: selected macrodiols used in thermoplastic poly(urethane/urea)s

Name Abbreviation	Chemical structure
poly(tetrahydrofuran) <sup>118,142,143*</sup> pTHF	
poly(hexamethylene carbonate)diol <sup>118*</sup> pHMC	
poly(caprolactone)diol <sup>114,118,133,143-147</sup> pCL	

\* used previously in our research group



The choice of diisocyanates used in TPU(U) synthesis also has a crucial influence on the final mechanical properties. While it is reported that aromatic diisocyanates like 4,4'-methylene diphenyl diisocyanate (MDI) or toluene diisocyanate (TDI) (Figure 10) show better mechanical behavior than non-aromatic diisocyanates, they cannot be used for degradable biomedical applications, as their diamines are considered carcinogenic.<sup>148,149</sup>

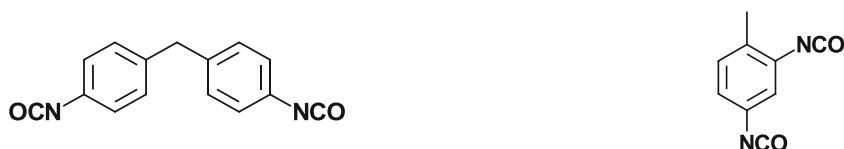


Figure 10: Chemical structures of 4,4'-methylene diphenyl diisocyanate (MDI) and toluene diisocyanate (TDI)

Therefore, a switch towards aliphatic diisocyanates had to be made, even at the cost of worse mechanical performance. Among the most common aliphatic diisocyanate are hexamethylene diisocyanate (HMDI),<sup>114,119,120,126,141,150</sup> 4,4'-diisocyanato dicyclohexylmethane (H12MDI)<sup>114,144</sup> or isophorone diisocyanate (IPDI).<sup>126,133,151</sup> These three and further established aliphatic diisocyanates bis(isocyanatomethyl)cyclohexane (BIMC)<sup>94</sup>, tetramethylene diisocyanate (BDI),<sup>130,152-154</sup> 2,2,4-trimethylene diisocyanate (TMDI)<sup>155</sup> and lysine diisocyanate (LDI)<sup>131,156-158</sup> are shown in Table 2.

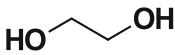
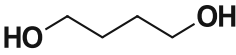
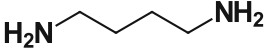
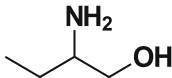
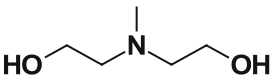
Table 2: selected diisocyanates used in biodegradable thermoplastic poly(urethane/ureas)

Name Abbreviation	Chemical structure
hexamethylene diisocyanate* <sup>114,119,120,126,141,150</sup> HMDI	
4,4'-diisocyanato dicyclohexylmethane* <sup>114,144</sup> H12MDI	
isophorone diisocyanate* <sup>126,133,151</sup> IPDI	
bis(isocyanatomethyl)cyclohexane* <sup>94</sup> BIMC	
tetramethylene diisocyanate <sup>130,152-154</sup> BDI	
2,2,4-trimethylene diisocyanate <sup>155</sup> TMDI	
lysine diisocyanate <sup>131,156-158</sup> LDI	

\* used previously in our research group

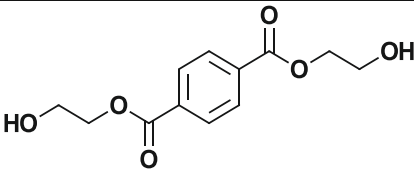
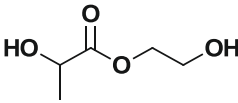
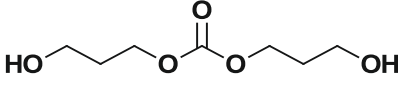
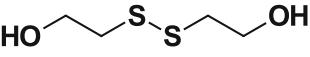
In segmented TPU(U)s, chain extenders are the components, which link the macrodiisocyanates formed between macrodiols and diisocyanates to achieve the final polymer chains. This monomer shows a wide variety: As a small molecule, the integration of desired functional groups can often be done more easily here than in other parts of the final chain. Also, as reactive monomers endgroups to form links with the isocyanate group, alcohols (to form urethane links), amines (to form urea links) or thiols (to form thiourethane links) are possible. The simplest chain extenders are diols and diamines without additional functional groups, like in the case of ethylene glycol (EG),<sup>114,144</sup> 1,4-butanediol (BDO),<sup>118,133,145,154,159</sup> 1,4-butane diamine (putrescine),<sup>130,153</sup> 2-amino-1-butanol (2AB)<sup>126</sup> and 2,2-(methylimino) diethanol (MDEA),<sup>137,145</sup> all of which are also non-cleavable. For hard block degradability, only a very limited amount of monomers is reported in diols with cleavable ester groups like bis(2-hydroxyethyl) terephthalate (BHET)<sup>110,120,136,160</sup> and lactic acid ethylene glycol ester/2-hydroxyethyl lactate (EGLA).<sup>119,160</sup> For cleavable chain extenders with carbonate functionalities, BHPC has been introduced by Ochiai et al.,<sup>135</sup> with alternative preparation methods by Potzmann<sup>132</sup> and Ehrmann.<sup>110</sup> In all these monomers, the functional groups act as target sites for the start of the degradation of the polymer, which was reported in different works.<sup>96,161</sup> A disulfide bond as cleavage site has been reported with 2,2'-dithiobisethanol (DIT).<sup>96,141</sup>

Table 3: diols/diamines/amino alcohols used as non-cleavable chain extender in thermoplastic poly(urethane/urea)s

Name Abbreviation	Chemical structure
ethylene glycol* <sup>114,144</sup> EG	
1,4-butanediol <sup>118,133,145,154,159*</sup> BDO	
1,4-butanediamine (putrescine) <sup>130,153</sup>	
2-amino-1-butanol <sup>126</sup> 2AB	
2,2-(methylimino) diethanol <sup>137,145</sup> MDEA	

\* used previously in our research group

Table 4: diols used as cleavable chain extender in thermoplastic poly(urethane/urea)s

Name Abbreviation	Chemical structure
bis(2-hydroxyethyl) terephthalate* <sup>110,120,136,160</sup> BHET	
lactic acid ethylene glycol ester* <sup>119,160</sup> EGLA	
bis(3-hydroxypropyl) carbonate* <sup>96,110,135</sup> BHPC	
2,2'-dithiobisethanol* <sup>96,141</sup> DIT	

\* used previously in our research group

In order to combine TPU(U) for tissue engineering with dynamic hindered urea bonds, a second chain extender with diamine groups with (bulky) substituents at the nitrogen like *tert*-butyl, isopropyl groups or ethyl groups or amino alcohols with *tert*-butyl aminoethanol is proposed; all of those monomers are commercially available. These compounds (as shown in Table 5 and 6) were all used by Ying *et al.*<sup>109,111</sup> as small monomers in polymerization or to prepare molecular model compounds to prove the cleavability and dynamic reversibility of their hindered urea bonds. However, a use as a chain extender in the synthesis of biocompatible, segmented TPU(U) for vascular tissue engineering has not been reported in literature yet. In this application, their reaction to form hindered urea bonds is desirable, as they are the building blocks that can introduce the proposed self-reinforcing properties shown in a first work by Ehrmann.<sup>109</sup>

Table 5: selected diamines used in the preparation of hindered urea bonds by Ying et al.<sup>111</sup>

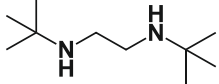
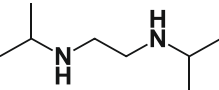
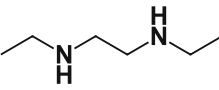
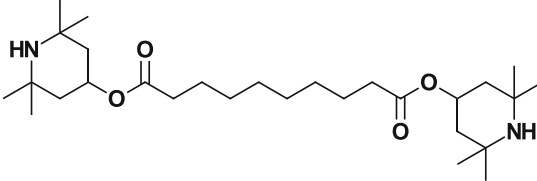
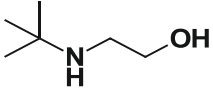
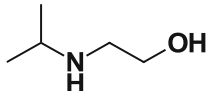
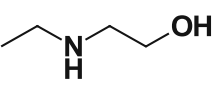
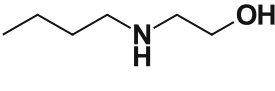
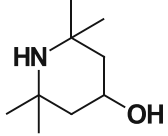
Name Abbreviation	Chemical structure
N,N'-di-tert-butylethylenediamine* TBEDA	
N,N'-diisopropylethylenediamine IPEDA	
N,N'-diethylethylenediamine EEDA	
ditetramethylpiperidine sebacate TMPCA	

Table 6: selected amino alcohols used in the preparation of hindered urea bonds by Ying et al.<sup>111</sup>

Name Abbreviation	Chemical structure
tert-butyl aminoethanol TBAE	
N-(isopropylamino)ethanol IPAE	
N-ethylaminoethanol EAE	
N-butylaminoethanol BAEA	
2,2,6,6-tetramethyl-4-piperidinol TMP-OH	

While both the concept of TPU(U) for vascular tissue engineering and the concept of hindered urea bonds for dynamic materials are established in separate areas of (bio)material engineering, there is no overlap reported yet. This circumstance should be changed with the results of this research combining knowledge of both fields towards new dynamic TPU(U) materials for vascular tissue engineering.

## Results and discussion

The main goal of this work was a systematic study on a system of thermoplastic poly(urethane/urea) elastomers with singular changes in their composition to show the influence of these variations on the final materials. With the preparation and characterization of these new TPUU wanted for vascular tissue engineering applications, which also incorporate dynamic bonds in the form of hindered urea bonds, these two fields should be combined towards new innovative materials. The results of this work to achieve this ambitious goal can therefore be mainly subdivided into two parts:

In the first part, all aspects regarding the synthesis process of TPUU is discussed. This includes preliminary work in the form of monomer synthesis, analysis and purification. Polymer synthesis is then described in general.

The variations are done in all parts of the TPUU starting from the standard material pTHF-HMDI-BHET-TBEDA 1:2:0.5:0.5, with its monomers shown in Figure 11.

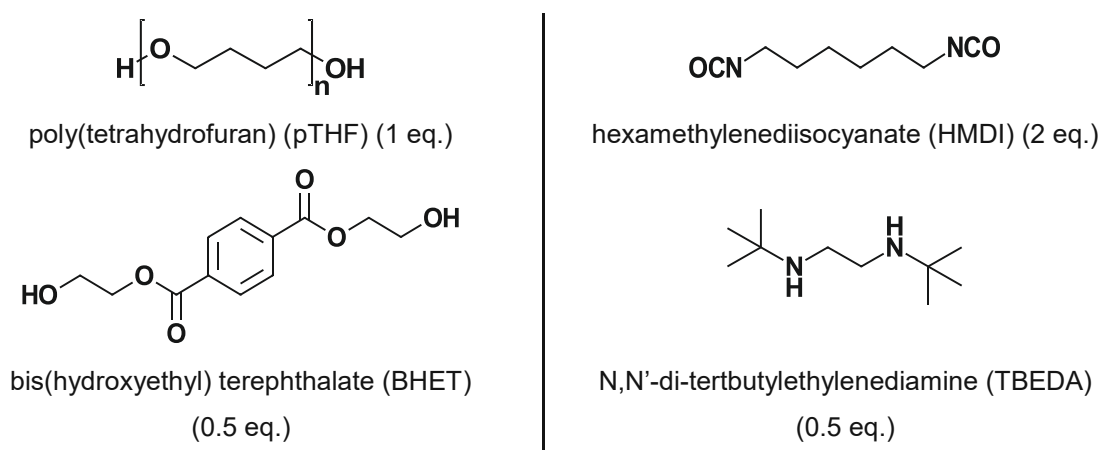


Figure 11: Monomers used in the synthesis of the standard polymer pTHF-HMDI-BHET-TBEDA 1:2:0.5:0.5

In a first change the ratio of the employed chain extenders bis(hydroxyethyl) terephthalate (BHET) and N,N'-di-*tert*-butylethylenediamine (TBEDA) is then changed to ratios of 25:75 and 75:25, leading to polymers with different amounts of hindered urea bonds (HUB) in their chains, which should correlate with the degree of self-reinforcement.

Afterwards, the initial TPUU is changed by exchanges of singular monomers. The first variation in the soft block is done with the exchange of pTHF with either poly(hexamethylene carbonate)diol (pHMC) or poly(caprolactone)diol (pCL). These changes should influence the stiffness of the final material, as they also contain the functional groups carbonates for pHMC

or esters which can form hydrogen bonding between different polymer chains. In the TPUU with pHMC as macrodiol a second change is then also conducted with the exchange of hexamethylenediisocyanate towards 4,4'-diisocyanato dicyclohexylmethane (H12MDI), which should make the material even stiffer. All structures are depicted in Figure 12.

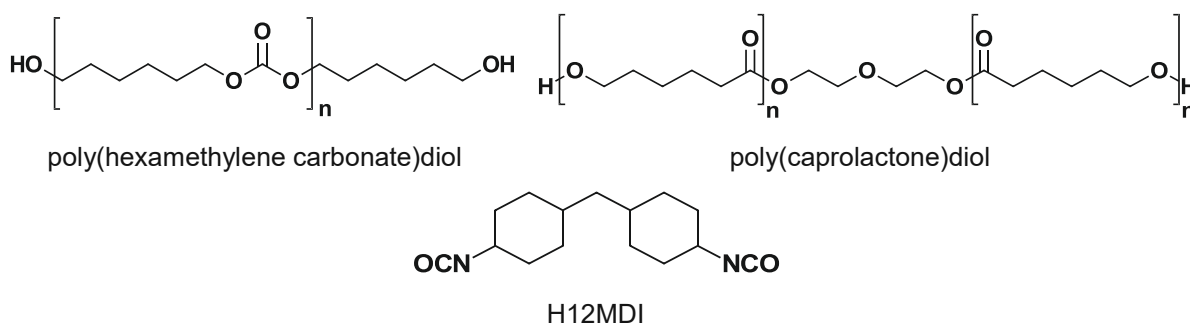


Figure 12: Macrodiols and diisocyanate used in the first variation of the initial polymer

The next variations are then done with the chain extenders. At first with the first chain extender, in which different diols are used, namely 1,4-butanediol (BDO), bis(3-hydroxypropyl) carbonate (BHPC), lactic acid ethylene glycol ester (EGLA) and hydroxypivalic acid neopentyl glycol ester (HPN). Their structures can be seen in Figure 13. All of these changes should influence the mechanical properties of the materials as they effect the hydrogen bonding in the hard block, which is needed for good mechanical performance.

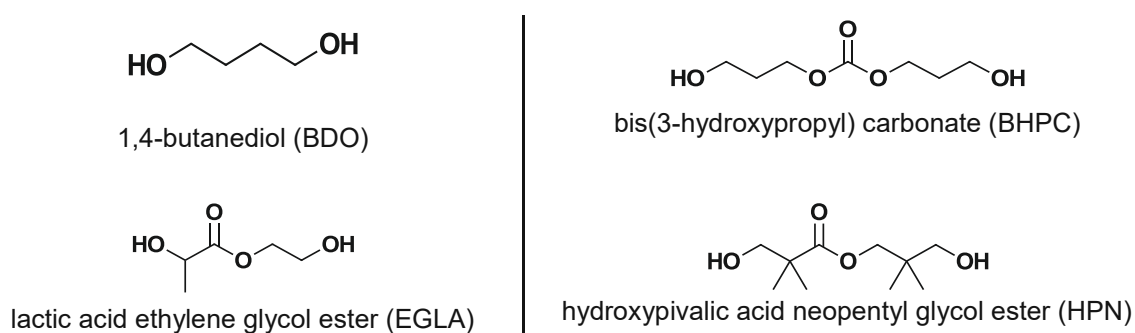


Figure 13: Structures of different small diols used as first chain extender

The final change is then in the second chain extender, which introduces the hindered urea bonds. With the exchange of TBEDA towards N,N'-diisopropylethylenediamine (IPEDA), the destabilization of the urea bond is lowered making it less susceptible towards cleavage and therefore more stable. *Tert*-butyl aminoethanol (TBAE) on the other hand shows the same destabilization of the HUB, however only on one side of the monomer making it an interesting

choice to study possible influences of single side cleavage. Both structures of these chain extenders are shown in Figure 14.



Figure 14: Structures of different amino-based chain extenders used as second chain extender to introduce HUBs

As reference polymers the TPU pTHF-HMDI-BHET 1:2:1 (“BHET-P”), containing the same monomers as the standard polymer as shown in Figure 11, however without TBEDA to not include HUBs. As second reference the commercial product Pellethane (from Lubrizol) is used. It contains the monomers pTHF, the aromatic 4,4'-methylene diphenyl diisocyanate (MDI) and the chain extender 1,4-butanediol (BDO), but with unknown exact stoichiometry. Its monomers are shown in Figure 15.

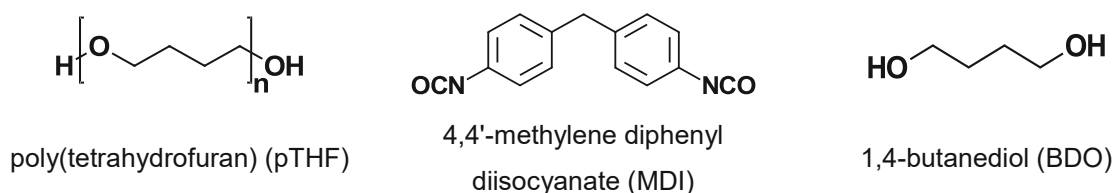


Figure 15: Monomers of the commercial TPU Pellethane used as benchmark

In the second part, the characterization of the previously described synthesized TPUUs from the shown monomers is done in regards to chemical composition, molecular weight, thermal and mechanical properties. Also, a short degradation study was done with one TPUU.

## 1. Synthesis

In order to prepare thermoplastic poly(urethane/urea) elastomers with high molecular weights, high purity and exact stoichiometry of the reactants has to be ensured, as the degree of polymerization follows the Carother's equation (further details see Introduction, chapter “3.2 Synthesis route and synthesis requirements”). To do so, used macrodiols were analyzed in regards to their molecular weight; the purity of diisocyanates and chain extenders was ensured

by application of different purification methods. Two used chain extenders were also not commercially available and had to be synthesized before their use in TPUU synthesis.

## 1.1 Chain extenders

Bis(3-hydroxypropyl) carbonate (BHPC) and lactic acid ethylene glycol ester (EGLA) (as shown in Figure 16) are both not commercially available and had to be synthesized. In both cases, transesterification reactions are employed to yield the desired product.

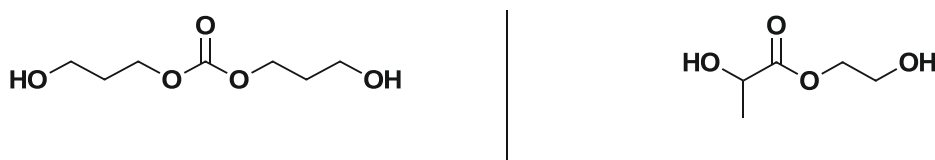


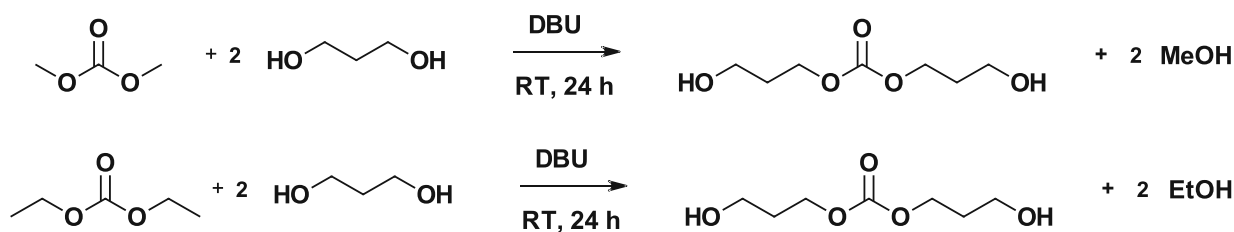
Figure 16: Structures of the synthesized chain extenders bis(3-hydroxypropyl) carbonate (BHPC) and lactic acid ethylene glycol ester (EGLA)

Bis(3-hydroxypropyl) carbonate (BHPC) can be synthesized from the starting material dimethyl carbonate or diethyl carbonate with 1,3-propanediol using different reaction conditions. While earlier works<sup>96</sup> used diethyl carbonate and 1,3-propanediol with  $\text{Ti}(\text{OiPr})_4$  as the catalyst and pushed the reaction equilibrium towards completion by removal of the side product ethanol with a parallel distillation, the applicability of this reaction is hindered by long reaction times at high temperatures and still relatively low yields after purification with column chromatography (46 % in literature). Also, unwanted oligomerization of BHPC can occur quickly.

The resulting oligomeric side products are difficult to separate by column chromatography given the similar  $R_f$ -values of monomeric BHPC and oligomers.

Therefore a newer synthesis route<sup>110</sup> was used, which can be seen in Scheme 3. The reaction time is shortened, and the reaction temperature is lowered to room temperature: in this simplified process di(m)ethyl carbonate is stirred with an excess of 1,3-propanediol for 24 hours at room temperature. The catalyst is also changed from  $\text{Ti}(\text{OiPr})_4$  to 1,8-diazabicyclo[5.4.0]undec-7-ene (DBU) in relatively high amounts to hinder unwanted oligomerization.

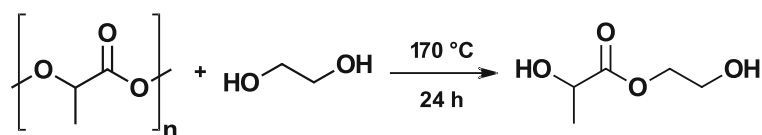




Scheme 3: Both possible syntheses of BHPC: dimethyl carbonate and 1,3-propanediol using DBU as the catalyst (top), diethyl carbonate and 1,3-propanediol using DBU as catalyst (bottom)

The side product (m)ethanol is not distilled off in parallel; therefore, the reaction goes towards an equilibrium with a maximum yield of 25 % BHPC. After stopping the reaction, the side product (m)ethanol and 1,3-propanediol are separated via distillation. Afterward, the crude product is purified using column chromatography with pure ethyl acetate as solvent (BHPC  $R_f = 0.40$ ). Although oligomerization can happen here, it is less of a problem because of lower temperatures and higher catalyst amounts. Therefore, the effort to obtain BHPC with the least possible oligomers for polymer synthesis is significantly eased.

The synthesis of lactic acid ethylene glycol ester (EGLA) is done similarly (Scheme 4), also using a transesterification reaction. However, in this reaction, instead of a transesterification of small molecules as starting material, the lactic acid comes from a poly(lactic acid) (pLA) source, which chains are cleaved and esterified by heating in an excess of ethylene glycol.



Scheme 4: Synthesis of EGLA from pLA and ethylene glycol

After removing ethylene glycol under reduced pressure, the product can be isolated by distillation under high vacuum. The reaction should be done parallel to the TPUU synthesis to ensure the purity of the monomer. Otherwise, even after short storage times, an increase in viscosity was noted, which was traced back to possible oligomerization reactions.

## 1.2 Polymers

### 1.2.1 Prerequisites for polymer synthesis

In order to achieve the high molecular weights, which are needed for the desired mechanical properties, several prerequisites must be fulfilled. Since the polymer is synthesized using a polyaddition mechanism between isocyanates and (macro)diols and diamines, exact stoichiometry must be used. For this, the purity and absence of water in the reactants must be ensured before syntheses. Previous works showed that water contents of monomers below 50 ppm are necessary to achieve good molecular weights.<sup>29</sup> In order to reduce the moisture to such low values, solid reagents and viscous macrodiols were dried under high vacuum ( $2 - 4 \cdot 10^{-2}$  mbar) with solids being dried at room temperature; macrodiols were also stirred at 90 °C. Liquid monomers (diisocyanates and chain extenders) were dried using 3 Å molecular sieves.

The water content of monomers is then monitored before addition to the reaction by utilizing Karl-Fischer titration (KFT). This analysis method relies on the reaction of iodine to iodide and methyl sulfite to methyl sulfate, which needs water in the system to occur.<sup>162</sup> Its exact reaction can be seen below, with RNH being an unspecified base.



KFT can be used for various substances, with only a few leading to undesired side reactions hindering the titration. For example, the application of KFT to determine the water content in reactants of polyurethane/urea synthesis is simple: liquid monomers can be tested directly using an automated titration device with coulometric detection for solids; the same can be done with the prior dissolving of the solid analyte in dry solvents.

Also, the molecular weights of macrodiols must be analyzed beforehand to calculate the needed amount of diisocyanate and chain extenders, which was done using two different analysis methods based on the reactivity of the alcohol endgroups. If the monomer's purity was not suitable for synthesis, the necessary purification was performed before using distillation or column chromatography. Furthermore, two chain extenders are not commercially available and were synthesized (as previously mentioned).

### 1.2.1.1 Analysis of macrodiols

All used macrodiols pTHF, pHMC and pCL were obtained from commercial sources in purities suitable for polyurethane/urea synthesis; hence, no purification was necessary. Since these monomers act as starting blocks of the final material, their exact molecular weights must be known to calculate the amount of diisocyanates and chain extenders needed for correct stoichiometry. Therefore, these molecular weights were analyzed with two different analytical methods relying on the principle of endgroup modification.

#### 1.2.1.1.1 Molecular weight of used macrodiols using OH-titration

The molecular weight can be calculated using the OH-value of the macrodiols. In this first method, the OH-value was determined using a method according to DIN 53240-1<sup>163</sup>. For this method, the macrodiol reacts with the acetylation agent (25:75 acetic anhydride/dry pyridine) with dry pyridine as solvent at elevated temperatures. After quenching with deionized water to hydrolyze the excess of acetic anhydride to acetic acid, the remaining acetic acid is back titrated using the automated titration device Metrohm Titrino (mode DET) with 0.5 N methanolic KOH (titer determination with benzoic acid in methanol). The same procedure without adding a sample was done to get the blank value. Blank values were determined in duplicates; sample titrations were done in triplicates.

Hydroxyl values were then calculated using the Formula 3 (taken from DIN 53240-1):

$$OH - number = \frac{(V_0 - V) \cdot 28.5 \cdot f}{m} \quad (3)$$

OH-number (mg KOH/g)	hydroxyl value
$V_0$ [mL]	blank value
$V$ [mL]	volume 0.5 M KOH in sample titration
$f$	titer 0.5 M KOH (0.9404)
$m$ [g]	mass of the sample
28.5	factor derived from the molecular weight of KOH (56.1 g mol <sup>-1</sup> ) and the molarity of the used solution (0.5 M)

Afterward, the hydroxyl values can be directly converted to the desired molecular weights with Equation 4, leading to the final results shown in Table 7.

$$M_n = \frac{2 \cdot 56.11 \cdot 1000}{OH - number} \quad (4)$$

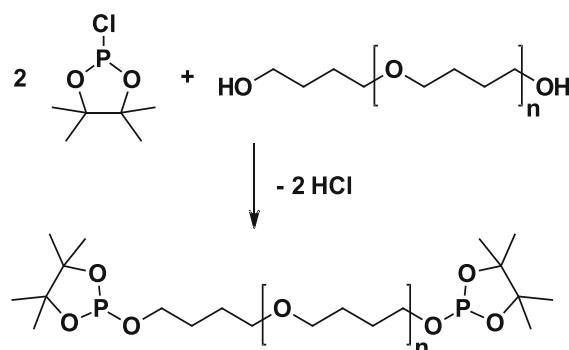
Table 7: Results of the hydroxyl value titrations and calculated molecular weights of used macrodiols

Macrodiol (CAS)	Supplier	Product name/ catalogue number	theor. $M_n$ [g mol <sup>-1</sup> ]	OH-number [mg KOH g <sup>-1</sup> ]	act. $M_n$ [g mol <sup>-1</sup> ]
<b>pTHF</b> (25190-60-1)	Sigma	345296	1000	111.6 ± 0.2	1005 ± 0.5
	Aldrich				
<b>pHMC</b> (61630-98-6)	UBE	Eternacoll UH-100	1000	91.1 ± 1.4	1232 ± 19
<b>pCL530</b> (36890-68-3)	Sigma	189405	530	205.6 ± 5.1	546 ± 14
	Aldrich				
<b>pCL2000</b> (36890-68-3)	Sigma	189421	2000	52.3 ± 1.1	2148 ± 46
	Aldrich				

Following these results, the deviations from the expected molecular weights from the manufacturers' product descriptions show considerable differences between the macrodiols. The deviation in molecular weight of pTHF1000 is negligibly small with 0.5% and can therefore be ignored in polyurethane/urea syntheses. The OH-values of pCL530 showed higher standard deviations between measurements leading to an averaged deviation in the molecular weight of 3.0. Therefore, the molecular weight found with this analysis should be used in polymer syntheses. pHMC1000 and pCL2000 have high deviations with 23.2, and 7.4%, respectively, which is in accordance with the low molecular weights of TPUUs made from these macrodiols in first syntheses attempts. In later attempts, the weigh-ins of the macrodiols pHMC1000 and pCL2000 were adjusted to correspond with the molecular weights from this analysis.

### 1.2.1.1.2 Molecular weight of macrodiols using quantitative $^{31}\text{P}$ -NMR-spectroscopy

Apart from the routine determination of the molecular weight of macrodiols through the OH-value by titration, a conceptually similar approach is quantitative  $^{31}\text{P}$ -NMR-spectroscopy.<sup>164</sup> While in the first case, the calculation of the OH-value depends on the reaction of OH-groups with acetic anhydride and back titration of the remaining acid surplus, in this experiment, the alcohol end groups of the macrodiols react with the phosphorous agent 2-chloro-4,4,5,5-tetramethyl-1,2,3-dioxaphospholane (TMDP), which can be quantified via internal standard in a  $^{31}\text{P}$ -NMR experiment (Scheme 5).



Scheme 5: Phosphorylation of a macrodiol (here: pTHF) using TMDP

The high reactivity of the phosphorous agent TMDP means that no separate reaction step is necessary since the phosphorylation happens almost instantly upon mixing of TMDP with reactants with OH-groups. Therefore, the sample has to be anhydrous; otherwise, hydrolysis reactions happen, which can be seen by the instant formation of HCl gas (Figure 17).

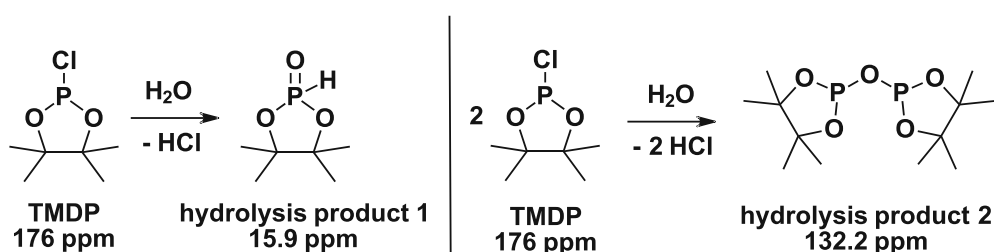


Figure 17: Possible hydrolysis reactions of TMDP

Pyridine is added to buffer the traces of HCl coming from the phosphorylation of the macrodiol and the hydrolysis reaction. Other reagents needed are an internal standard (cyclohexanol), which also reacts with TMDP allowing the quantification of the NMR signals. The cyclohexanol standard is prepared beforehand with a known concentration (around 40 mg mL<sup>-1</sup> in pyridine), and to this prepared solution, the relaxation agent chromium(III)acetylacetonate (Cr(acac)<sub>3</sub>) is also added ( ~ 5 mg mL<sup>-1</sup>). As an NMR solvent, CDCl<sub>3</sub> is used.

### Sample preparation:

An exact amount of dry macrodiol is dissolved in CDCl<sub>3</sub> and mixed with an internal standard solution made from pyridine with approx. 40 mg mL<sup>-1</sup> cyclohexanol and 5 mg mL<sup>-1</sup> chromium(III)acetylacetonate. This solution is then finally mixed with a solution of TMDP in CDCl<sub>3</sub>, transferred to an NMR-tube, and a <sup>31</sup>P-NMR spectrum is measured immediately.

### NMR evaluation:

All <sup>31</sup>P-NMR measurements were conducted with a 600 MHz NMR spectrometer (128 scans) and analyzed with MestreNova. After an automated phase correction and a manual baseline correction using polynomial fit, the spectrum was referenced to the signal at 132.2 ppm (CDCl<sub>3</sub>). Following the peak assignments, all NMR signals were integrated, and the integral of the internal standard cyclohexanol at 145 ppm was set to 1.

The OH-value can then be calculated from the integrals in the spectrum by using Equation 5:

$$\frac{c_{IS} \cdot V_{IS} \cdot I_{aliph.OH}}{M_{IS} \cdot I_{IS} \cdot m} = OH - value \left[ \frac{mmol\ OH}{g} \right] \quad (5)$$

$c_{IS}$	concentration of the internal standard (40.58 mg mL <sup>-1</sup> )
$V_{IS}$	volume of the internal standard (100 μL)
$I_{aliph.OH}$	integral of aliphatic OH-groups (found in 145.2 – 150.0 ppm range)
$M_{IS}$	molecular mass of the internal standard cyclohexanol (100.158 g mol <sup>-1</sup> )
$I_{IS}$	Integral of the internal standard (set to 1)
$m$	mass of macrodiol sample in mg

The OH-value as result of Equation 5 represents the number of OH-groups in mmol g<sup>-1</sup> polymer, which can be converted in the molecular weight of the macrodiol by using Equation 6.

$$\frac{z \cdot f}{OH - value} = M_n \left[ \frac{g}{mol} \right] \quad (6)$$

z	number of OH-groups per macrodiol (2)
f	conversion factor from mol to mmol (1000)
OH-value	result from equation 1 [mmol g <sup>-1</sup> ]
M <sub>n</sub>	number average molar mass [g mol <sup>-1</sup> ]

Following these steps for all macrodiols then leads to the following results listed in Table 8.

Table 8: Results of the quantitative <sup>31</sup>P-NMR spectroscopy

macrodiol	I <sub>aliph.OH</sub> *	mass of macrodiol [mg]	OH-value [mmol g <sup>-1</sup> ]	M <sub>n</sub> [g mol <sup>-1</sup> ]
pTHF1000	1.58	31.92	2.0055	997
pHMC1000	1.33	32.87	1.6394	1220
pCL530	2.73	29.91	3.6980	541
pCL2000	0.73	31.39	0.9422	2123

\* manual integration, derivations between different integration ranges in a range of < 1%

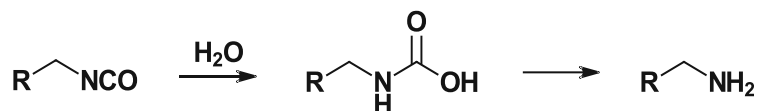
These results can then be compared to the molecular weights of the macrodiols calculated from previous OH-titrations, as done in Table 9. It could be shown that the deviation between the methods is roughly around one percent. With the exception of pTHF, all results from the <sup>31</sup>P-NMR method lie within the standard deviation of the respective titrations.

Table 9: Comparison of molecular weights given by the supplier and values calculated from titration and quantitative <sup>31</sup>P-NMR

macrodiol	theor. M <sub>n</sub> [g mol <sup>-1</sup> ]	M <sub>n</sub> from titration [g mol <sup>-1</sup> ]	M <sub>n</sub> from quant. <sup>31</sup> P-NMR [g mol <sup>-1</sup> ]	deviation between methods [%]
pTHF1000	1000	1005 ± 0.5	997	0.8
pHMC1000	1000	1232 ± 19	1220	1.5
pCL530	530	546 ± 14	541	0.9
pCL2000	2000	2148 ± 46	2123	1.2

### 1.2.1.2 Purification of diisocyanates

Diisocyanates can hydrolyze, leading to amines through a carbamic acid intermediate (Scheme 6).



Scheme 6: Hydrolytic degradation of isocyanates to an amine through a carbamic acid intermediate step

This degradation reaction can happen during storage with even small amounts of moisture resulting in impurities of partially hydrolyzed diisocyanates, fully hydrolyzed diisocyanates to diamines and different possible addition products of newly formed amine groups with isocyanates. As all these unwanted products could interfere with the polymerization reaction by shifting the stoichiometry, they had to be removed before use. To achieve this, the diisocyanates were distilled before polymer synthesis and stored under argon in the fridge during storage times.

Two different diisocyanates were used in the polymer syntheses, namely hexamethylene diisocyanate (abbreviated HMDI, CAS 822-06-0) and 4,4'-diisocyanato dicyclohexylmethane (H12MDI, CAS 5124-30-1), as shown in Figure 18.

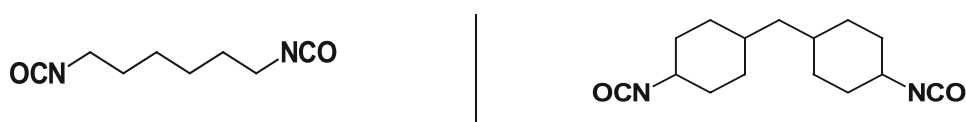


Figure 18: Structures of the diisocyanates hexamethylene diisocyanate (HMDI) and 4,4'-diisocyanato dicyclohexylmethane (H12MDI) used in TPUU synthesis

Both diisocyanates were purified via vacuum distillation, in the case of HMDI at 104 °C at 10 mbar and for H12MDI at 147-154 °C at  $3.8 \cdot 10^{-2}$  mbar.

### 1.2.1.3 Purification of chain extenders

In contrast to the macrodiols and diisocyanates, not all chain extenders were commercially available. As mentioned in the previous chapter, the two chain extenders bis(3-hydroxypropyl) carbonate (BHPC) and lactic acid ethylene glycol ester (EGLA) were synthesized using known transesterification reactions from previous works.<sup>29,110</sup>



For the use of all chain extenders in polymerization reactions, purity was checked before usage and purification was done if necessary. Also, all monomers were dried before use and their water contents checked with KFT and only used in synthesis if the water content was below 50 ppm (this requirement was shifted to 100 ppm for the di-*tert*-butylamino-based monomers TBEDA and TBAE, as well as the isopropyl amino-based monomer IPEDA (shown in Figure 18/Table 10) as their drying procedure often leads to water contents slightly above 50 ppm, which still showed good results in polymer synthesis).

All commercially available chain extenders were purchased in high purity. To ensure the purity of all chain extenders, they were analyzed before use and purified using different methods.

As solid chain extenders, bis(2-hydroxyethyl) terephthalate (BHET), hydroxypivalic acid neopentyl glycol ester (HPN) and *tert*-butyl aminoethanol (TBAE) were used, which are shown in Figure 19.

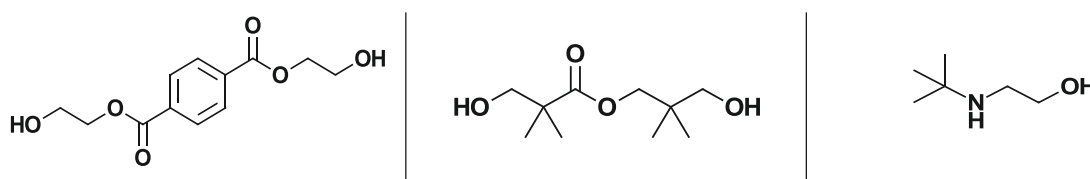


Figure 19: Structures of the solid chain extenders used in TPUU synthesis: bis(2-hydroxyethyl) terephthalate (BHET), hydroxypivalic acid neopentyl glycol ester (HPN) and *tert*-butyl aminoethanol (TBAE)

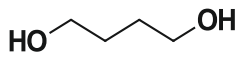
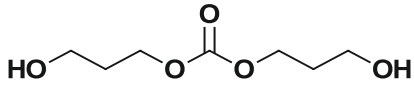
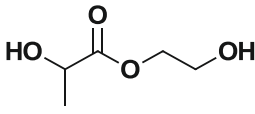
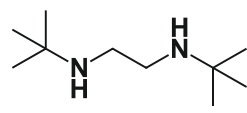
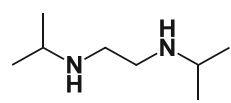
BHET was purified via recrystallization in distilled water. Given its low solubility in water, an excess of BHET was heated in water at reflux, filtered while hot, and slowly precipitated. Drying of the filtered white crystalline solid was done under high vacuum at room temperature.

As the purity of HPN was considered suitable for synthesis after analysis, it could be used as purchased after drying under high vacuum at room temperature.

TBAE was also purified before use. Given its low melting point of 41-43 °C and suitable boiling point of 90-92 °C/25 mmHg, it was melted at first and distilled under vacuum. Drying was then done under high vacuum at room temperature in the solid-state.

As liquid chain extenders, the following monomers listed in Table 10 were used.

Table 10: All liquid chain extenders used in polymer synthesis

Name (abbreviation)	CAS	Structure
1,4-butanediol (BDO)	110-63-4	
bis(3-hydroxypropyl) carbonate (BHPC)	-	
lactic acid ethylene glycol ester (EGLA)	-	
N,N'-di-tert-butylethylenediamine (TBEDA)	4062-60-6	
N,N'-diisopropylethylenediamine (IPEDA)	4013-94-9	

Bis(3-hydroxypropyl) carbonate (BHPC) and lactic acid ethylene glycol ester (EGLA) were synthesized as described in the previous chapter “1.1 Chain extenders”, page 26. BHPC was purified after synthesis using column chromatography with pure ethyl acetate as eluent. EGLA was purified using distillation under high vacuum.

The three remaining liquid chain extenders, 1,4-butanediol (BDO), N,N'-di-tert-butylethylenediamine (TBEDA) and N,N'-diisopropylethylenediamine (IPEDA), were purified via distillation under vacuum. This was combined with a first drying step by stirring over dry molecular sieves (3 Å) before distilling. The distilled, pure monomer was then stored under argon over molecular sieves. Water content was checked before use in synthesis via KFT.

## 1.2.2 General polymer synthesis procedure

The synthesis of all polymers was done using Schlenk-technique with completely dry monomers, which was checked before synthesis using KFT. Synthesis was only done if the water content was determined to be below 50 ppm. For the chain extenders TBEDA/IPEDA/TBAE, this was adjusted to 100 ppm H<sub>2</sub>O for handling reasons.

The synthesis following a prepolymer synthesis route was done similar to previous works<sup>29,94,96,110</sup> with the incorporation of two different chain extenders. After the transfer of the predried macrodiol to the reaction vessel, another short drying step at 90 °C was performed before adding two equivalents of freshly distilled diisocyanate to the reaction under argon flux while ensuring quantitative transfer by dilution and rinsing with dry DMF, which also acts a solvent to ensure homogenous conditions; otherwise, unwanted crosslinking reactions can happen.<sup>110</sup> The formation of the macro-diisocyanate prepolymers is catalyzed with three drops Sn(Oct)<sub>2</sub> while stirring for three hours at slightly elevated temperatures of 60 °C. Afterward, the first chain extender is added substoichiometrically with 0.5 equivalents for most polymers, which is only changed to 0.25 and 0.75 equivalents in the variation of chain extender ratios. Here, again the quantitative transfer is guaranteed by rinsing off all used transfer equipment with dry DMF. The addition reaction of the first chain extender is done at 60 °C for three hours before adding the second, amino-based chain extender, which introduces the hindered urea bonds, in the same way. After rinsing with dry DMF, the reaction is kept stirring at either room temperature or 60 °C under argon atmosphere overnight, depending on the monomers used.

After one night, the polymer solution was diluted with a small amount of dry DMF if there was a strong increase in viscosity and transferred to a separation funnel. Afterward, the reaction flask was rinsed with dry DMF to ensure a quantitative transfer of the product to the separation funnel.

Precipitation of the polymer was done by dropwise addition to dry diethyl ether under stirring at room temperature. This precipitation step showed two different behaviors for the different polymer variations: If flaky polymer fell out of solution, the product was filtered off using a glass funnel and filter paper. If the polymer stayed as a polymer film in the precipitation solution, the precipitation agent diethyl ether and remaining reaction solvent DMF was decanted off. The polymer film, which was often sticking to the beaker walls, was afterward manually extracted with a spatula. To limit the loss of polymer with this method, the beaker was rinsed with dry THF into a rotavapor flask, and the solvent was then removed under vacuum.

Using all the before mentioned suitable monomers for thermoplastic poly(urethane/urea)s, many different compositions are possible. Thirteen different polymers are proposed as a selection to test the usability of the different monomers and investigate the influence of each

exchange in monomers on the properties of the final polymer. The variations of the initial material (shown in Table 11) are done in different parts of the TPUU and to introduce different changes:

The first variation was done by changing the **chain extender ratio** of the TPUU with the building blocks pTHF-HMDI-BHET-TBEDA. The initial material with a chain extender ratio of 50 % BHET, 50 % TBEDA, was changed in two different directions, once towards a lower content of hindered urea bonds with the chain extenders in a ratio of 75 % BHET to 25 % TBEDA and then with more HUBs with a content of 25 % BHET to 75 % TBEDA. With this change the influence in the number of HUBs on the initial mechanical properties as well as its impact on the degree of possible self-reinforcement should be analyzed.

In the second variation, the **macrodiol** building block was altered so that each final polymer still has a composition with a consistent stoichiometry of macrodiol/diisocyanate/chain extender 1/chain extender 2 = 1/2/0.5/0.5, with the chain extenders being the standard BHET and TBEDA. Starting from the macrodiol poly(tetrahydrofuran) (pTHF), this was changed to poly(hexamethylene carbonate)diol (pHMC) (with a molecular weight of 1000 Da) with the diisocyanates HMDI (polymer pHMC/HMDI) and H12MDI (pHMC/H12MDI). The second different macrodiol used was poly(caprolactone)diol (pCL), which had molecular weights of 530 Da (pCL530/HMDI) and 2000 Da (pCL2000/HMDI) as per manufacturer specified. With this change the influence of the soft-block on the material properties can be seen; also pHMC and pCL are interesting from an tissue engineering standpoint and would be a useful expansion in the monomer choice.

The third variation was in **chain extender 1**, which has its name from the fact that it is added as the first chain extender after the formation of macrodiisocyanates. As all of these chain extenders are small diols, they react to form urethane bonds with free isocyanates groups and do not lead to the incorporation of hindered urea bonds into the final polymer, but are still important as they can influence the interaction of chains in the hard blocks.

The fourth variation then alters the **second chain extender**, which is the key monomer responsible for the incorporation of hindered urea bonds in the final polymer. Coming from the standard TBEDA, which is a symmetrical diamine with *tert-butyl* substituents on each side, this is first changed to IPEDA swapping *tert-butyl* with *isopropyl* substituents. This change should also lead to a polymer with hindered urea bonds, although the different destabilizing groups on the urea bond can alter the reactivity. The other variation in chain extender 2 is from a symmetrical diamine to an amino alcohol with the usage of *tert-butyl* amino ethanol. With this monomer, the destabilizing substituent at the hindered urea bond stays the same, allowing a bond cleavage under the same conditions as with TBEDA. However, this cleavage is only on one side, as the other side is bound by a stable urethane group.

Finally, two **reference materials** were also tested under the same conditions. Pellethane is a commercially available product from Lubrizol which is FDA approved and applied in electrospun vascular grafts,<sup>165</sup> consisting of pTHF-MDI-BDO (with unknown exact stoichiometry) and as second reference material the TPU “BHET-P”, a polyurethane without hindered urea bonds made from pTHF-HMDI-BHET (ratio 1:2:1).

Table 11: Variations of the initial polymer with macrodiol:diisocyanate:chain extender 1:chain extender 2 1:2:0.5:0.5 with a change in the chain extender ratio macrodiol, chain extender 1 and chain extender 2. Changes to the initial polymer (in the first row) are highlighted in gray.

Polymer	Macrodiol (1 eq.)	Diisocyanate (2 eq.)	Chain extender 1 [mol%]	Chain extender 2 [mol%]
<b>Changes in the chain extender ratio</b>				
pTHF-HMDI-BHET-TBEDA 50/50	pTHF	HMDI	BHET 50 %	TBEDA 50 %
pTHF-HMDI-BHET-TBEDA 75/25	pTHF	HMDI	BHET 75 %	TBEDA 25 %
pTHF-HMDI-BHET-TBEDA 25/75	pTHF	HMDI	BHET 25 %	TBEDA 75 %
<b>Changes in the macrodiol (and diisocyanate)</b>				
pHMC-HMDI-BHET-TBEDA	pHMC	HMDI	BHET 50 %	TBEDA 50 %
pHMC-H12MDI-BHET-TBEDA	pHMC	H12MDI	BHET 50 %	TBEDA 50 %
pCL530-HMDI-BHET-TBEDA	pCL530	HMDI	BHET 50 %	TBEDA 50 %
pCL2000-HMDI-BHET-TBEDA	pCL2000	HMDI	BHET 50 %	TBEDA 50 %
<b>Changes in the first chain extender</b>				
pTHF-HMDI-BDO-TBEDA	pTHF	HMDI	BDO 50 %	TBEDA 50 %
pTHF-HMDI-BHPC-TBEDA	pTHF	HMDI	BHPC 50 %	TBEDA 50 %
pTHF-HMDI-EGLA-TBEDA	pTHF	HMDI	EGLA 50 %	TBEDA 50 %
pTHF-HMDI-HPN-TBEDA	pTHF	HMDI	HPN 50 %	TBEDA 50 %
<b>Changes in the second chain extender</b>				
pTHF-HMDI-BHET-TBAE	pTHF	HMDI	BHET 50 %	TBAE 50 %
pTHF-HMDI-BHET-IPEDA	pTHF	HMDI	BHET 50 %	IPEDA 50 %
<b>Reference materials</b>				
pTHF-HMDI-BHET	pTHF	HMDI	BHET	
Pellethane*	pTHF	MDI	BDO	

\* commercial product, exact stoichiometry unknown

## 2. Polymer analysis

The success in the preparation of TPUU was then judged with different analytical methods. With the use of  $^1\text{H-NMR}$  and ATR-FTIR, the chemical composition of each individual polymer could be determined to show if each monomer takes part in the polyaddition reaction, while GPC is used to analyze the final molecular weights of the prepared TPUU. Afterwards, thermal properties are evaluated by the means of DSC and TGA. While DSC was used to show the glass transition temperature and melting of the ordered hard blocks of new, promising polymers in order to predict their mechanical properties, thermal degradation via TGA can be an early indicator to show the nature of the dynamic HUBs with mass loss under thermal stress. The core aspect in TPUU analysis was done with tensile testing to demonstrate changes coming from the self-reinforcement effect after preconditioning in water. Finally, one TPUU was analyzed in a short degradation study under aqueous conditions.

### 2.1 Chemical constitution and polymer composition

The chemical constitution of the polymers were analyzed with  $^1\text{H-NMR}$  and ATR-FTIR.  $^1\text{H-NMR}$  was used to determine if all monomers were built into the polymer chain by confirming the presence of each monomer's signals in the spectrum. This could be successfully done for all TPUUs except with the chain extender BDO as it has the exact same signals as the used macrodiol pTHF. Also, by integrating the signals, the final ratio of the monomers can be judged; however, due to the often overlapping signals (pTHF and BDO, pHMC/pCL and TBEDA) and low intensities of the same, the ratios are often not exact but give a good indication if the wanted reaction stoichiometry was achieved. This was done for all TPUUs and led to the conclusion that the deviation of the wanted stoichiometry was in an approximate range of 10 % to around 20 % (Table 12).

Table 12: Deviation ranges in the TPUU composition calculated from <sup>1</sup>H-NMR

polymer	wanted stoichiometry	achieved stoichiometry	deviation range [%]
<b>Changes in chain extender ratio</b>			
pTHF-HMDI-BHET-TBEDA 50/50	1:2:0.50:0.50	1.06:2.02:0.50:0.45	10
pTHF-HMDI-BHET-TBEDA 75/25	1:2:0.75:0.25	1.06:2.20:0.75:0.28	20
pTHF-HMDI-BHET-TBEDA 25/75	1:2:0.25:0.75	1.15:2.10:0.25:0.56	20
<b>Changes in the macrodiol (and diisocyanate)</b>			
pHMC-HMDI-BHET-TBEDA	1:2:0.50:0.50	1.15:2.30:0.50:0.50	10-20*
pHMC-H12MDI-BHET-TBEDA	1:2:0.50:0.50	-*	-*
pCL530-HMDI-BHET-TBEDA	1:2:0.50:0.50	0.89:2.08:0.50:0.56	10-20
pCL2000-HMDI-BHET-TBEDA	1:2:0.50:0.50	1.20:2.20:0.50:0.47	20
<b>Changes in the first chain extender</b>			
pTHF-HMDI-BDO-TBEDA	1:2:0.50:0.50	-#	-#
pTHF-HMDI-BHPC-TBEDA	1:2:0.50:0.50	1.00:20.2:0.60:0.40	25
pTHF-HMDI-EGLA-TBEDA	1:2:0.50:0.50	1.00:2.17:0.45:0.43	25
pTHF-HMDI-HPN-TBEDA	1:2:0.50:0.50	1.00:2.30:0.65:0.40	40
<b>Changes in the second chain extender</b>			
pTHF-HMDI-BHET-TBAE	1:2:0.50:0.50	0.90:1.81:0.50:0.50	< 10
pTHF-HMDI-BHET-IPEDA	1:2:0.50:0.50	1.09:2.20:0.50:0.49	< 10

\* signals of pHMC (and H12MDI) overlap with TBEDA, no exact determination possible

#pTHF and BDO have the same signals, no exact determination possible

With ATR-FTIR, the characteristic bands of each group were identified, and the absence of unreacted isocyanate (band at 2300 – 2250 cm<sup>-1</sup>) was confirmed for all polymers.

## 2.2 Molecular weight via GPC

The molecular weight of polymers directly correlates with the mechanical properties, with higher molecular weights leading to better performance.<sup>126</sup> It is, therefore, a good indicator in regards to the usability of a polymer. All prepared polymers were tested using a gel permeation chromatography system (GPC) with dry THF (spiked with butylhydroxytoluol BHT as flowrate marker) as eluent with conventional calibration. In order to do this, samples of the polymers

and the reference standard Pellethane were prepared by dissolving the polymer in THF. The desired final concentration of the polymer depends on the expected molecular weight and should be in the range of 2-3 mg mL<sup>-1</sup> for such polymers. This was done by weighing approx. 8-12 mg with mg accuracy and dissolving in the appropriate amount of THF in a test tube to get the desired concentration. Due to strong hydrogen bonding, many of the analyzed TPUs are difficult to solve at room temperature; therefore, the samples were either heated with a heat gun and shaken or suspended into a 60 °C water bath until the polymer was completely in solution. If these methods were deemed unsuccessful, 1,1,1,3,3,3-hexafluoroisopropanol (HFIP) can be used to break hydrogen bonds between polymer chains by using a maximum of around 10/90 % v/v HFIP/THF. For measurements using the triple detection method, the possible loss of volatile solvent must be accounted for in order not to distort the final polymer concentration, which is needed to determine the refractive index increment (dn/dc). This can be done either by weighing or marking of the solvent level. The polymer solution was then filtered into a GPC vial through a syringe filter to ensure complete dissolving of the polymer and afterwards measured. The results of these measurements using conventional calibration can be seen in in Figure 20 and Table 13.

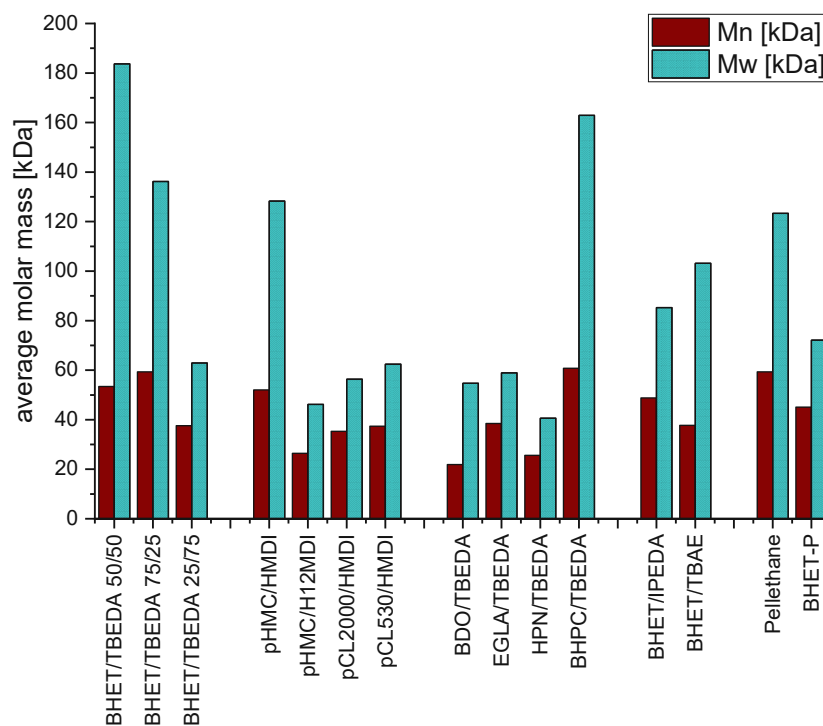


Figure 20: Overview of all different polymers in regards to number average molar mass and weight average molar mass determined via GPC using THF as eluent and conventional calibration against polystyrene standards



Table 13: GPC results with conventional calibration against polystyrene standards, measured directly after synthesis (the reference material Pellethane is a commercial product, while the reference material BHET-P was synthesized)

Abbreviation	M <sub>n</sub> [kDa]	% Pell.	M <sub>w</sub> [kDa]	% Pell.	PDI
<b>Changes in the chain extender ratio</b>					
<b>for the stoichiometry pTHF/HMDI/BHET/TBEDA 1/2/X/(1-X)</b>					
BHET/TBEDA 50/50	53.4	90.1	183.7	149.0	3.4
BHET/TBEDA 75/25	59.3	100.0	136.2	110.5	2.3
BHET/TBEDA 25/75	37.6	63.4	62.9	51.0	1.7
<b>Changes in the macrodiol (and diisocyanate)</b>					
<b>for the stoichiometry macrodiol/diisocyanate/BHET/TBEDA 1/2/0.5/0.5</b>					
pHMC/HMDI	52.0	87.7	128.3	104.1	2.5
pHMC/H12MDI	26.4	44.5	46.2	37.5	1.8
pCL2000/HMDI	35.3	59.5	56.4	45.7	1.6
pCL530/HMDI	37.4	63.1	62.4	50.6	1.7
<b>Changes in the first chain extender</b>					
<b>for the stoichiometry pTHF/HMDI/CE1/TBEDA 1/2/0.5/0.5</b>					
BDO/TBEDA	21.9	36.9	54.7	44.4	2.5
EGLA/TBEDA	38.5	64.9	58.9	47.8	1.5
HPN/TBEDA	25.6	43.2	40.6	32.9	1.6
BHPC/TBEDA	60.8	102.5	162.9	132.1	2.7
<b>Changes in the second chain extender</b>					
<b>for the stoichiometry pTHF/HMDI/BHET/CE2 1/2/0.5/0.5</b>					
BHET/IPEDA	48.8	82.3	85.3	69.2	1.8
BHET/TBAE	37.7	63.6	103.2	83.7	2.7
<b>Reference materials</b>					
Pellethane	59.3	-	123.3	-	2.1
BHET-P	45.1	76.1	72.1	58.5	1.6

The results of these measurements evaluated with conventional calibration against polystyrene standards showed that the choice of monomers has a significant influence on the molecular weights and polydispersity of the final polymers. Although all polymers were prepared with the same synthesis route with only minor adjustments, the range of the final results regarding molecular weights is relatively high. TPUUs with different macrodiols showed lower molecular weights, which could be attributed to the fact, that the initial synthesis is optimized for the macrodiol pTHF and further optimization could be useful. On the contrary, the polymer BHPC/TBEDA showed a remarkably high molecular weight, which is similar to previous research<sup>96</sup> with the TPU pHMC/HMDI/BHPC 1/2/1 also with higher than usual molecular weight. A definitive reason for this behavior was not found though. Overall, the molecular weights are however in a comparable range to the reference polymers BHET-P and Pellethane, which leads to the conclusion that there is a certain limitation to the achievable molecular weight given by the nature of polyaddition reactions following Carother's law.

As the behavior of thermoplastic poly(urethane/urea) elastomers is quite different from polystyrene in regards to the shape of dissolved polymer in solution, which is crucial in this analysis method, a comparison to the commercially available reference material Pellethane is done. This comparison shows that the molecular weights are in a similar range but mostly (slightly) lower to the commercial product, which can already be expected given the higher susceptibility to errors in a new synthesis compared to established and optimized routines in commercial products. As the molecular weight determined by GPC is used as a criterion to judge the success of a TPUU synthesis, it can be said that the synthesis of all listed polymers was successful and should lead to polymers, which can be tested for their mechanical properties. Nevertheless, the influence of the varying molecular weights should be kept in mind while judging the final mechanical properties.

For more exact determination of the molecular weights, measurements using triple detection were also done. For these triple detection measurements, the sample preparation is done analog. Each measuring solution is then injected into the device in five separate runs with injection volumina ranging from 80 to 120  $\mu\text{L}$  with 10  $\mu\text{L}$  increments. This allows a variation of the polymer concentration and, as a consequence, the determination of the refractive index increment (often abbreviated to  $dn/dc$ ), which describes the change in response of the IR detector depending on the polymer concentration.  $Dn/dc$  values are characteristic for each polymer class/composition and solvent (at isothermal conditions), allowing the determination of absolute molecular weight values. The results of the measurements can be seen in Table 14.

Table 14: GPC results with triple detection method

Abbreviation	M <sub>n</sub> [kDa]	M <sub>w</sub> [kDa]	PDI	dn/dc
<b>Changes in the chain extender ratio</b>				
<b>for the stoichiometry pTHF/HMDI/BHET/TBEDA 1/2/X/(1-X)</b>				
BHET/TBEDA 50/50	44.7	164.4	3.7	0.0838
BHET/TBEDA 75/25	31.1	66.7	2.1	0.0850
BHET/TBEDA 25/75	102.6	213.4	2.1	0.0154 <sup>#</sup>
<b>Changes in the macrodiol (and diisocyanate)</b>				
<b>for the stoichiometry macrodiol/diisocyanate/BHET/TBEDA 1/2/0.5/0.5</b>				
pHMC/HMDI	19.6	108.6	5.5	0.0689
pHMC/H12MDI	10.2	23.7	2.3	0.0774
pCL2000/HMDI	35.9	80.9	2.3	0.0341
pCL530/HMDI	32.5	94.9	2.9	0.0574
<b>Changes in the first chain extender</b>				
<b>for the stoichiometry pTHF/HMDI/CE1/TBEDA 1/2/0.5/0.5</b>				
BDO/TBEDA	25.3	45.4	1.8	0.0668
EGLA/TBEDA	-*	-*	-*	-*
HPN/TBEDA	10.9	34.1	3.1	0.0643
BHPC/TBEDA	50.6	255.1	5.0	0.0146 <sup>#</sup>
<b>Changes in the second chain extender</b>				
<b>for the stoichiometry pTHF/HMDI/BHET/CE2 1/2/0.5/0.5</b>				
BHET/IPEDA	60.7	415.4	6.8	0.0192 <sup>#</sup>
BHET/TBAE	29.2	93.9	3.2	0.0878
<b>Reference materials</b>				
Pellethane	34.9	92.6	2.7	0.1131
BHET-P	25.6	68.4	2.7	0.0774

\* showed strong signs of degradation in the later triple detection measurement and was therefore not evaluated

<sup>#</sup> unusually low values for dn/dc (normally dn/dc ≥ 0.05)

A comparison of the results between conventional calibration and triple detection method shows lower values for the latter in most cases. Also, while the measurements with conventional calibration were done immediately after synthesis, triple detection measurements were done at a later time and most polymers already showed (slight) signs of degradation,

lowering these values. For several polymers, the  $dn/dc$  value determined by the device was unusually low compared to literature values, which often state that  $dn/dc \geq 0.05$  for similar polymers. It could not be determined, though, if this is an error of the device or its calculation method or a result of only a slight refractive index change between these solutions of TPUU in THF and pure THF. Therefore, the results of the measurements in these cases should be judged critically, and only seen as additional results together with the conventional calibration.

## 2.3 Thermal properties

In order to analyze the thermal properties of the materials, DSC and TGA measurements of the polymers were conducted. Polymers with the composition pTHF-HMDI-BHET-TBEDA with a change in chain extender ratio and the reference materials BHET-P and Pellethane had been measured in previous works;<sup>110</sup> therefore, only polymers with the new macrodiols pHMC and pCL and the chain extenders BDO, BHPC, EGLA and HPN were analyzed.

### 2.3.1 Glass transition temperatures and melting behavior *via* DSC

For each polymer, the parameters glass transition temperature and melting behavior were analyzed following two heating cycles. After staying isothermal at the starting temperature of  $-90\text{ }^{\circ}\text{C}$  for 5 minutes, the temperature was raised to  $150\text{ }^{\circ}\text{C}$  with a temperature ramp of  $10\text{ }^{\circ}\text{C}/\text{min}$ . After another isothermal step with a duration of 2 min. at this temperature, the sample was cooled down to  $-90\text{ }^{\circ}\text{C}$  with a temperature ramp of  $-10\text{ }^{\circ}\text{C}/\text{min}$ , and the first cycle was repeated. The signals of the measurements were then analyzed, with glass transition temperatures being determined as the inflection in the second heating cycle of each polymer. Melting points were determined as endothermic peaks with the first heating cycle of each polymer and melting enthalpy as the area under the curve for each peak. The results of the measurements can be seen in Table 15.

Table 15: Results of the DSC measurements for all tested polymers

Polymer	Thermal property	
<b>Changes in the chain extender ratio for the stoichiometry pTHF/HMDI/BHET/TBEDA 1/2/X/(1-X)</b>		
BHET/TBEDA 50/50 <sup>\$</sup>	T <sub>g</sub> [°C] (1 <sup>st</sup> cycle)	-66.7
	T <sub>m</sub> [°C]	81.1
	ΔH <sub>m</sub> [J g <sup>-1</sup> ]	7.0
BHET/TBEDA 75/25 <sup>\$</sup>	T <sub>g</sub> [°C] (1 <sup>st</sup> cycle)	-62.6
	T <sub>m</sub> [°C]	91.3
	ΔH <sub>m</sub> [J g <sup>-1</sup> ]	26.8
BHET/TBEDA 25/75 <sup>\$</sup>	T <sub>g</sub> [°C] (1 <sup>st</sup> cycle)	-60.5
	T <sub>m</sub> [°C]	75.4
	ΔH <sub>m</sub> [J g <sup>-1</sup> ]	9.3
<b>Changes in the macrodiol (and diisocyanate) for the stoichiometry macrodiol/diisocyanate/BHET/TBEDA 1/2/0.5/0.5</b>		
pHMC/HMDI	T <sub>g</sub> [°C] (1 <sup>st</sup> cycle)	-33.1
	T <sub>g</sub> [°C] (2 <sup>nd</sup> cycle)	-31.6
	T <sub>m</sub> [°C]	47.5* / 55.2* / 105.2
	ΔH <sub>m</sub> [J g <sup>-1</sup> ]	12.07 / 9.72
pHMC/H12MDI	T <sub>g</sub> [°C] (1 <sup>st</sup> cycle)	_#
	T <sub>g</sub> [°C] (2 <sup>nd</sup> cycle)	-28.9
	T <sub>m</sub> [°C]	46.1
	ΔH <sub>m</sub> [J g <sup>-1</sup> ]	23.87
pCL2000/HMDI	T <sub>g</sub> [°C] (1 <sup>st</sup> cycle)	-54.5
	T <sub>g</sub> [°C] (2 <sup>nd</sup> cycle)	-54.0
	T <sub>m</sub> [°C]	20.4 / 49.8 / 89.1
	ΔH <sub>m</sub> [J g <sup>-1</sup> ]	3.91 / 28.77 / 6.01
pCL530/HMDI	T <sub>g</sub> [°C] (1 <sup>st</sup> cycle)	-27.1
	T <sub>g</sub> [°C] (2 <sup>nd</sup> cycle)	-16.2
	T <sub>m</sub> [°C]	92.6
	ΔH <sub>m</sub> [J g <sup>-1</sup> ]	19.2
<b>Changes in the first chain extender for the stoichiometry pTHF/HMDI/CE1/TBEDA 1/2/0.5/0.5</b>		
BDO/TBEDA	T <sub>g</sub> [°C] (1 <sup>st</sup> cycle)	-67.5
	T <sub>g</sub> [°C] (2 <sup>nd</sup> cycle)	-65.6
	T <sub>m</sub> [°C]	96.1
	ΔH <sub>m</sub> [J g <sup>-1</sup> ]	15.71
BHPC/TBEDA	T <sub>g</sub> [°C] (1 <sup>st</sup> cycle)	-66.4
	T <sub>g</sub> [°C] (2 <sup>nd</sup> cycle)	-62.1
	T <sub>m</sub> [°C]	70.9
	ΔH <sub>m</sub> [J g <sup>-1</sup> ]	11.46
EGLA/TBEDA	T <sub>g</sub> [°C] (1 <sup>st</sup> cycle)	-62.5
	T <sub>m</sub> [°C]	22.0
	ΔH <sub>m</sub> [J g <sup>-1</sup> ]	16.7

<b>Continuation of Table 15</b>		
<b>Polymer</b>	<b>Thermal property</b>	
HPN/TBEDA	$T_g$ [°C] (1 <sup>st</sup> cycle)	-62.0
	$T_m$ [°C]	34.5
	$\Delta H_m$ [J g <sup>-1</sup> ]	14.9
<b>Changes in the second chain extender for the stoichiometry pTHF/HMDI/BHET/CE2 1/2/0.5/0.5</b>		
BHET/IPEDA	$T_g$ [°C] (1 <sup>st</sup> cycle)	-67.0
	$T_g$ [°C] (2 <sup>nd</sup> cycle)	-58.1
	$T_m$ [°C]	85.0
	$\Delta H_m$ [J g <sup>-1</sup> ]	11.87
BHET/TBAE	$T_g$ [°C] (1 <sup>st</sup> cycle)	-66.6
	$T_g$ [°C] (2 <sup>nd</sup> cycle)	-56.7
	$T_m$ [°C]	94.7
	$\Delta H_m$ [J g <sup>-1</sup> ]	13.29
<b>Reference materials:<sup>§</sup></b>		
BHET-P	$T_g$ [°C]	-66.2
	$T_m$ [°C]	55.1 / 108.7
	$\Delta H_m$ [J g <sup>-1</sup> ]	34.7
Pellethane	$T_g$ [°C]	-46.1
	$T_m$ [°C]	68.9 / 160.2
	$\Delta H_m$ [J g <sup>-1</sup> ]	5.1

\*overlapping melting peaks

# no  $T_g$  found

§ reference values taken from Ehrmann (2020), page 110<sup>112</sup>

The thermal properties of the polymers analyzed with DSC show expected behavior (exact measurement curves are can be found in the Appendix under “DSC measurement curves”):

For all polymers with pTHF as soft-block, the  $T_g$  stays in a range of around -65 to -55 °C, which is comparable to the reference polymers BHET-P (also shown in Table 15), which has the composition pTHF-HMDI-BHET 1:2:1, with the same macrodiol pTHF and differences in the hard block without having hindered urea bonds, and slightly lower compared to the commercial polymer Pellethane.

With changes in the macrodiol, the glass transition temperature also shifts to other temperature values. For the polymers with pHMC as macrodiol, it falls into a range of around – 30 °C, for polymers with poly(caprolactone) as macrodiols, the  $T_g$  seems to depend on the molecular

weight of the poly(caprolactone) used as prepolymer with around  $-54\text{ }^{\circ}\text{C}$  for pCL2000 and around  $-27$  to  $-16\text{ }^{\circ}\text{C}$  for pCL530.

The melting behavior of the polymers also shows interesting results: One melting point in a range of around  $70.9\text{ }^{\circ}\text{C}$  (BHPC/TBEDA) to  $105.2\text{ }^{\circ}\text{C}$  (pHMC/HMDI) is present for all polymers except pHMC/H12MDI and can be attributed to the melting of hard-blocks in the polymer structure. However, in the polymers pHMC/HMDI, pHMC/H12MDI, and pCL2000, additional melting peaks at lower temperatures can be seen at around  $50\text{ }^{\circ}\text{C}$ . This melting behavior could indicate additional chain interaction *via* hydrogen bonding in the soft blocks between the carbonate moieties (pHMC polymers) or ester moieties (pCL2000), which would hinder the flexibility of these chains and therefore change the mechanical properties dramatically towards stiffer materials. Interestingly, no additional melting peak was found for the polymer with pCL530 as soft-block. One possible explanation could be the shorter length of the soft-blocks between the hard-blocks: in long pCL soft-block chains, certain sections of these chains could align and form several hydrogen bonds in between, which melt at low temperatures. With more hard-blocks, the structure is dominated by these blocks, and the probability that the soft-blocks between can align and form physical crosslinking *via* hydrogen bonding is lower.

While these results allow no direct conclusions to be drawn towards the mechanism of self-reinforcement, a prediction of mechanical properties can be made: With the additional melting peaks in the polymers pHMC/HMDI, pHMC/H12MDI and pCL2000 and the resulting conclusion of additional more ordered domains, materials from these polymers should be stiffer.

### 2.3.2 Thermal stability *via* TGA

The thermal stability of the thermoplastic poly(urethane/urea) elastomers (as bulk material) was analyzed using a standalone TGA device. Due to the limited availability of the device, again, only promising materials were analyzed, which had not been measured in previous works.

For TGA measurements, two different temperature cycles were chosen. With the first heating cycle, the dryness of the samples was judged before determining the mass loss steps with a separate measurement following the second temperature cycle. In the first cycle starting at 30 °C, a temperature plateau at 150 °C was reached with a temperature ramp of 10 °C/min, held for 1 minute before cooling down back to 30 °C with -5 °C/min. After an isothermal step at this temperature for 2 min, the sample was heated to 500 °C with a rate of 10 °C/min, leading to nearly complete thermal decomposition. Since these measurements showed that all samples were sufficiently dry, a second measurement for each polymer was done with a simpler cycle starting isothermal at 30 °C for 1 min and heating up to 500 °C without a temperature plateau with a rate of 10 °C/min. The curves of the measurements following the second heating cycle can be seen in Figure 21 and the numerical results in Table 16.

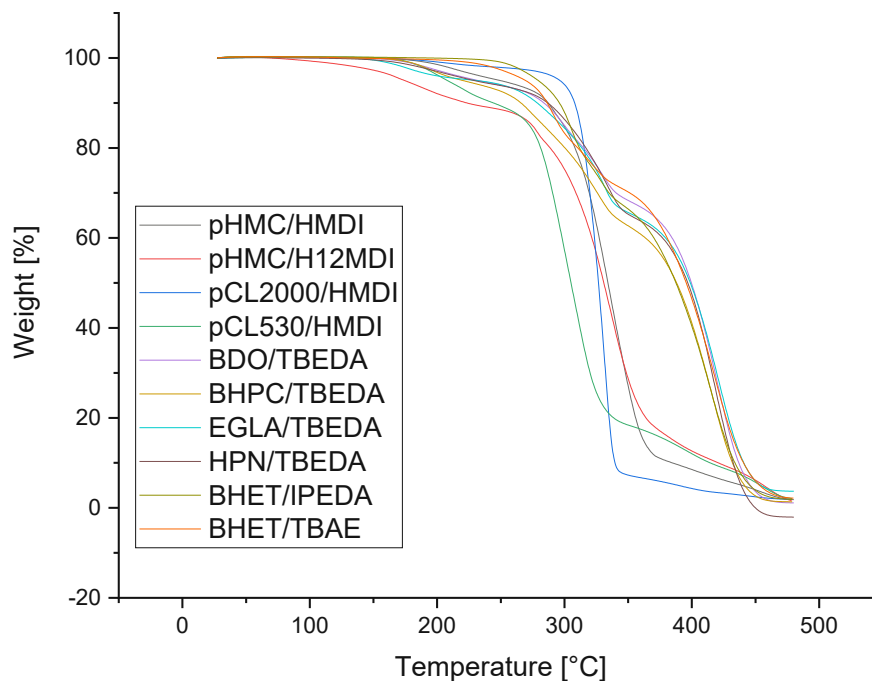


Figure 21: TGA curves of all measured polymers (second heating cycle)



Table 16: Results of the TGA measurements for all tested polymers

Polymer	onset temperature [°C]	mass change [%]	residual mass [%]
<b>Changes in the chain extender ratio for the stoichiometry pTHF/HMDI/BHET/TBEDA 1/2/X/(1-X)</b>			
BHET/TBEDA 50/50 <sup>§</sup>	111	-4.37	95.63
	276	-25.8	69.83
	377	-66.86	2.97
BHET/TBEDA 75/25 <sup>§</sup>	274	-27.48	72.52
	377	-65.77	6.75
BHET/TBEDA 25/75 <sup>§</sup>	170	-9.81	90.19
	291	-21.74	68.45
	383	-66.40	2.05
<b>Changes in the macrodiol (and diisocyanate) for the stoichiometry macrodiol/diisocyanate/BHET/TBEDA 1/2/0.5/0.5</b>			
pHMC/HMDI	185	-5.16	94.9
	308	-83.97	10.93
	402	-9.11	1.82
pHMC/H12MDI	154	-9.42	89.92
	305	-77.72	12.20
	494	-10.60	1.60
pCL2000/HMDI	169	-2.85	97.32
	315	-94.82	2.44
pCL530/HMDI	175	-10.18	90.08
	282	-71.60	18.27
	375	-15.07	3.16
<b>Changes in the first chain extender for the stoichiometry pTHF/HMDI/CE1/TBEDA 1/2/0.5/0.5</b>			
BDO/TBEDA	168	-6.75	93.32
	291	-25.84	67.48
	393	-66.27	1.21
BHPC/TBEDA	175	-6.00	94.20
	283	-31.95	62.26
	390	-60.60	1.51
EGLA/TBEDA	148	-4.47	95.70
	293	-29.80	65.89
	392	-62.24	3.65
HPN/TBEDA	161	-5.50	94.48
	298	-30.16	64.31
	393	-61.37	2.94

**Continuation of Table 16**

Polymer	onset temperature [°C]	mass change [%]	residual mass [%]
<b>Changes in the second chain extender for the stoichiometry pTHF/HMDI/BHET/CE2 1/2/0.5/0.5</b>			
BHET/IPEDA	195	-34.02	66.20
	392	-64.17	1.92
BHET/TBAE	269	-18.47	81.74
	314	-12.47	69.00
	401	-66.66	2.16
<b>Reference materials</b>			
BHET-P <sup>§</sup>	285	-3.9	96.1
Pellethane <sup>§</sup>	274	-3.5	96.5

<sup>§</sup> reference values taken from Ehrmann (2020), page 114 and A39-A40<sup>112</sup>

Although these measurements were conducted with bulk samples, judging by the percentual mass changes with regards to the known composition of the polymers, an essential hint regarding self-reinforcing can be drawn: All polymers with the exception of BHET/IPEDA 50/50 and BHET/TBAE 50/50 show a first mass loss already at relatively low temperatures of around 155 – 185 °C. As the only polymers not showing this step do not contain the monomer TBEDA and the mass change is correlating with the mass percentage of TBEDA in these polymers, the lability of the hindered urea bonds coming from this monomer can be seen under thermal stress indicating similar behavior in all of these polymers. It is reasonable to assume that this degradation step is linked to a thermal cleavage of the hindered urea bonds and the following loss of the split-off TBEDA monomer. For polymers not containing the TBEDA moiety, this first degradation step is shifted to higher temperatures with 195 °C for the IPEDA variant and 269 °C for the TBAE variant. This can be easily explained: for IPEDA, the destabilization of the hindered urea bond is simply lower, making the bond more stable before breaking at higher temperatures. Although this measurement is only indicating lower reactivity of hindered urea bonds with isopropyl substituents in regards to thermal cleavage, a transfer of this lower reactivity for self-reinforcement in aqueous media seems plausible. This could either be in the form of slower self-reinforcement at the same temperature or in the need for higher temperatures or increased time periods to achieve the same degree of self-reinforcement. Also, with the shift to higher temperatures for this step in the polymer, the determination of the

starting and end point proves to be difficult, resulting in a merge with the next degradation step. For TBAE, the hindered urea bond has the same steric hindrance as TBEDA, but the cleavage can only happen at one side, therefore a complete cleavage at the same lower temperature as polymers containing TBEDA is prevented. This also means that the vast majority of TBAE monomers have to be part of the chain, with no or only very few TBAE monomers being chain endgroups connected through a HUB moiety. Otherwise, a smaller but significant degradation step with a lower onset would also be visible for this polymer.

The following degradation steps are then traced back to the degradation of macrodiols and the remaining hard blocks. For polymers with pHMC as macrodiol, the next step at 305 – 308 °C is credited to the degradation of its macrodiol, losing about 80 % of total mass before a final degradation happens at 402 °C or 494 °C depending on diisocyanate.

For polymers with pCL as macrodiol, the first degradation step comes from the TBEDA monomer; afterward, the pCL block degrades, starting at 315 °C (for pCL2000) and 285 °C (for pCL530), respectively. For pCL530, an intermediate step in this second degradation was determined at 375 °C, which was far less prominent in pCL2000 and could therefore not be determined precisely.

## 2.4 Mechanical properties

The mechanical properties of TPUU are analyzed through tensile testing of polymer films. These films were prepared by the already established solution casting method. Afterwards, an additional preconditioning step is done to trigger the self-reinforcement. The influence of this effect on the mechanical properties is then determined by the tensile tests.

### 2.4.1 Preparation of films for tensile testing

#### *Solution casting method*

For the tensile tests, polymer films were prepared following a standard solution casting method using polymer solutions with a concentration of  $0.1 \text{ g mL}^{-1}$  polymer in 1,1,1,3,3,3-hexafluoroisopropanol (HFIP). This was done by dissolving 0.5 g polymer in 5 mL solvent under stirring at  $40 - 50 \text{ }^\circ\text{C}$  until the polymer was fully dissolved. These viscous polymer solutions were then poured into Teflon molds, which were kept under reverse funnels to prevent contamination during the drying of the films. The volatile solvent evaporated overnight under ambient conditions leaving the desired polymer films.

#### *Conditioning of films*

After removal from the molds, these films were cut in half, with one half being stored under dry conditions in a desiccator, the other half was stored in porcelain dishes submerged in deionized water for different time periods (1 day (= 24 hours), seven days and 28 days). To prevent the polymer films from floating to the surface and therefore being only partially in contact with water, they were weighed down. Optical differences in the films were already visible after several hours: the transparent films often turned white and opaque under water. However, this change was often not permanent and after drying, the films often partially or entirely reversed to their initial appearance.

During the conditioning, the pH values were also monitored. However, due to the very low ionic strength of the deionized water in which the films were stored, the measurement times of the pH-values using a pH-electrode were very high, and the precision was rather poor. Also, during conditioning, several opposite reactions are at work, with the hydrolysis of HUBs releasing new amine end groups pushing the pH towards basic values. In contrast, the hydrolysis of free isocyanates releases  $\text{CO}_2$ , pushing back towards a slightly acidic milieu leading to an erratic pH curve over longer periods.

Therefore, no exact curves could be measured. At the same time, no strong trends could be seen, indicating a relatively constant aqueous milieu. If this should be further investigated, more standardized methods must be developed with exact test specimens and volumes to ensure equal surface areas in well-defined amounts of deionized water. To decrease the measurement times and increase precision, a neutral salt should also be added to increase the ionic strength of the liquid. This, however, may be counterproductive for evaluating the self-reinforcing effect since difficulties with salt removal may lead to weakened hydrogen bonding.

While monitoring the pH values shows no clear trends, it can be handy to recognize degradation behavior during longer incubation periods. Here, after hydrolysis of most isocyanates from HUBs to amines and no subsequent reaction to close the open chain links, the pH should change to a noticeably basic value. With a maximum incubation period of 28 days, such behavior was not seen in any polymer, though, which corroborates the suspicion that only a fraction of the HUBs engages in self-strengthening, while many HUBs remain within the material.

## 2.4.2 Tensile tests

In order to test the mechanical properties of the polymer films, dog-bone shaped test specimens were punched out and tested on a universal testing machine (Zwick 050) until material failure, while recording stress-strain curves and extracting Young's modulus  $E$ , ultimate tensile strength  $UTS/\sigma_B$  and elongation at break  $\epsilon_B$ , which are defined by Equation 7 and 8.

$$\sigma = \frac{F}{A} \quad (7)$$

$\sigma$	tensile stress [MPa]
$F$	tensile force [N]
$A$	initial cross-section [mm <sup>2</sup> ]

$$\epsilon = \frac{\Delta L}{L_0} \cdot 100 \% \quad (8)$$

$\epsilon$	tensile strain [%]
$\Delta L$	elongation [mm]
$L_0$	initial length [mm]

For clarity, the results of the tensile tests are presented in two different ways. At first, the changes in each individual thermoplastic poly(urethane/urea) elastomer are shown by comparing the mechanical properties of the films of every single polymer after dry storage and different incubation times. Then a comparison of the different polymer compositions is made to show how each substitution of a monomer changed the properties of the material.

The TPUUs are also categorized to show which part of the polymer was varied:

The first variation was done by changing the **chain extender ratio** of the TPUU with the building blocks pTHF-HMDI-BHET-TBEDA. Here, starting with a chain extender ratio of 50 % BHET, 50 % TBEDA, this was changed towards lower contents of hindered urea bonds with the chain extenders in a ratio of 75 % BHET to 25 % TBEDA and then with more HUBs with a content of 25 % BHET to 75 % TBEDA.

In the second variation, the **macrodiol** building block was altered so that each final polymer still has a composition with a consistent stoichiometry of macrodiol/diisocyanate/chain extender 1/chain extender 2 = 1/2/0.5/0.5, with the chain extenders being the standard BHET and TBEDA. Starting from the macrodiol poly(tetrahydrofuran) (pTHF), this was changed to poly(hexamethylene carbonate)diol (pHMC) (with a molecular weight of 1000 Da) with the diisocyanates HMDI (polymer pHMC/HMDI) and H12MDI (pHMC/H12MDI). The second different macrodiol used was poly(caprolactone)diol (pCL), which had molecular weights of 530 Da (pCL530) and 2000 Da (pCL2000) as per manufacturer specified.

The third variation was in **chain extender 1**, which has its name from the fact that it is added as the first chain extender after the formation of macrodiisocyanates. As all of these chain extenders are small diols, they react to form urethane bonds with free isocyanates groups and do not lead to the incorporation of hindered urea bonds into the final polymer.

The fourth variation then alters the **second chain extender**, which is the key monomer responsible for the incorporation of hindered urea bonds in the final polymer. Coming from the standard TBEDA, which is a symmetrical diamine with *tert-butyl* substituents on each side, this is first changed to IPEDA swapping *tert-butyl* with *isopropyl* substituents. This change should also lead to a polymer with hindered urea bonds, although the different destabilizing groups on the urea bond can alter the reactivity. The other variation in chain extender 2 is from a symmetrical diamine to an amino alcohol with the usage of *tert-butyl* amino ethanol. With this monomer, the destabilizing substituent at the hindered urea bond stays the same, allowing a bond cleavage under the same conditions as with TBEDA. However, this cleavage is only on one side, as the other side is bound by a stable urethane group.

Finally, two **reference materials** were also tested under the same conditions. Pellethane is a commercially available product from Lubrizol, consisting of pTHF-MDI-BDO and a polyurethane without hindered urea bonds made from pTHF-HMDI-BHET (“BHET-P”).

## 2.4.3 Results of tensile tests

### 2.4.3.1 Change in chain extender ratio between BHET and TBEDA

For the polymer **pTHF-HMDI-BHET-TBEDA 50/50**, conditioning was done for the three time periods of one day (=24 hours), seven days and 28 days at room temperature. As it was a repetition of the synthesis by Ehrmann,<sup>110</sup> a comparison can also be done, which shows very similar results for Young's modulus and elongation at break. The ultimate tensile strength is also similar; however, several films underperformed compared to the previous study.

In terms of self-reinforcement, similar results can be seen (Figure 22). While the ultimate tensile strength (UTS) of the conditioned film halves with a preconditioning period of 7 days and 28 days increased significantly compared to the halves stored under dry conditions, Young's modulus increases to a lesser degree and only after 28 days are statistically significant increase can be measured. This preconditioning time period was not studied before, but the slow continuation of hardening makes sense with the assumed improvement in the hydrogen bonding of hard blocks. To discuss the changes happening because of precondition more easily, a look at the relative changes can be done as both halves of the film tested for 24 h preconditioning time performed significantly better than the comparable films. In order to do this, the relative change in each parameter was calculated using Equation 9.

$$\text{rel. change} = \frac{p_{\text{prec.}} - p_{\text{unprec.}}}{p_{\text{unprec.}}} \cdot 100 \% \quad (9)$$

rel. change	relative change in mechanical parameter p (Young's modulus, UTS, elongation at break) between two film halves of the same film (preconditioned/unpreconditioned) [%]
$p_{\text{prec.}}$	tested parameter for the preconditioned half [MPa for Young's modulus and UTS, % for elongation at break]
$p_{\text{unprec.}}$	tested parameter for the unpreconditioned half [MPa for Young's modulus and UTS, % for elongation at break]

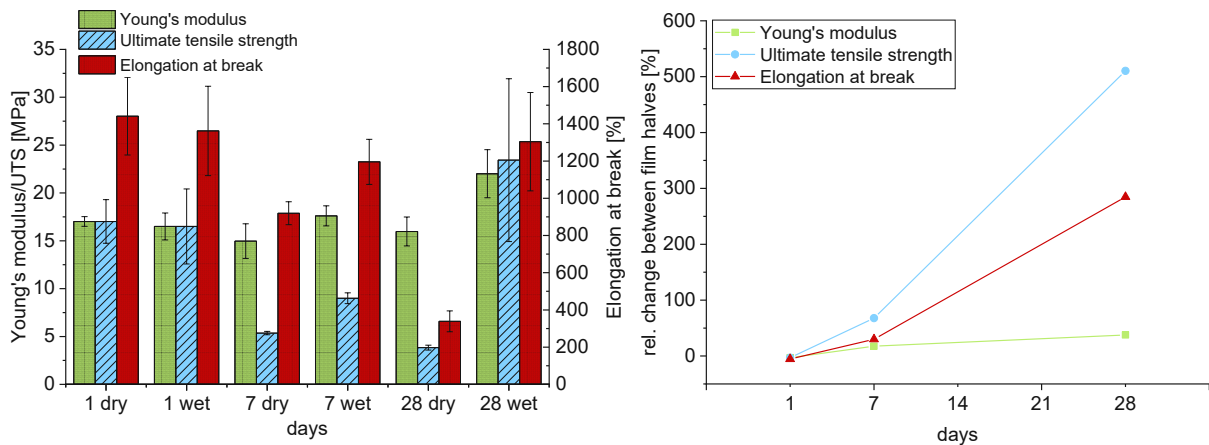


Figure 22: Results of the tensile tests for pTHF-HMDI-BHET-TBEDA 50/50 after different incubation periods at room temperature (absolute and relative values)

In relative changes (Figure 22, right), the transformation of the mechanical properties is even more apparent and easier to discuss. While the Young's modulus only increases slightly, the UTS and elongation at break both show positive changes to a higher degree, with the increase in elongation at break set in later and staying behind for all preconditioning times. Combining the results of all three mechanical properties, this means that this increase is different from a simple hardening of the material, which would lead to a stiff material with decreased elongation at break. Such a hardening would also be unwanted for the desired application, as the stiffness of the material should not change much to avoid problems with compliance at the tissue-graft interface. The observed change is positive on the application, though: With only slight changes in the stiffness of the material (determined by the Young's modulus) but higher tensile strength and increased elongation at break the material changes towards optimized properties on its own with an easy setup (in a separate preconditioning step) or also in the application environment after implantation in the body.

So, since this polymer is the standard polymer from which the first research combining HUBs with tissue engineering TPUUs was conducted, it was also tested after the same preconditioning times at higher temperature of 37 °C (Figure 23), which can be used to mimic the conditions in the human body more closely. This rise in temperature influences the kinetics of chemical reactions happening at the HUBs, which should be accelerated according to the Arrhenius equation.



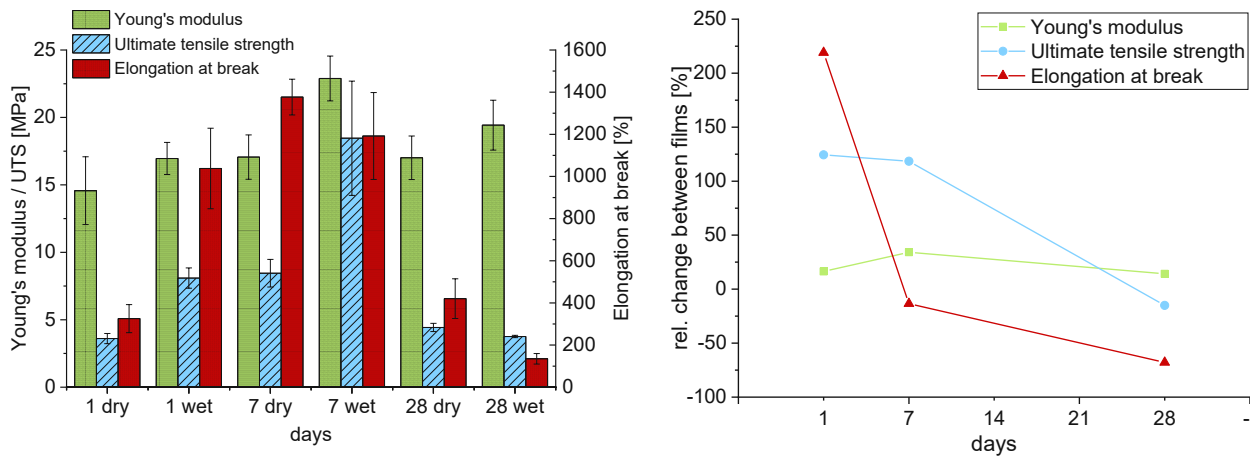


Figure 23: Results of the tensile tests for pTHF-HMDI-BHET-TBEDA 50/50 after different incubation periods at 37°C (absolute and relative values); the dry stored halves were kept at room temperature

A look at the results shows similarities to the previous results after preconditioning at room temperature: While the Young's modulus again only showed small and often non-significant changes, the UTS demonstrates a significant increase in the comparison of the film halves stored dry and preconditioned and very similar relative changes for the time periods of one and seven days. After 28 days of preconditioning, a slight decrease in this material property was measured. With the higher temperature, this behavior can be explained by the accelerated reaction rate of the self-reinforcement, which means that the maximum UTS is reached faster. However, at higher temperatures, the degradation of the material also sets in faster; and here, with the data point at 28 days, indications of a slowly starting degradation process can already be seen. However, this is only an indication as this is only a single data point and the corresponding film underperformed compared to the rest; for more statistically significant results, further tests are necessary.

For the elongation at break, the film with a seven-day preconditioning period also severely outperformed the other films. Here again, a conditioning period of one day showed a substantial increase in this parameter, whereas at seven days, it slightly decreased, and at 28 days, it decreased significantly, again indicating that the self-reinforcement is accelerated and the start of degradation of the material had already happened after 28 days.

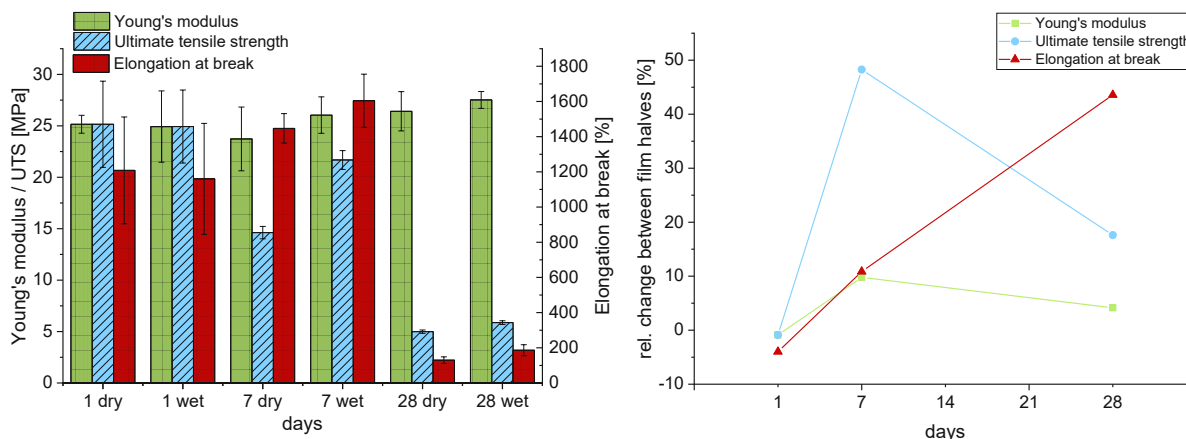


Figure 24: Results of the tensile tests for pTHF-HMDI-BHET-TBEDA 75/25 after different incubation periods at room temperature (absolute and relative values)

The second polymer with the identical monomers and different chain extender ratio was the polymer **pTHF:HMDI:BHET:TBEDA** in a ratio of 1:2:0.75:0.25, with the results of the tensile tests of this material shown in Figure 24. With the decrease in the number of HUBs in the material, self-reinforcement should also be less prominent in the results after preconditioning.

This trend can already be seen in the comparison of the Young's moduli between film (halves), which showed no increase and stayed the same before and after preconditioning (within the margin of error). For the UTS, the variance between the films is again visible. Comparing the relative changes between two film halves, after one day, the conditioning shows no difference, whereas, after seven days, a statistically significant increase has occurred. The comparison of the two halves of the polymer film conditioned for 28 days shows only a slight increase, which could mean that the self-reinforcement reached its peak between seven days and 28 days and is again declining in a similar way to the previous polymer. However, again this film was severely underperforming compared to the other films of this polymer. For the elongation at break, the films with one- and seven-days preconditioning periods showed high values. After one day, the elongation at break remains the same, while after seven days a slight, but not statistically significant increase occurs. The film conditioned for 28 days also underperforms in this parameter in both states, with dry storage and preconditioned in deionized water.

The last chain extender ratio that was tested was BHET/TBEDA 25/75, leading to a thermoplastic polyurethane/urea elastomer with a stoichiometry of **pTHF:HMDI:BHET:TBEDA 1:2:0.25:0.75**. This polymer showed worse mechanical properties than the other two chain extender ratios, which was already apparent during the synthesis due to a lower yield as well as during solvent casting, which proved to be far more complicated than with other polymers.

Here, the casted film was often gluey, and therefore the removal from the mold had to be done with additional care since the films often stuck to the mold even after complete drying and pulling the film off the mold could create defects. These worse mechanical properties can be explained by the hindrance to forming strong hydrogen bonding in the hard blocks, with the higher amount of TBEDA importing more sterically demanding *tert*-butyl substituents into the structure.

As can be seen in Figure 25 showing the results of the tensile tests, one film (preconditioning time of one day) outperformed the other two quite significantly.

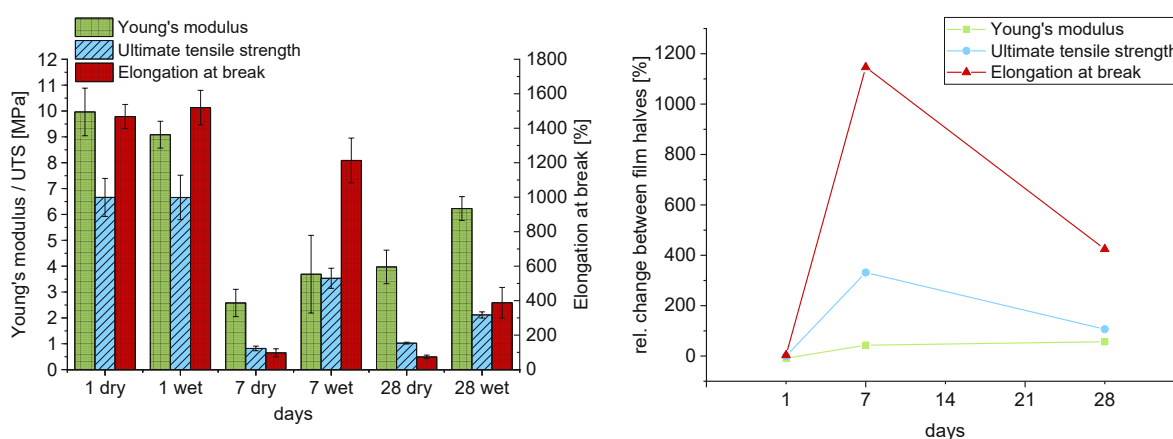


Figure 25: Results of the tensile tests for pTHF-HMDI-BHET-TBEDA 25/75 after different incubation periods at room temperature (absolute and relative values)

Regarding the Young's modulus, both halves of the film with a preconditioning period of one day showed higher values than the other films, with no significant change in between them. For the two films used for incubation periods of seven and 28 days, there are increases visible in both of them, with the increase for the seven-day film not being statistically significant, whereas the change during the 28 days incubation period is.

For the ultimate tensile strength, the first film again outperforms the other two by a significant margin, but no change between the two halves of this film can be determined. In between the film halves of incubation periods seven days and 28 days, a strong relative increase can be measured, with the increase being higher after seven days compared to 28 days, which could mean that the self-reinforced polymer is already starting to degrade by hydrolysis of further hindered urea bonds.

The same can also be said about the elongation at break. The first film outperforms the other two halves again, with no change between the halves of the film. For the film conditioned for seven days, the strongest relative increase is measured. For 28 days, the increase is also quite high, but compared to 7 days incubation period, again somewhat lower, which is in accordance with the results of the ultimate tensile strength.

After showing the influence of preconditioning on each of the individual polymers, a comparison of the three previously discussed polymers is necessary in order to evaluate the influence of the change in chain extender ratio on the material properties. To do this, representative, single films were compared to each other both in the preconditioned and unpreconditioned state. For preconditioned films, the best-achieved values of films are chosen, independent of different precondition conditions (times and temperatures). As always, the comparison is made against the first such polymer with the monomers pTHF:HMDI:BHET:TBEDA in a ratio of 1:2:0.5:0.5.

In the unpreconditioned state (shown in Figure 26), all three parameters, Young's modulus, UTS and elongation at break, increased with higher BHET contents. This behavior can be explained by the results of previous research quite easily, as these show, that the good mechanical properties of TPUU highly depend on flexible soft blocks and hard blocks with strong hydrogen bonding to physically crosslink the chains. BHET was determined as an excellent monomer to allow this behavior, whereas, with the steric hindrance of TBEDA, this wanted chain interaction can be difficult, leading to a worse influence of the hard block to achieve good mechanical properties.

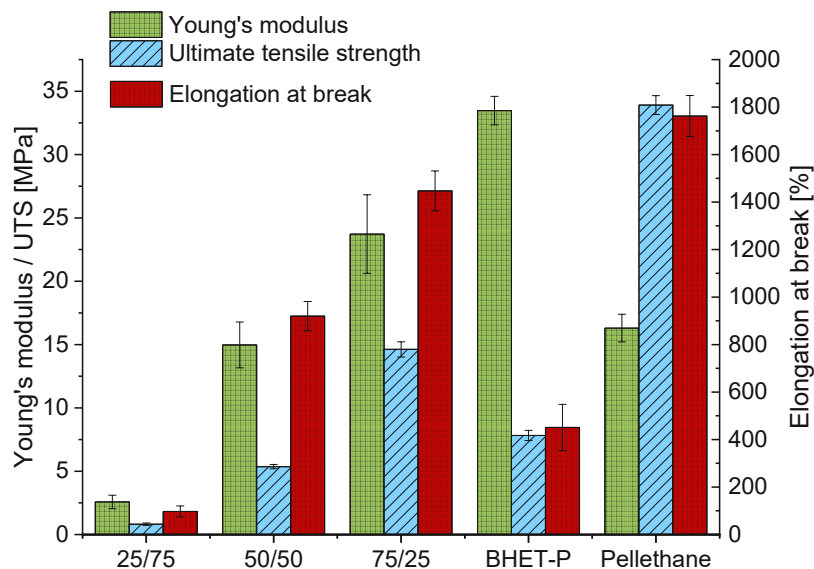


Figure 26: Comparison of Young's modulus, ultimate tensile strength and elongation at break for single unpreconditioned films of polymers with the monomers pTHF:HMDI:BHET:TBEDA with changes in the ratio of BHET:TBEDA and the reference materials BHET-P and Pellethane

The comparison of the same polymers after preconditioning (Figure 27) shows a different picture. Even though the polymer with the highest TBEDA content stayed behind the others in regards to the Young's modulus and UTS, its elongation at break rose up the other polymers, showing that the formerly poorly performing polymer becomes quite elastic. For the two other polymers with higher BHET contents, the three tested parameters are in a very similar range after starting from a different starting position. This could indicate the presence of a certain plateau of mechanical properties that can be reached in the best case depending on the monomers used. However, given the high deviations between films (which were already discussed previously) and the limited amount of testing possible in the scope of this work, such a claim cannot be proven yet and would require further investigation.

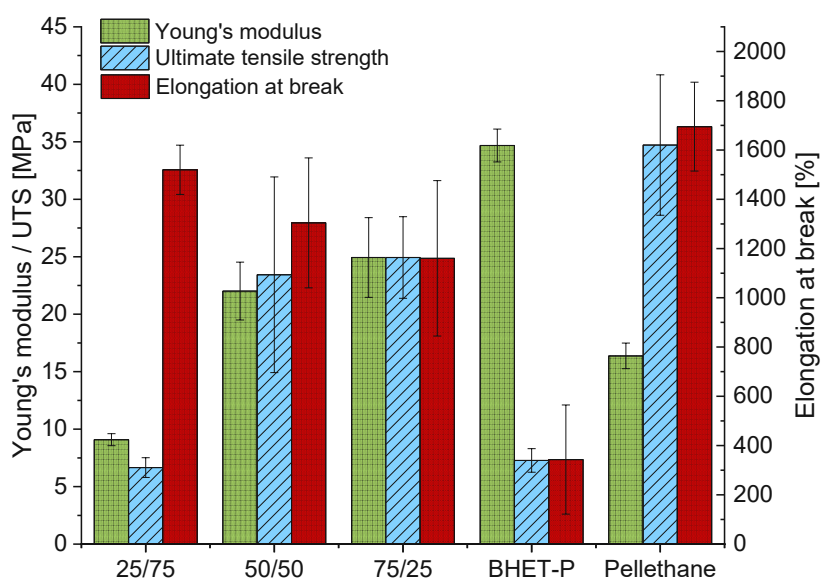


Figure 27: Comparison of Young's modulus, ultimate tensile strength and elongation at break for single preconditioned films of polymers with the monomers pTHF:HMDI:BHET:TBEDA with changes in the ratio of BHET:TBEDA and the reference materials BHET-P and Pellethane

#### 2.4.3.2 Change in macrodiol

For the change in macrodiol, pTHF is replaced with either diols of poly(hexamethylene carbonate) (pHMC) or poly(caprolactone) (pCL), which leads to a different soft block of the final material which now includes ester or carbonate groups in its chain. For reasons of commercial availability, the normally used pTHF with a molecular weight of  $1000 \text{ g mol}^{-1}$  was replaced with pHMC with a nearly identical molecular weight of  $1200 \text{ g mol}^{-1}$ ; for poly(caprolactone), this had to be changed to 530 and  $2000 \text{ g mol}^{-1}$ . This also means that for polymers with pCL as macrodiol, the soft block to hard block length changes.

Also, as an additional change, in one polymer with the macrodiol pHMC, the diisocyanate HMDI was replaced with H12MDI, which should lead to a stiffer material.

### 2.4.3.2.1 TPUU with pHMC as macrodiol

The first polymer with pHMC replacing pTHF was the TPUU with composition **pHMC:HMDI:BHET:TBEDA 1:2:0.5:0.5**, with the results of the tensile tests shown in Figure 28. For this polymer, the material hardened already after a preconditioning period of one day (shown in the increase in the Young's modulus). In the UTS, which is used to determine self-reinforcement behavior, an increase could also be observed, which manifested in a slight increase after seven days, which then became significant after 28 days preconditioning with a final UTS of 31.6 MPa. Interestingly, although the Young's modulus increased, which would correlate with hardening and therefore a loss of elasticity, such a behavior was not observed: The elongation at break remained consistently high at around 900 – 1000%, regardless of storage conditions or preconditioning times and did not change significantly between the unpreconditioned and preconditioned state. Similar to the previous results, this leads to the conclusion that the self-reinforcement is different from a simple hardening of the material, since the soft block which imports the elasticity is unaffected; only the quality of the hard blocks is improved by the self-reinforcing effect.

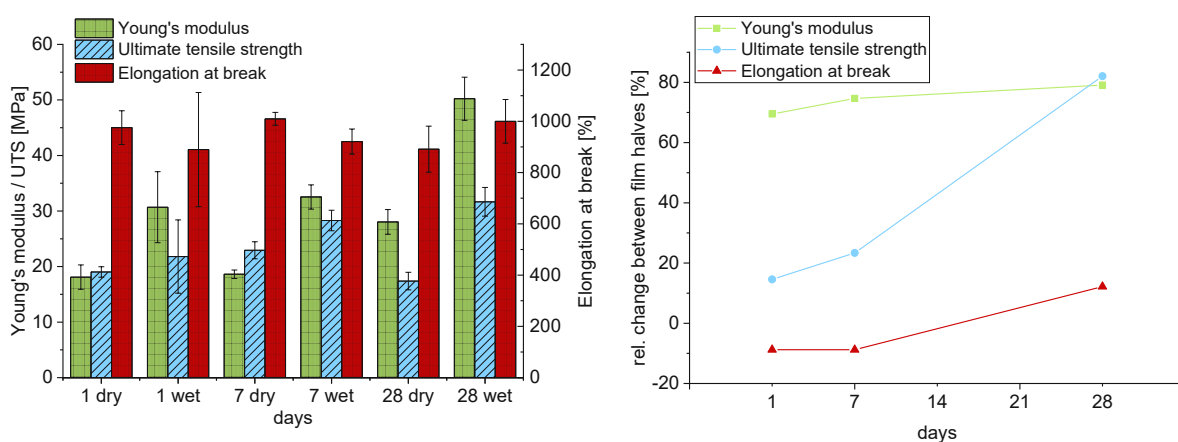


Figure 28: Results of the tensile tests for pHMC/HMDI after different incubation periods at room temperature (absolute and relative values)

The second polymer built from the macrodiol pHMC utilized H12MDI as diisocyanate, with a TPUU with the composition **pHMC:H12MDI:BHET:TBEDA 1:2:0.5:0.5** (Figure 29). This diisocyanate changed the material properties in an extreme way: As the previous DSC measurements showed, additional crystallinity was introduced into the material, which then became extremely stiff with a Young's modulus of around 200 MPa, with one film reaching even up to 350 MPa. Such high Young's moduli were not reached by similar materials of previous works,<sup>94</sup> which only showed values up to around 35 MPa in a polymer with the composition pTHF-H12MDI-BHET 1:2:1.

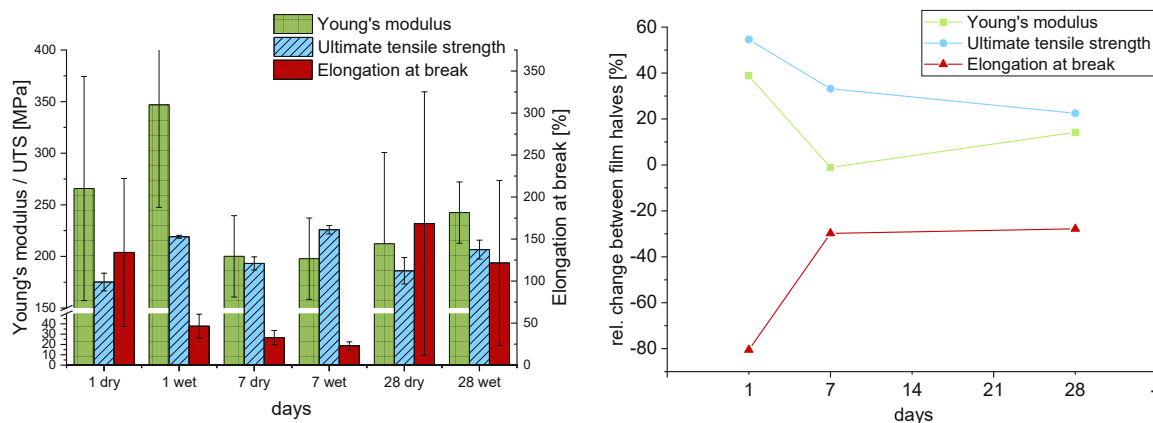


Figure 29: Results of the tensile tests for pHMC/H12MDI after different incubation periods at room temperature (absolute and relative values)

The mechanical tests of this polymer showed several changes (Figure 29): First of all, the homogeneity of the films was worse than in previous cases, which was already apparent during the solution casting process, which produced irregular films more often. This problem can also be seen by the high standard deviations between singular measurements of films with no visible defects. While the Young's modulus and elongation at break showed no statistically significant changes before and after preconditioning, the UTS improved for all time periods after preconditioning. However, the changes were only minor compared to other polymers. One possible explanation could be the high stiffness of the material, which could hinder the self-reinforcement reaction with low mobility in the hard blocks. Also, this material is not suitable for the application as a blood vessel scaffold given its high stiffness, which could lead to compliance issues.

#### 2.4.3.2.2 TPUU with pCL as macrodiol

The second different macrodiol used as a substituent for pTHF was poly(caprolactone)diol. For the polymers with this macrodiol, molecular weights of around  $530 \text{ g mol}^{-1}$  (pCL530) and  $2000 \text{ g mol}^{-1}$  (pCL2000) were used. As previously mentioned, this also means that the weight ratio of soft and hard blocks in the final thermoplastic poly(urethane/urea) elastomer is changed parallel to the change in chemical properties of the soft block from pTHF to pCL.



As shown in the results of the tensile tests (Figure 30) for the polymer with pCL530 as macrodiol (**pCL530:HMDI:BHET:TBEDA 1:2:0.5:0.5**), the Young's modulus is slightly higher than that of other TPUUs with the exception of the pHMC/H12MDI, which can be attributed to both the higher hard block content and the possibility of interaction in the soft block with the ester groups in the chain introducing unwanted semi crystalline behavior.<sup>124</sup> Similar to previously discussed polymers, the tensile tests after preconditioning also showed a slight increase in the Young's modulus, which can be traced back to the improvements in the hydrogen bonding in the hard blocks. Regarding the UTS, an increase after preconditioning in water can also be seen, which is lower than in previously discussed polymers. This can be explained in two ways: either the self-reinforcement is weaker in this polymer or happening slower than in the other polymer compositions, meaning that it is still incomplete after 28 days of preconditioning. However, although the change is not as prominent as in other compositions, it is still statistically significant.

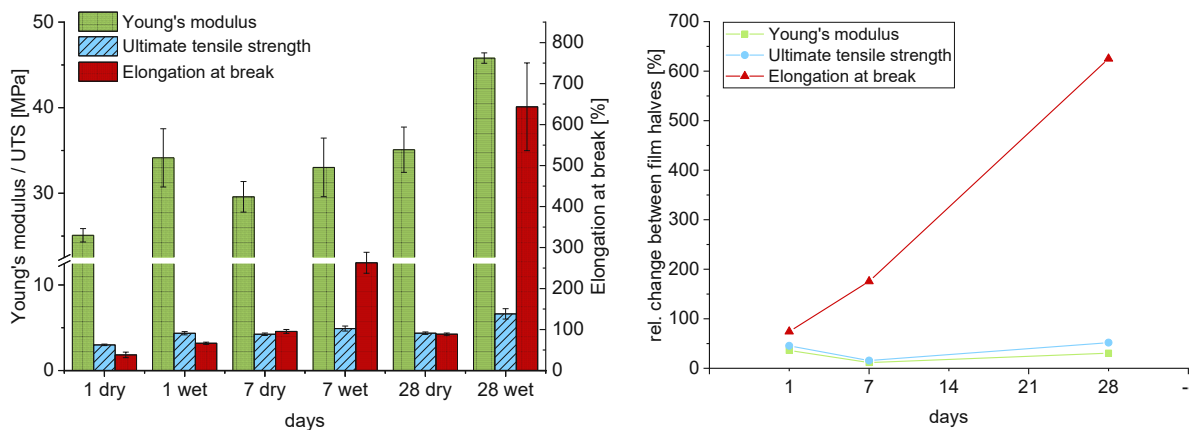


Figure 30: Results of the tensile tests for pCL530 after different incubation periods at room temperature (absolute and relative values)

While the impact of self-reinforcement on the UTS was relatively low, the change in elongation at the break of the pCL530-TPUU after preconditioning happens to a higher degree. With changes already visible after one day, the increase rises already after seven days, and after 28 days, an elongation at break of roughly 650 % of the initial value is reached. With the high difference between seven days and 28 days, again a slower self-reinforcement than in the other polymers may be likely and even longer preconditioning periods could be needed to reach the full potential of the material, presumably, due to the more rigid matrix.



The last polymer with a change in the macrodiol was the TPUU with the stoichiometry of **pCL2000:HMDI:BHET:TBEDA 1:2:0.5:0.5**, with its performance in the tensile tests shown in Figure 31. This polymer had the second-highest Young's modulus of the tested polymers at around 60 – 100 MPa, with slight variance between the films, which can again be explained by unwanted, additional hydrogen bonding in the soft block, which leads to a stiffening of the material. An increase in Young's modulus linked to the preconditioning was only determined for the sample preconditioned for seven days. While the UTS increases with preconditioning for all tested time periods, this increase is again relatively low and nearly the same between the preconditioning times of one and seven days before it rises after 28 days. Again, as with the polymer with pCL530 as macrodiol, this could indicate that the self-reinforcement of this polymer happens much slower due to the stiffer matrix, and longer preconditioning periods could be necessary to reach the full potential as the increase shows a linear behavior in the relative comparison with no obvious plateau being reached. Also, the maximum increase achievable with self-reinforcement should be lower in this material, as the longer soft-block length also leads to a lower number of HUB in the final polymer, which induce self-reinforcement.

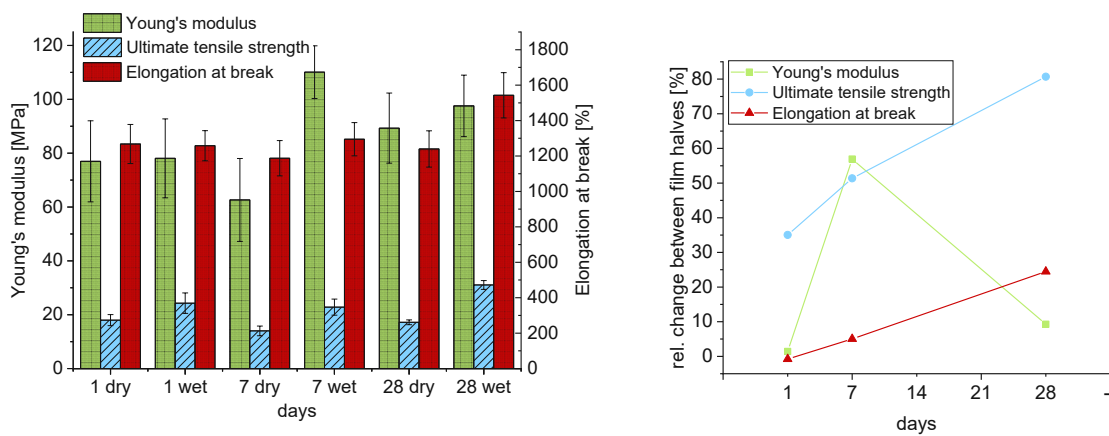


Figure 31: Results of the tensile tests for pCL2000 after different incubation periods at room temperature (absolute and relative values)

Here also, the elongation at break stayed nearly the same after preconditioning times of one day and seven days and increased only slightly after 28 days. All films also showed quite high values, around 1200 % for halves stored under dry conditions and incubation periods of one day and seven days and 1500 % after conditioning for 28 days.

The comparison of polymers with a change in the macrodiol is also necessary. While the ratio of chain extenders only showed small changes, a change in the macrodiol showed greater influence (Figure 32). While the change to pHMC showed similar results regarding the Young's modulus and elongation at break in the unconditioned state, the UTS increased slightly. With the additional second change of the diisocyanate HMDI to H12MDI, the material properties are, however, entirely different: The Young's modulus rose to about 200 MPa, which is an increase to over tenfold, which had not been achieved in previous works with similar polymers.<sup>94</sup> While the ultimate tensile strength remained in the same range, the elongation at break is drastically decreased, further demonstrating the complete change of a flexible soft material to a rigid polymer; an alteration in material properties which could already be anticipated from the change in crystallinity determined with DSC analysis. This also means that this monomer combination is not suitable for vascular prostheses. For polymers using poly(caprolactone)diol as macrodiol, a similar change happens to varying degrees, which was again in line with the results of the DSC analysis. With a molecular weight of around 2000 Da for the macrodiol, the material properties fall in-between the standard polymer using pTHF and the variation with pHMC and H12MDI as diisocyanate. While the Young's modulus rose to around 75 MPa, the material still stays flexible with very high elongation at break. For the polymer with poly(caprolactone)diol with molecular weight around 530 Da as starting point, the Young's modulus increased noticeably, however less than in the other variations. Also, both ultimate tensile strength and elongation at break were rather low.

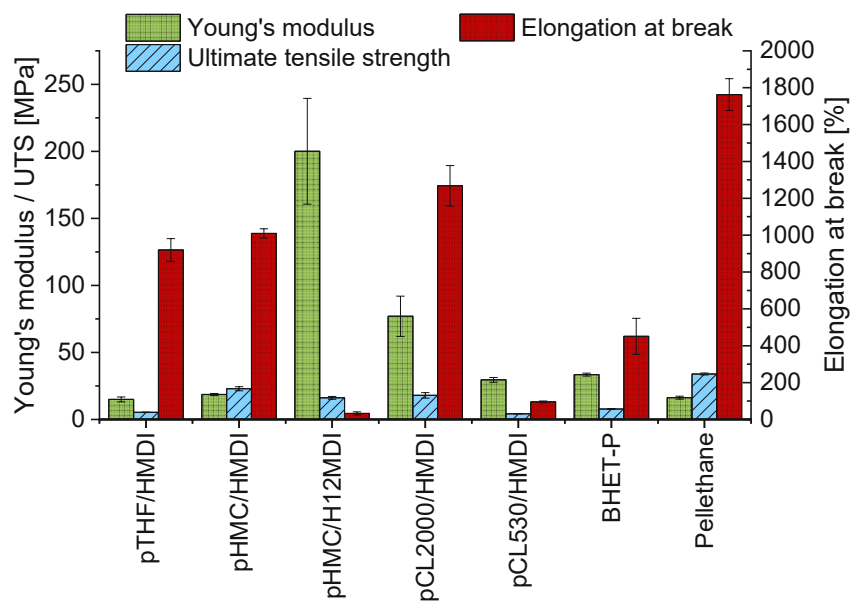


Figure 32: Comparison of Young's modulus, ultimate tensile strength and elongation at break for single unpreconditioned films of polymers with changed macrodiols for a final material of macrodiol:HMDI:BHET:TBEDA 1:2:0.5:0.5 and the reference materials BHET-P and Pellethane

After preconditioning, the previously discussed material changes after macrodiol substitution remain intact (Figure 33). Interestingly, while improvements in the ultimate tensile strength are visible for all polymers, the increase varies between the different polymers, indicating a different self-reinforcement behavior depending on the polymer. While the self-reinforcement leads to higher UTS with similar elongation at break for some materials, others show only slight improvements in the UTS while becoming more elastic with higher elongation at break.

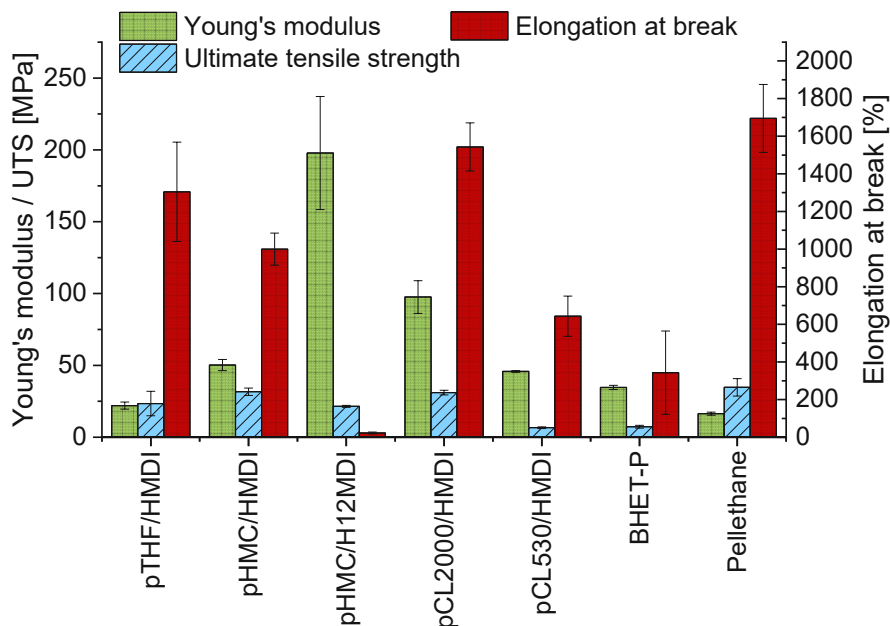


Figure 33: Comparison of Young's modulus, ultimate tensile strength and elongation at break for single preconditioned films of polymers with changed macrodiols for a final material of macrodiol:HMDI:TBEDA 1:2:0.5:0.5 and the reference materials BHET-P and Pellethane

#### 2.4.3.3 Change in the first chain extender

The first TPUU with a changed first chain extender was the polymer BDO/TBEDA 50/50 in which the first chain extender bis-(2-hydroxyethyl) terephthalate was replaced with 1,4-butanediol (BDO) to yield a TPUU with a composition of **pTHF:HMDI:BDO:TBEDA 1:2:0.5:0.5**. The tensile tests of this polymer showed Young's moduli in a range between 15 – 25 MPa depending on the film. Comparison of the dry stored and preconditioned film halves of each film showed a slight and rather constant increase in this parameter for preconditioning times, as shown in Figure 34.

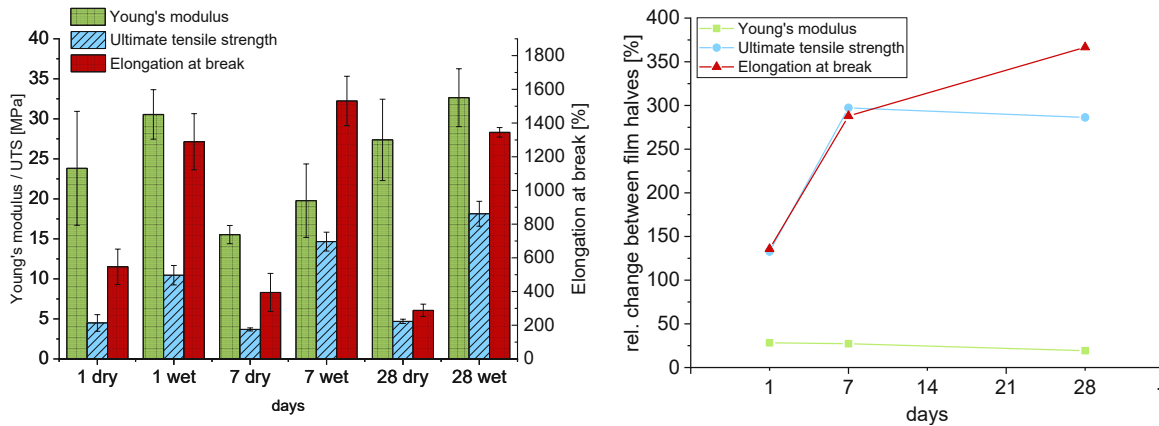


Figure 34: Results of the tensile tests for BDO/TBEDA 50/50 after different incubation periods at room temperature (absolute and relative values)

The UTS of the different films showed nearly no difference in the halves stored under dry conditions speaking in favor of good film reproducibility for this particular polymer. After preconditioning, an increase can be seen, which already starts after a preconditioning period of one day. After this time period, an increase of + 130 % occurs, which rises to + 285 % after 28 days, and the comparison of relative changes indicates that a plateau has been reached.

For the elongation at break, this increase also happens immediately after preconditioning for one day. In contrast to the other parameters, however, this then stays around the same for the films preconditioned for seven days and 28 days at a high value of around 1400 – 1500 %.

In the second polymer with a change in chain extender 1, the cleavable chain extender bis-(hydroxypropyl)carbonate (BHPC) was used in a ratio BHPC/TBEDA 50/50 for a TPUU with composition **pTHF:HMDI:BHPC:TBEDA 1:2:0.5:0.5**. Since this polymer had higher molecular weight at around 60 kDa and since it was known that polymers with BHPC as single chain extenders have good mechanical properties,<sup>96</sup> the self-reinforcement was tested after preconditioning both at room temperature and 37 °C.

For the preconditioning at room temperature, the tensile tests show no significant changes in the Young's modulus regardless if stored dry or incubated for different time periods. The ultimate tensile strength, however, increases tremendously. Starting slowly at 2.5 -3.7 MPa, slight changes are already visible after one day, which increases after seven days before reaching around 15 MPa after 28 days, which is equal to a relative increase of + 550 % (as can be seen in Figure 35).

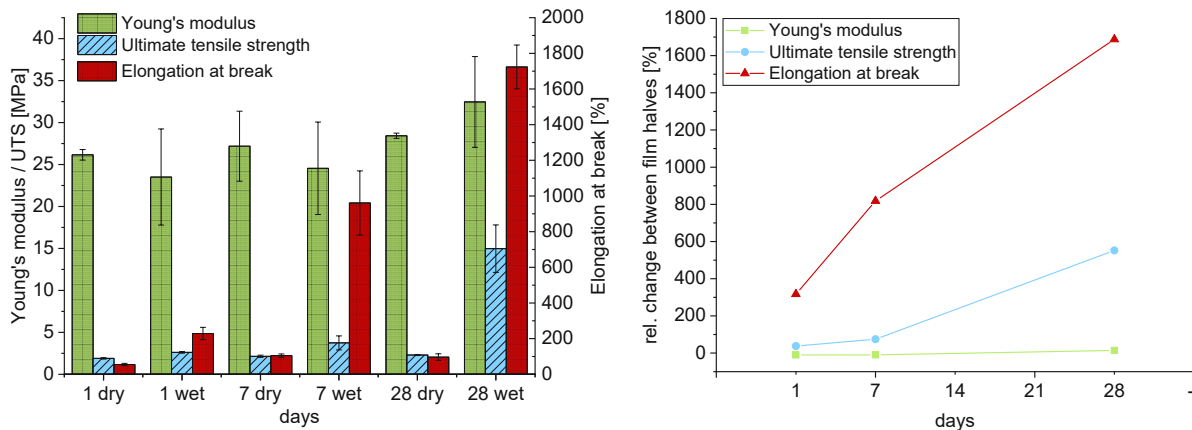


Figure 35: Results of the tensile tests for BHPC/TBEDA 50/50 after different incubation periods at room temperature (absolute and relative values)

The elongation at break shows a similar picture with even more significant relative changes between film halves. Starting with elongation at breaks of around 60 – 100 % (absolute value) for dry stored halves, this property increases to 230 % after 24 hours, 960 % after seven days and 1720 % after 28 days, which was the highest elongation at break achieved for all tested polymers.

The conditioning at elevated temperatures of 37 °C showed very similar results (Figure 36). Here, the Young's modulus slightly increases, and the ultimate tensile strength reaches 20 MPa after 28 days of preconditioning. With higher temperatures, the self-reinforcing effect is again accelerated: The UTS of the film half conditioned for 24 hours at 37 °C is already higher than the film half conditioned for seven days at room temperature. Also, the UTS of the film half conditioned for seven days at 37 °C is also slightly higher than 28 days at room temperature and nearly as high as the one at 28 days/37 °C.

The elongation at break also increases very fast during conditioning at 37 °C. Already after preconditioning for one day, this parameter rises up to around 1400 % before staying at around 1600 – 1800 % after seven and 28 days preconditioning periods.

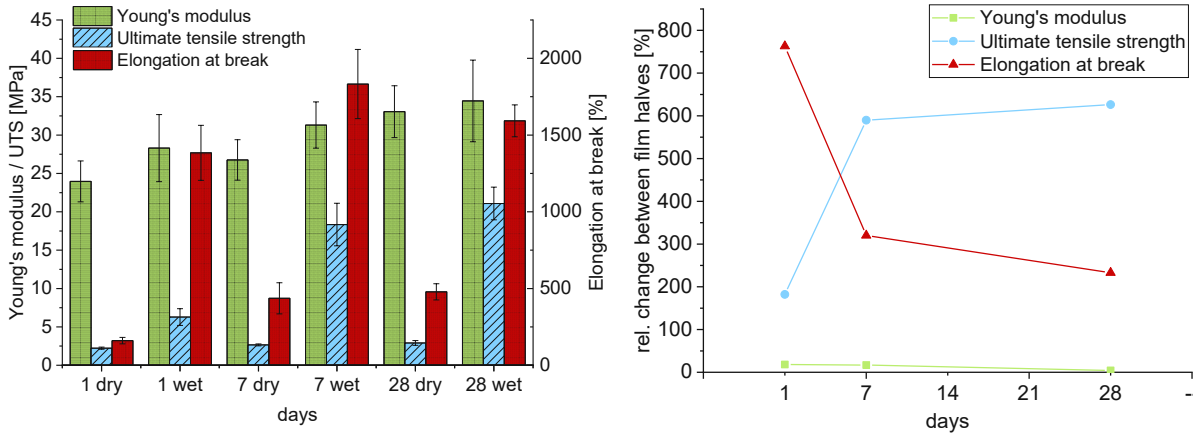


Figure 36: Results of the tensile tests for BHPC/TBEDA 50/50 after different incubation periods at 37°C (absolute and relative values); the dry stored halves were kept at room temperature

With a change in the first chain extender, the differences between polymers in the unconditioned state are less prominent compared to other substitutions, which can be seen in Figure 37. For both changed polymers, the Young's modulus increased and the elongation at break decreased with the monomer substitution indicating a slight shift towards a stiffer material compared to the benchmark TPUU pTHF:HMDI:BHET:TBEDA 1:2:0.5:05. Also, the TPUU with BHPC as chain extender showed a slightly lower UTS in this state.

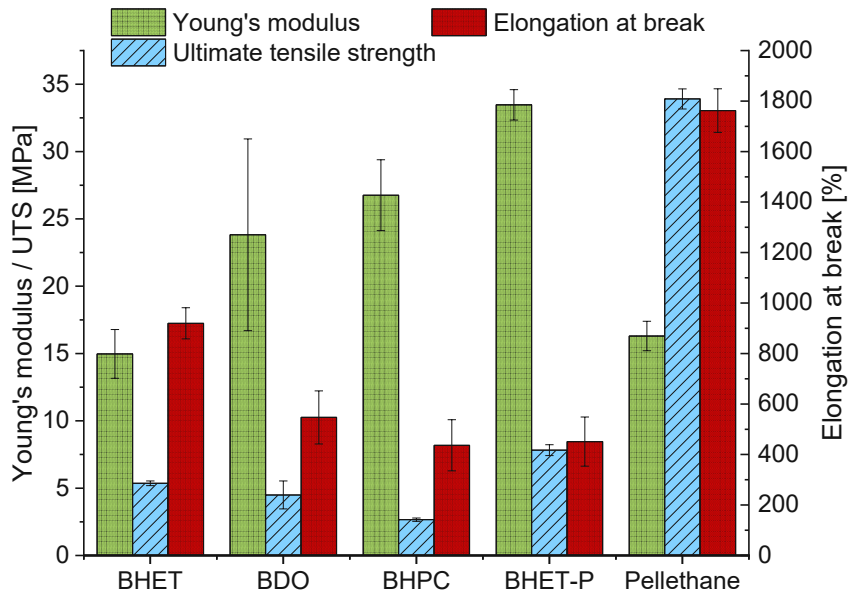


Figure 37: Comparison of Young's modulus, ultimate tensile strength and elongation at break for single unpreconditioned films of polymers with changed chain extender 1 for a final material of pTHF:HMDI:CE1:TBEDA 1:2:0.5:0.5 and the reference materials BHET-P and Pellethane

A comparison of the best-achieved results after preconditioning (Figure 38) of these polymers shows similarities to the unconditioned state. For the Young's modulus, the values of polymers with BDO and BHPC are still higher compared to the polymer with BHET. For the UTS, the BHPC-polymer showed a stronger increase and catches up to the other two polymers, with all of them having very similar results. The same can be said about the elongation at break, which is very comparable between polymers and often in the margin of error given by the standard deviation.

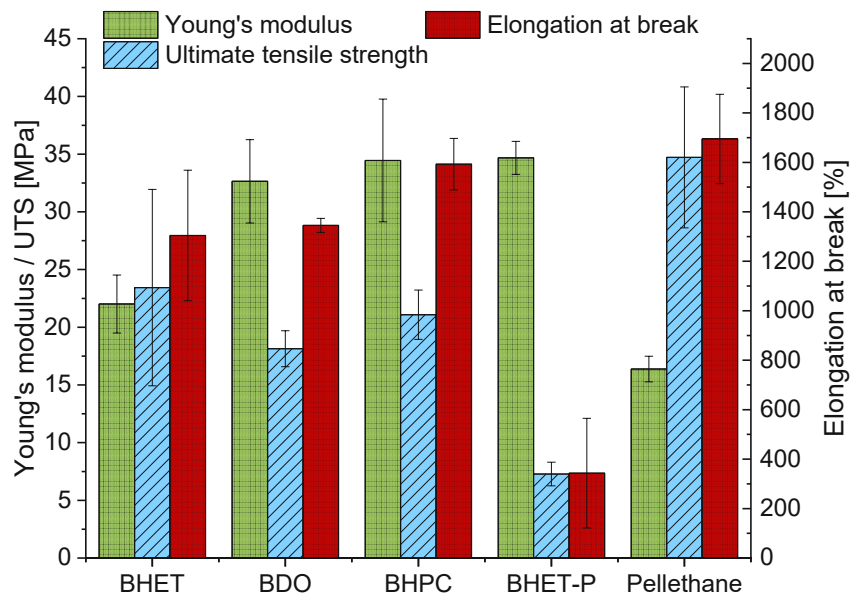


Figure 38: Comparison of Young's modulus, ultimate tensile strength and elongation at break for single preconditioned films of polymers with changed chain extender 1 for a final material of pTHF:HMDI:CE1:TBEDA 1:2:0.5:0.5 and the reference materials BHET-P and Pellethane

#### 2.4.3.4 Change in the second chain extender

In order to show if other chain extenders with sterically hindered amines can also lead to a self-reinforcing effect through the reversible cleavage by destabilization of the urea bond, the chain extenders N,N'-diisopropylethylenediamine (IPEDA) and N-(*tert*)-butylaminoethanol (TBAE) were chosen to replace TBEDA in a ratio of 50/50 with BHET.

In the first TPUU with a change in the second chain extender, N,N'-di-*tert*-butylethylenediamine (TBEDA) was replaced with N,N'-diisopropylethylenediamine (IPEDA) for the TPUU **pTHF:HMDI:BHET:IPEDA 1:2:0.5:0.5**. Since preconditioning at room temperature and 37 °C showed no quantifiable self-reinforcing effect for this TPUU (results listed in the Appendix), another preconditioning study at 60 °C was done, which results are shown in Figure 39. Here, the first significant changes happen in the UTS of the material. While the Young's modulus does not change significantly, the UTS already shows a significant increase after 24 hours with 55 %, which increases after seven days to 150 % and after 28 days to 155 % compared to the film half stored under dry conditions. The only slight difference in UTS between preconditioning periods of seven and 28 days also shows that the self-reinforcement effect is happening quite fast, with the TPUU reaching its full potential between seven and 28 days preconditioning at 60 °C. Regarding the elongation at break, the polymer shows no significant increase or decrease for all incubation periods. This material property remains at very high values at roughly 1300 – 1500 %, which again shows, similarly to previous polymers, that the self-reinforcement is different from a simple hardening of the material, which would lead to higher stiffness and lower elongation at break.

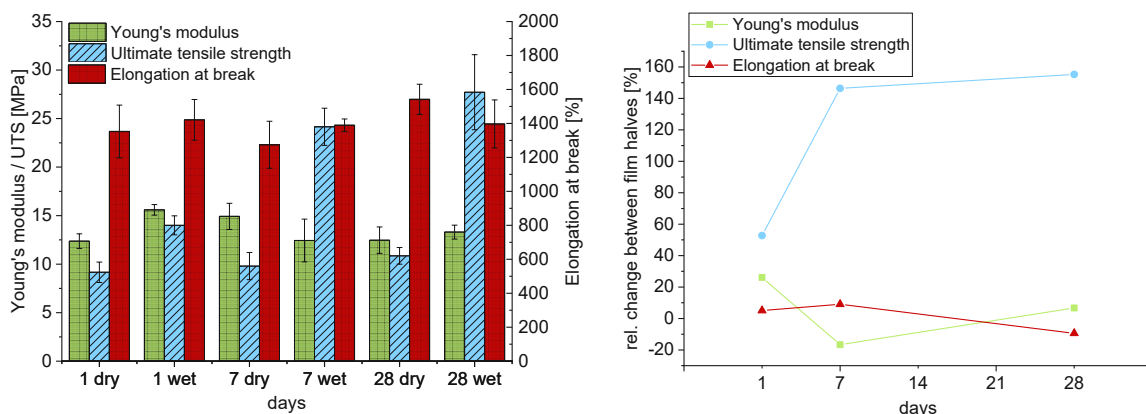


Figure 39: Results of the tensile tests for BHET/IPEDA 50/50 after different incubation periods at 60 °C (absolute and relative values); the dry stored halves were kept at room temperature



The second polymer with a change in chain extender 2 is the TPUU with a molecular ratio of **pTHF:HMDI:BHET:TBAE 1:2:0.5:0.5** (BHET/TBAE 50/50), in which N,N'-di-(*tert*)-butylethylenediamine (TBEDA) is replaced with N-(*tert*)-butylaminoethanol (TBAE). The new chain extender leads to the hindered urea bonds with the same steric hindrance through a *tert*-butyl substituent with its *tert*-butyl-amine side; the alcohol on the other end, however, forms stable urethane bonds. Therefore, the amount of hindered urea bonds in the final TPUU is reduced, and this chain extender can only be cleaved off at one side. This is especially important since it prevents the leaking of monomers during self-reinforcement, which also happens in the body.

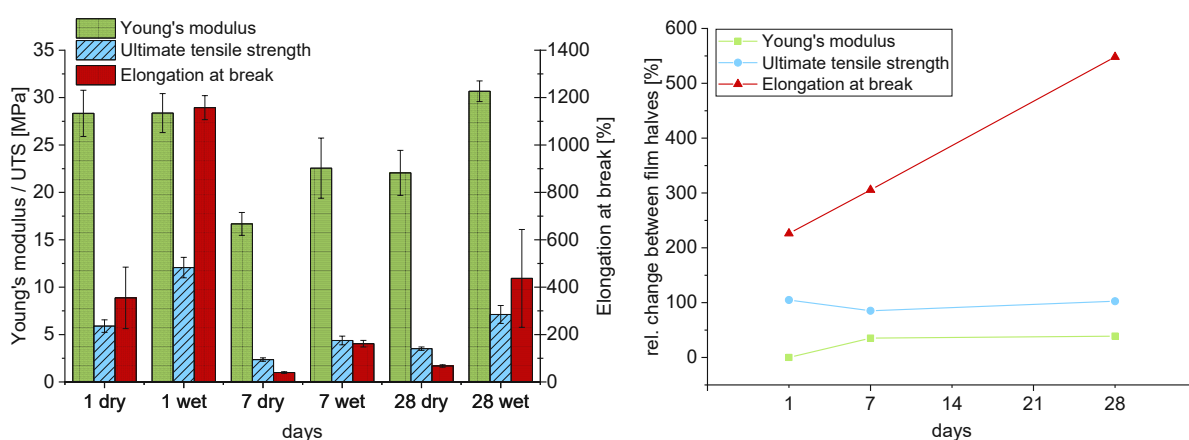


Figure 40: Results of the tensile tests for BHET/TBAE 50/50 after different incubation periods at room temperature (absolute and relative values)

The results of the tensile tests of this polymer can be seen in Figure 40. The polymer BHET/TBAE 50/50 showed significant changes in the ultimate tensile strength between film halves at all incubation periods. For the Young's modulus, no difference between film halves can be seen after one day, but with incubation periods of seven and 28 days, the Young's modulus increases significantly. However, comparing the different films with each other, the film, which was used for testing the one-day preconditioning period, had significantly better performance in terms of the UTS than the films preconditioned for seven and 28 days. For the elongation at break, the differences are pretty similar. All films showed significant increases between the film halves. However, in this parameter, the films with preconditioning periods of 7 days and 28 days also underperformed compared to the film with a one-day preconditioning period regarding both the dryly stored and the preconditioned half.

The TPUU BHET/TBAE 50/50 was then also conditioned for one day, seven and 28 days at an elevated temperature of 37 °C, with the results of the tensile tests shown in Figure 41. Here, the film halves stored under dry conditions with preconditioning periods of seven days and 28 days show comparable results with the film, which was preconditioned at room temperature for one day, whereas the film for one day preconditioning at 37 °C shows mechanical properties similar to the films for seven days and 28 days incubation at room temperature. For the Young's modulus, both films preconditioned for one day and 28 days show an increase; the film preconditioned for seven days has no change. For the UTS, however, this material property increases significantly for all films. For a preconditioning period of seven days, the UTS increases by around 80 %, but the wet film half has a relatively high standard deviation. With a preconditioning period of 28 days, the UTS increases to + 250 %, with a maximum UTS of ~ 25 MPa. Due to the big difference between the values of seven days and 28 days preconditioning periods, it is unclear if the self-reinforcement is complete after 28 days.

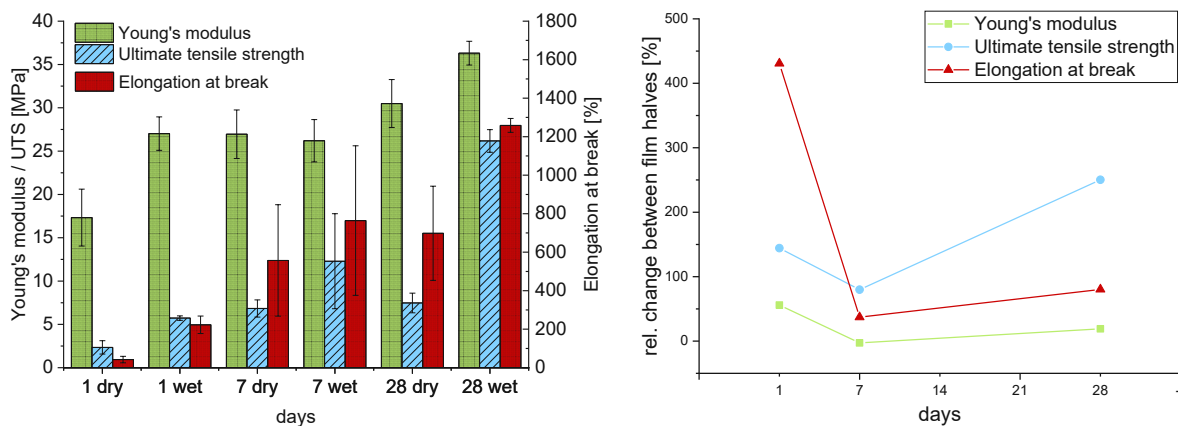


Figure 41: Results of the tensile tests for BHET/TBAE 50/50 after different incubation periods at 37 °C (absolute and relative values); the dry stored halves were kept at room temperature

The elongation at break also showed similar results. The film with a preconditioning period of one day showed extremely low values compared to the others, which also raises the suspicion that some problem occurred during the solution casting of this particular film. For the two other films with preconditioning times of seven and 28 days, the preconditioned half always shows higher elongation at break compared to the dry stored counterpart. Both halves of the film for 7-day preconditioning and the dry stored half of the film for 28 days incubation show high standard deviation, leading to the conclusion that these films could be inhomogeneous. Therefore, even though the film for seven days incubation shows an increase, this increase is not statistically significant given the high standard deviation. At 28 days, this is changed, however: The elongation at break of the self-reinforced half rises to such high values at around 1300 % that even the high standard deviation in the tensile tests of the dry stored half do not impair the statistical significance of the self-reinforcing effect.

The last comparison between TPUUs with a change in one monomer is between polymers with a difference in the second chain extender, which introduces the hindered urea bonds. For all these polymers with the monomers pTHF, HMDI, BHET and the TBEDA/IPEDA/TBAE, representative single film measurements were again chosen as a starting point for comparison of which the results can be seen in Figure 42. In the unconditioned state, the change of TBEDA to IPEDA, which is a simple exchange of *tert*-butyl to isopropyl substituents at the hindered urea bonds, improved both ultimate tensile strength and elongation at break, but otherwise, the material properties as soft and elastic stayed very similar. However, the substitution with TBAE changed this: The Young's modulus increased while the elongation at break decreased, indicating either a change in the material properties towards stiffer properties or a worse behavior of this material regarding elasticity in the unconditioned state in general.

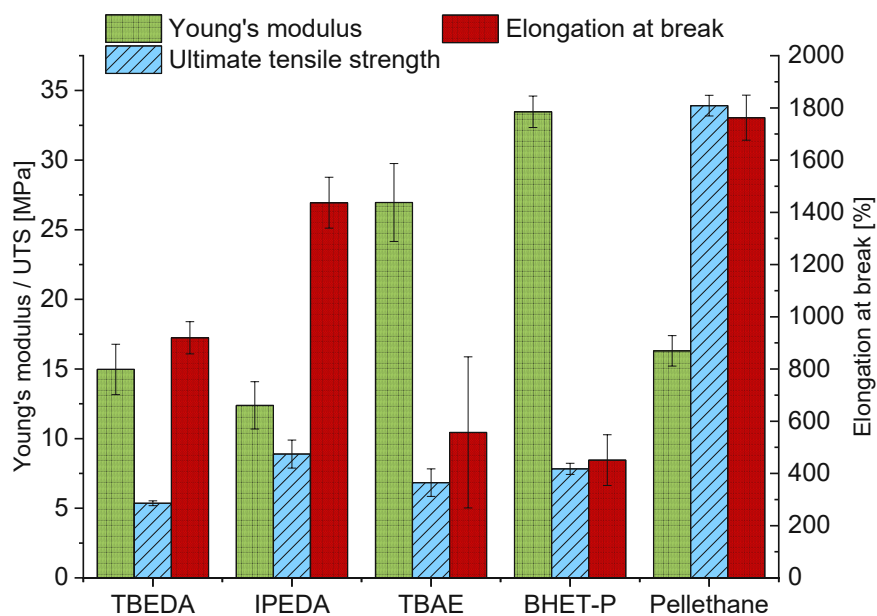


Figure 42: Comparison of Young's modulus, ultimate tensile strength and elongation at break for single unpreconditioned films of polymers with changed chain extender 2 for a final material of pTHF:HMDI:BHET:CE2 1:2:0.5:0.5 and the reference materials BHET-P and Pellethane

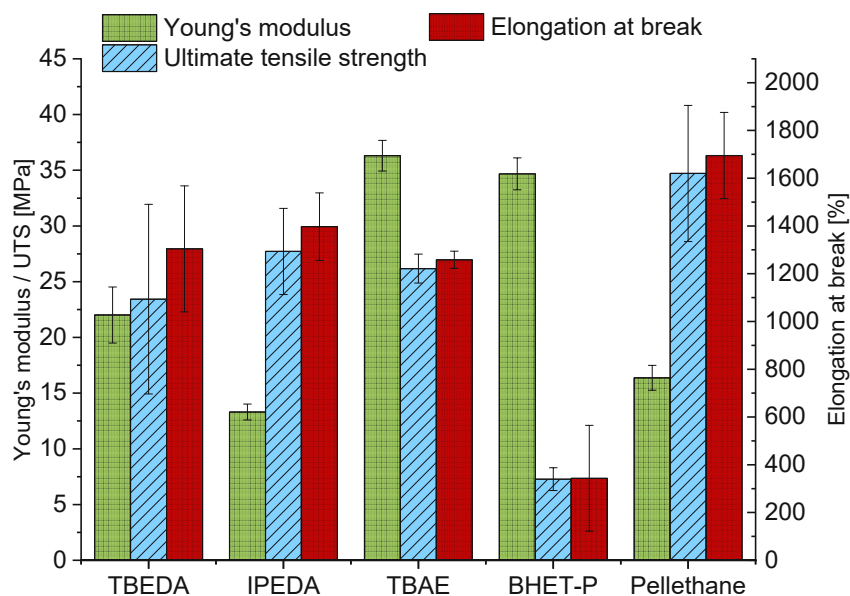


Figure 43: Comparison of Young's modulus, ultimate tensile strength and elongation at break for single preconditioned films of polymers with changed chain extender 2 for a final material of pTHF:HMDI:BHET:CE2 1:2:0.5:0.5 and the reference materials BHET-P and Pellethane

After preconditioning, all three materials showed more similarities in their mechanical properties (Figure 43). As this is a comparison of the best-achieved results, it has to be noted, though, that the compared polymer films were treated differently during preconditioning as the TBEDA film was stored at room temperature, the IPEDA film at 60 °C and the TBAE film at 37 °C. After these treatments, the materials are very elastic and have a high ultimate tensile strength. The most significant difference is in the Young's modulus: While this value increases slightly for each individual polymer after preconditioning, the degree of increase is not the same. Therefore, the polymer with TBEDA has a higher value than the IPEDA-polymer, which stays relatively low and shows the second lowest value for any preconditioned polymer.

### Reference materials

In order to show that the self-reinforcing effect must be linked to the incorporation of hindered urea bonds in the TPUU, the same conditioning protocols were applied to other thermoplastic polyurethane elastomers without these reversible covalent bonds in their chain. As a reference, the well-studied hard block degradable polymer pTHF:HMDI:BHET 1:2:1 (BHET-P) and the commercially available non-degradable benchmark polymer pTHF-MDI-BDO ("Pellethane" with no known exact stoichiometry) were used.

For the polymer BHET-P, no significant changes in the three tested mechanical parameters (Young's modulus, UTS, elongation at break) were visible after preconditioning (Figure 44). Also, in the Young's modulus and elongation at break, a higher variance was observed with even bigger differences between the films.

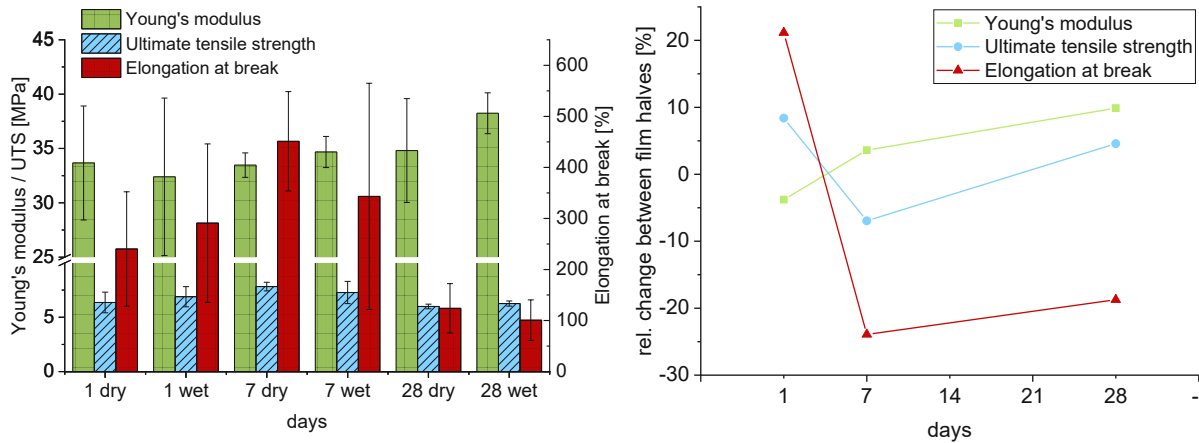


Figure 44: Results of the tensile tests for BHET-P after different incubation periods at room temperature (absolute and relative values)

The same can be said for the commercially available thermoplastic polyurethane elastomer Pellethane. No significant changes in the mechanical properties were observed between the two states (dry storage vs. preconditioning), as can be seen in Figure 45. This polymer also showed low variance between different samples, which can be expected from a commercial product.

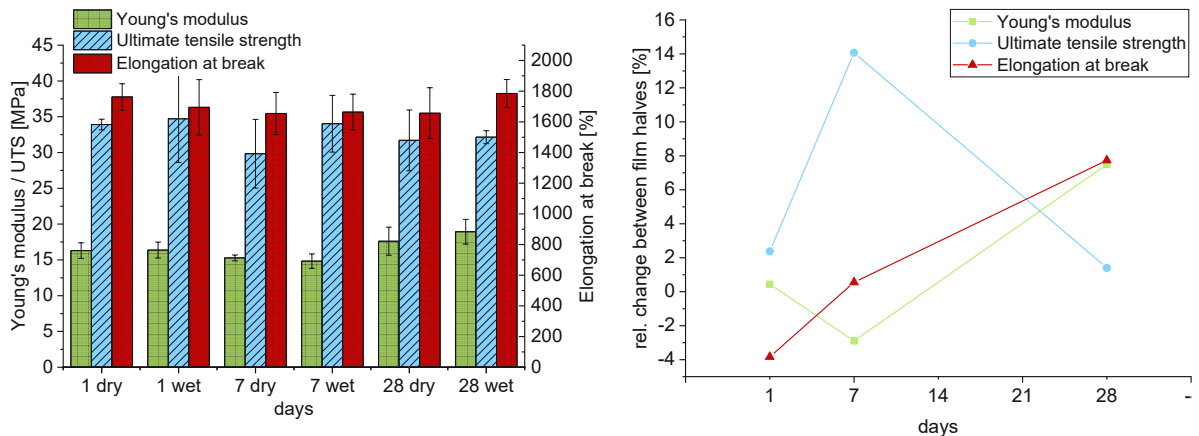


Figure 45: Results of the tensile tests for Pellethane after different incubation periods at room temperature (absolute and relative values)

## 2.5 Degradation behavior

For the degradation study of pTHF-HMDI-BHET-TBEDA 50/50, one polymer film was prepared by standard solution casting method (see “Preparation of films for tensile testing”). From this film, round platelets with a diameter of 5 mm were punched out and weighed in the dry state. Then, after preconditioning at 37 °C for 28 days in PBS buffer with four times buffer capacity, the samples were weighed again in the wet and dry state. Afterward, the samples were put into separate test tubes in the autoclave again in PBS buffer with four times buffer capacity and taken out in triplicates after specific time periods.

Since a pre-experiment showed very fast degradation for such polymer samples with such a high surface-to-bulk ratio at 90 °C, the first samples were already taken after two days and every other day after that.

The degradation was then judged by the residual mass. In order to determine this, the buffer solution was decanted off, and the polymer samples were washed with distilled water to remove the remaining buffer salts. The swelling of the samples could not be determined since they lost their mechanical stability completely, rendering their transfer to small vials in which they could be dried difficult. Therefore, the high deviation between triplicates of one degradation time can be partially traced back to this step. The final remaining mass was then analyzed by weighing after drying to constant weight.

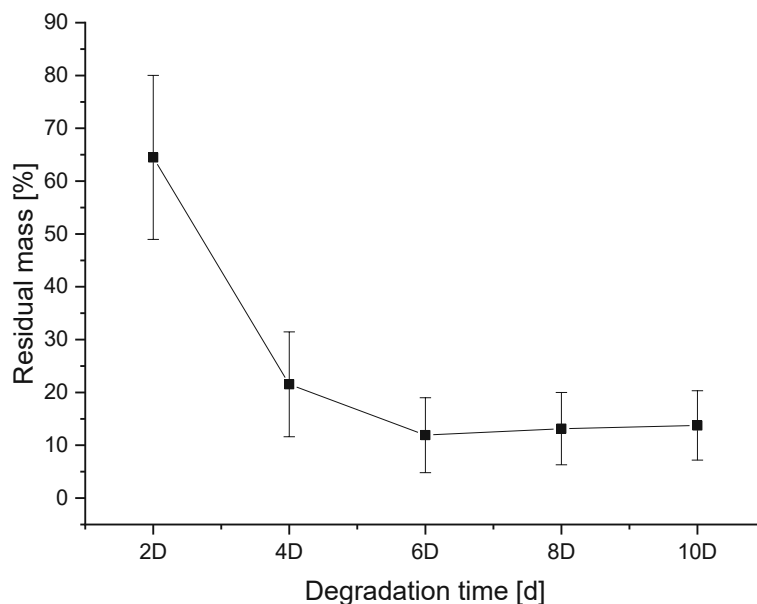


Figure 46: Results of the mass loss after degradation for the polymer pTHF-HMDI-BHET-TBEDA 50/50 after preconditioning at 37°C for 28 days in PBS buffer solution and degrading afterward at 90°C in PBS buffer solution

As shown in Figure 46, the mass loss starts almost instantly at such high temperatures for samples with this geometry. However, as further samples were kept at 37 °C in parallel for months, no optical changes could be seen there yet. The samples at 90 °C lost their shape already after two days and their mechanical stability after four days. This seems to show an apparent problem using an accelerated degradation study at high temperatures for such a material containing dynamic bonds: at room and body temperature, the cleavage and bonding of hindered urea bonds are in a certain equilibrium, at 90 °C, the behavior seems to be the altered, which could be correlating with the melting temperature of the polymer. At this elevated temperature and therefore a melted state, the cleaving reaction seems to be strictly favored, and the freed isocyanates hydrolyze to amines afterward with no backward reaction. Once this happens, the loss of mechanical stability sets in and the samples start to fall apart, increasing the exposed surface area tremendously and further accelerating the degradation. However, this irreversibility in the cleavage of the hindered urea bonds at 90 °C is different from the conditions in the application in tissue engineering, and the comparability is limited. Therefore, while this short degradation study shows that the polymer is degradable under aqueous conditions, the time periods in which this realistically happens cannot be determined. Longer degradation studies at 37 °C make more sense to provide reliable results and will be conducted in the future.

## Summary

Thermoplastic poly(urethane/urea) elastomers (TPUU) are promising polymer class for use as scaffolds in biodegradable blood vessel substitutes. Previous research showed that many different monomers are usable for these applications: With the starting point of Baudis,<sup>29</sup> the first biodegradable TPU from the variation of the commercially available product “Pellethane” with the possibility for application in vascular tissue engineering was achieved. In subsequent further works by Potzmann,<sup>96</sup> Seidler<sup>94</sup> and others, the range of applicable monomers was expanded, and additional possibilities of biodegradable cleavage in the polymers through carbonates and esters were introduced. Finally, with the newest findings of Ehrmann,<sup>112</sup> who described a so-called “self-reinforcing effect” in thermoplastic poly(urethane/urea) elastomers a first introduction of dynamic bonds in TPUU for vascular tissue engineering was achieved. The monomers and monomer ratios of this first TPUU can be seen below in Figure 47.

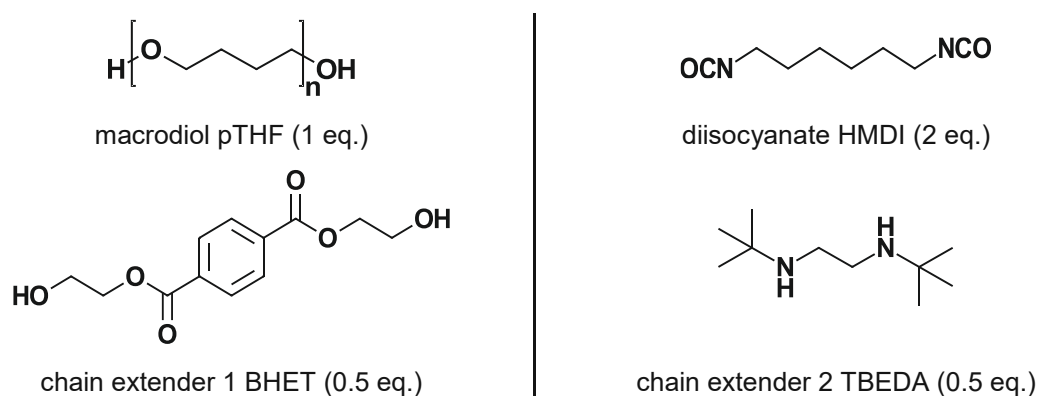


Figure 47: Monomers used in the standard polymer introduced by Ehrmann

Combining the previous findings, the most promising of the previously studied monomers were again applied in this work to achieve a merge of biocompatible and biodegradable TPUU with good mechanical properties and dynamic behavior.

In the first step, three already known polymers with hindered urea bonds were resynthesized and tested for their performance. These polymers contain the above-pictured monomers, and only the chain extender ratio between BHET and TBEDA changes, therefore altering the amount of hindered urea bonds in the chain (Table 17).

Table 17: TPUU compositions used with a change in chain extender ratio

Macrodiol	Diisocyanate	Chain extender 1	Chain extender 2
pTHF (1 eq.)	HMDI (2 eq.)	BHET (0.25 eq.)	TBEDA (0.75 eq.)
pTHF (1 eq.)	HMDI (2 eq.)	BHET (0.5 eq.)	TBEDA (0.5 eq.)
pTHF (1 eq.)	HMDI (2 eq.)	BHET (0.75 eq.)	TBEDA (0.25 eq.)



After this reproduction of previous work, the next step was an extension in the range of polymers in which hindered urea bonds are employed to introduce dynamic behavior. First variations were done in the soft-block with an exchange of poly(tetrahydrofuran) (pTHF) with poly(hexamethylene carbonate)diol (pHMC) and poly(caprolactone)diol (pCL) as pictured in Figure 48 and the exact thermoplastic poly(urethane/urea) elastomers listed in Table 18.

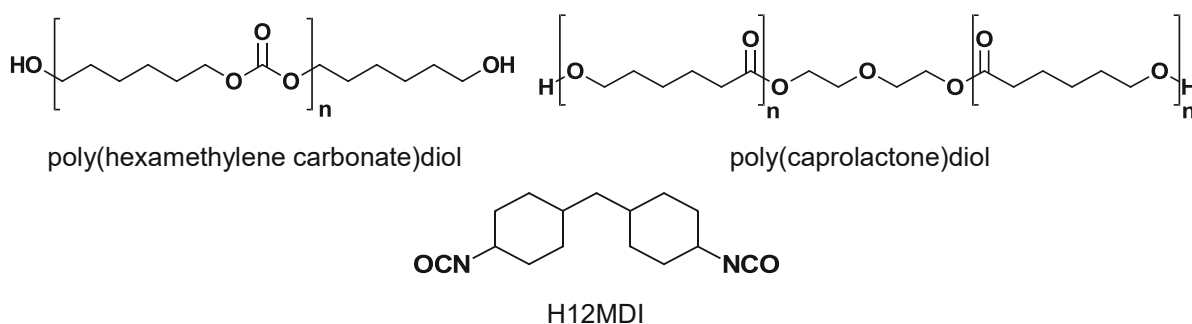


Figure 48: Used macrodiols (and diisocyanate) in the first variation in the soft block

Table 18: TPUU compositions used with a change in macrodiol (and diisocyanate) (CE1 and CE2 were the same in all shown TPUUs)

Macrodiol (1 eq.)	Diisocyanate (2 eq.)	Chain extender 1 (0.5 eq.)	Chain extender 2 (0.5 eq.)
pHMC	HMDI		
pHMC	H12MDI	BHET	TBEDA
pCL2000	HMDI		
pCL530	HMDI		

The exchange of macrodiol changed the material properties in different ways: while the single substitution of pTHF with pHMC still led to similar properties, the additional exchange of HMDI to H12MDI or the exchange of pTHF with pCL makes the final polymer very stiff and unusable for an application as vascular tissue graft.

After the variation in the soft block, the next alteration of the initial TPUU was then done by substituting BHET with other small diols as chain extender 1, which introduces changes in the hard block. The alternative first chain extenders, which were used, are pictured in Figure 49.

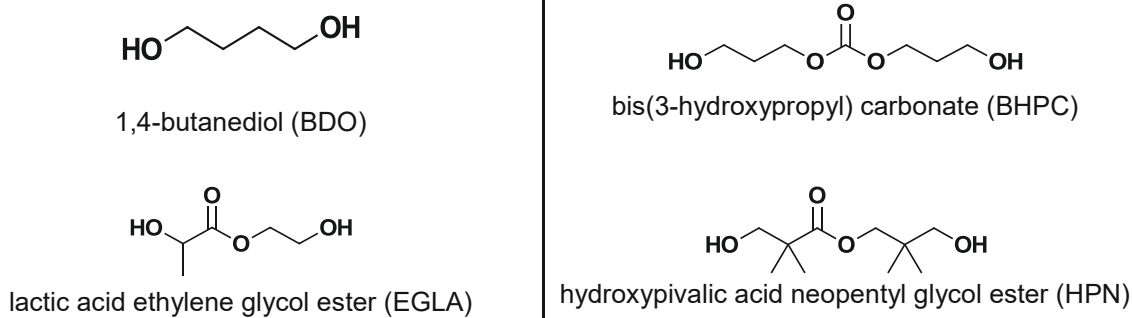


Figure 49: Small diols used as first chain extender in TPUU synthesis

The composition of the TPUUs synthesized with these monomers are listed in table 19.

Table 19: TPUU compositions used with a change in chain extender 1 (macrodiol, diisocyanate and CE2 were the same in all shown TPUUs)

Macrodiol (1 eq.)	Diisocyanate (2 eq.)	Chain extender 1 (0.5 eq.)	Chain extender 2 (0.5 eq.)
pTHF	HMDI	BDO	TBEDA
		BHPC	
		EGLA	
		HPN	

Changes in the first chain extender showed different results depending on the used monomer: BDO and BHPC resulted in polymers with very similar mechanical properties compared to the initial TPUU, whereas the chain extenders EGLA and HPN led to final materials, which were unusable given their lackluster properties.

After changing all other components, the last variation was in the second chain extender, which introduces the hindered urea bonds in the hard blocks and, therefore, the dynamic behavior. Changes in this monomer are especially interesting: with the substitution of TBEDA to IPEDA, the *tert*-butyl substituents at the nitrogen are exchanged with isopropyl groups, which are less stabilizing at the urea bond. In the change of TBEDA to TBAE, the destabilizing group stays the same; however, only one side forms hindered urea bonds, the other, as an alcohol group, forms stable urethane bonds (Structures depicted in Figure 50, TPUU compositions Table 20).



Figure 50: Structures of the second chain extenders used to introduce HUBs in the TPUU

Table 20: TPUU compositions used with a change in chain extender 2 (macrodiol, diisocyanate and CE1 were the same in all shown TPUUs)

<b>Macrodiol (1 eq.)</b>	<b>Diisocyanate (2 eq.)</b>	<b>Chain extender 1 (0.5 eq.)</b>	<b>Chain extender 2 (0.5 eq.)</b>
pTHF	HMDI	BHET	IPEDA TBAE

The change in the second chain extender also had only a slight impact on the mechanical properties compared to the base TPUU. With the chain extender IPEDA, the self-reinforcement however happens only at higher temperatures, making it interesting as a building block to introduce temperature control into the self-reinforcement process. The HUBs built by TBAE are the same as from TBEDA, therefore showing the same self-reinforcement behavior; however, with the reversible bond only on one side of the monomer it is a promising alternative if the release of cleaved off TBEDA monomer is deemed problematic.

All synthesized polymers were then analyzed using different analytical methods. First, the chemical composition of each polymer was investigated using  $^1\text{H-NMR}$  and ATR-IR measurements. This analysis had good correspondence with the expected values, showing that the synthesis procedure is adaptable from the first TPUU to other monomers. Also, thermal properties were determined with DSC and TGA measurements.

Molecular weights and polydispersity of each polymer were analyzed using GPC in conventional calibration and triple detection mode. These measurements were used as a tool to confirm the successful reaction to polymers of all monomer combinations to the final materials. While the final results regarding molecular weights and polydispersities were in a range from low to high ( $M_n$  20-60 kDa), the achieved molecular weights were suitable for mechanical testing. Further optimization of the synthesis procedures in each individual polymer composition to push the molecular weights to higher values could be possible. Since the aim of this thesis was a study showing the possibility of synthesis in a wide range of materials and the applicability of the self-reinforcing effect, this was not done in the scope of this work.

In order to test the mechanical properties and the applicability of a self-reinforcing effect for each of the different polymers, tensile testing of thin-film samples was done. Through the method of solution casting with hexafluoro isopropanol, polymer films were prepared at first. Then, after cutting in half to allow comparison between films, one half was stored under dry conditions. In contrast, the other half was submerged in deionized water for different time periods (one day, seven days, 28 days). While the standard incubation procedure was done at room temperature, several polymers were also tested at 37 °C and the polymer with IPEDA as chain extender at 60 °C.

The results of these tests showed one major problem in film reproducibility: Like already shown in the previous work of Ehrmann, the age of the polymers and films seems to play a role in the mechanical properties. Also, since the hindered urea bonds are specifically designed to be in an equilibrium between open and closed form, the final polymer films prepared by the solution casting method are very susceptible to variations in quality with even slight alterations in the process or different time periods of storage between preparation and tensile testing, even if moisture was avoided as well as possible. Nevertheless, the use of two film halves coming from the same solution casting process allowed judging of relative changes even in polymers in which the absolute change of mechanical properties could not be easily determined. Furthermore, with a large number of tensile tests, outliers in film quality could also often be discovered quickly in the analysis of data and therefore, trends could be determined even in polymers with high variation between films.

From the tensile tests, several conclusions can be drawn:

- The **self-reinforcing effect** under wet conditions applies **to all polymers containing hindered urea bonds**, although happening at different speeds and to different degrees. Especially with more stiff materials coming from the variation in the soft block macrodiol, the self-reinforcing seems to be slower.
- **Reference materials without hindered urea bonds** show **no such effect**; therefore, they must be linked to these dynamic bonds.
- Variations in monomers show **different effects** on the behavior of the final polymer depending if done **in the soft or hard block**.
  - Exchange of the macrodiol pTHF with pHMC or pCL leads to a stiffer material which can be easily explained by the additional hydrogen bonding ability in the soft block.
  - Exchange of chain extender 1 has a relatively low impact on mechanical properties under the premise that hydrogen bonding is still possible; otherwise, the mechanical properties suffer.
  - Exchange in chain extender 2 shows less influence on the mechanical properties but can be either used for tuning of the hindered urea to different temperatures (TBEDA vs. IPEDA) or to prevent total cleavage of the monomer from the polymer chain (TBEDA vs. TBAE).

Finally, a short degradation study of the first polymer pTHF:HMDI:BHET:TBEDA 1:2:0.5:0.5 was done. In this study, with thin samples punched out from a standard polymer film after incubation at 37 °C for 28 days, the degradation was accelerated at 90 °C. The high reactivity of hindered urea bonds was again a significant issue here: While hindered urea bonds are in a certain equilibrium at ambient temperatures, at these elevated temperatures, the cleavage and hydrolysis of freed isocyanates is strictly favored leading to a very fast loss of all mechanical stability within only several days. This behavior is quite different from normal conditions in which the mentioned reaction is much more balanced between the opening and closing of the chains. Therefore, further samples were stored at 37 °C to monitor degradation in a realistic application setup; however, at the writing of this master thesis, no results have been determined yet, as the degradation is significantly slower.

# Experimental

## 1. Synthesis

### 1.1. Chain extenders

#### 1.1.1. Synthesis of Bis-hydroxypropyl-carbonate (BHPC)

Table 21: Used reactants in the synthesis of BHPC

Name (CAS)	M [g mol <sup>-1</sup> ]	Eq.	N [mol]	$\rho$ [g mL <sup>-1</sup> ]	m [g]	V [mL]	V used [mL]
Dimethyl carbonate (616-38-6)	90.08	1	118.8	1.07	10.7	10.0	10.0
1,3-propanediol (504-63-2; 45853)	76.10	2.8	325.9	1.05	25.3	24.1	24.1
DBU (6674-22-2)	152.2					5 drops	6 drops

The synthesis of BHPC was done using a method proposed by Ehrmann.<sup>110</sup> 1 eq. dimethyl carbonate and 2.8 eq. 1,3-propanediol were stirred at room temperature for 24 hours to undergo a transesterification reaction catalyzed by DBU. During the work-up, the generated methanol was removed under vacuum, and the remaining crude product was afterward adsorbed into silica gel for column chromatography. Purification with MPLC (eluent ethyl acetate) led to three fractions (BHPC, BHPC oligomers and unreacted 1,3-propanediol). The pure product BHPC (*R<sub>f</sub>* 0.40) was recovered with a yield of 5.26 g (24.9 %).

#### 1.1.2. Synthesis of lactic acid ethylene glycol ester (EGLA)

Table 22: Used reactants in the synthesis of EGLA

Name (CAS)	M [g mol <sup>-1</sup> ]	Eq.	m [g]	m used [g]
poly(lactic) acid (26100-51-6)	72.06*	1	12.5	12.36
ethylene glycol (107-21-1)	62.07	4.6	50	51

\* molar mass of the repeating unit

The synthesis of EGLA was done using a method proposed by Baudis.<sup>29</sup> 12.36 g PLA (from PLA cups, cut into 1 cm<sup>2</sup> pieces), which corresponds to 172 mmol monomer units, were added to 51 g ethylene glycol (822 mmol) in a 250 mL three-necked flask with a reflux condenser and magnetic stirring. The reaction was stirred at 170 °C for 24 hours. The orange reaction solution was then transferred to a distillation apparatus, and the excess of ethylene glycol (approx. 40 mL) was distilled off at 8 mbar / 110 °C (oil bath) / 83 °C (head). The remaining liquid was then fractionally distilled under high vacuum, with the product EGLA being distilled at 2.2·10<sup>-2</sup> mbar / 112 °C (oil bath) / 80 °C (head) as a colorless liquid in a yield of 14.69 g (64 %). A dark red residue was left behind in the distillation flask, probably from different, non-identified additive components of the PLA cups. The purified monomer was then directly weighed in the appropriate amount and transferred under argon for the polymer synthesis conducted in parallel.

## 1.2 Polymers

### 1.2.1 Prerequisites for polymer synthesis

#### 1.2.1.1 Analysis of macrodiols

##### 1.2.1.1.1 Molecular weight of used macrodiols using OH-titration

In order to calculate the molecular weight from the OH-value of the macrodiols, the OH-value was analyzed analog to DIN 53240-1.<sup>163</sup> For this method, 1.5 g macrodiol were weighed into a penicillin flask, and 3 mL of acetylation agent (25:75 acetic anhydride/dry pyridine) and 5 mL dry pyridine as solvent were added. After heating to 120 °C and stirring for 70 min, 5 mL deionized water were added through the septum, and the sample was kept at 120 °C for another 20 min before removing it from the heating block and letting it cool to room temperature. The contents were then transferred to a 100 mL beaker, and the penicillin flask was washed with two portions of 10 mL pyridine each. Back titration of the remaining acetic acid was done using the automated titration device Metrohm Titrino (mode DET) with 0.5 N methanolic KOH (titer determination with benzoic acid in methanol). The same procedure without adding a sample was done to get the blank value. Blank values were determined in duplicates; sample titrations were done in triplicates.

The values determined by the analysis can be seen in Table 23.

Table 23: Results of the hydroxyl value titrations and calculated molecular weights of used macrodiols

measurement	weigh-in [g]	V <sub>0</sub> <sup>#</sup> [mL]	V [mL]	OH-number [mg KOH g <sup>-1</sup> ]	M <sub>n</sub> [g mol <sup>-1</sup> ]
pTHF 1	1.5778	32.432	25.870	111.5	
pTHF 2	1.4965	32.432	26.198	111.7	
pTHF 3	1.6188	32.432	25.679	111.8	
			<b>pTHF</b>	111.6±0.2	1005±0.5
pHMC 1	1.5336	32.432	27.196	91.5	
pHMC 2	1.5559	32.432	27.080	92.2	
pHMC 3	1.5383	32.432	27.294	89.5	
			<b>pHMC</b>	91.1±1.4	1232±19
pCL530 1	1.9461	32.432	17.769	201.9	
pCL530 2	1.7435	32.432	18.824	209.2	
			<b>pCL530*</b>	205.6±5.1	546±14
pCL2000 1	1.7296	32.432	29.109	51.5	
pCL2000 2	1.7841	32.432	28.867	53.6	
pCL2000 3	1.6402	32.432	29.268	51.7	
			<b>pCL2000</b>	52.3±1.1	2148±46

\* the third pCL530 measurement was removed due to an error of the titration device

<sup>#</sup>V<sub>0</sub> is the volume of methanolic KOH used in the blank titration

#### 1.2.1.1.2 Molecular weight of macrodiols using quantitative <sup>31</sup>P-NMR-spectroscopy

Roughly 30 mg dry macrodiol (weighed with 0.01 mg accuracy) are prepared in a vial. After the addition of 100 µL CDCl<sub>3</sub>, the vial is shaken with the vortexer for several minutes until the macrodiol is fully dissolved. Next, 100 µL of the internal standard solution (pyridine with 40.58 mg mL<sup>-1</sup> cyclohexanol and 5.001 mg mL<sup>-1</sup> chromium(III)acetylacetonate) are added, and the vial is again shaken with the vortexer. In parallel, a second vial is prepared in which 400 µL CDCl<sub>3</sub> are mixed with 100 µL TMDP and also shaken with the vortexer. Finally, the content of the second vial is transferred to the first vial containing the sample and internal standard using a syringe, mixed again with the vortexer and transferred into an NMR tube. The <sup>31</sup>P-NMR must then be measured immediately.



### 1.2.1.2 Purification of diisocyanates

Both diisocyanates HMDI and H12MDI were purified via vacuum distillation, in the case of HMDI at 104 °C at 10 mbar and for H12MDI at 147-154 °C at  $3.8 \cdot 10^{-2}$  mbar.

### 1.2.1.3 Purification of chain extenders

1,4-Butanediol (BDO) was freshly distilled before use in polymers following a procedure from Armarego et al.<sup>166</sup> Its high boiling point of 230 °C also allows to pre-dry the monomer in this step. For this, BDO was freshly distilled from Na<sub>2</sub>SO<sub>4</sub> under vacuum parallel to the polymer synthesis. This distillation was heated up very slowly with several temperature plateaus at which the small residual amount of water was distilled off while BDO remained. These intermediate steps were as follows:

Table 24: Distillation procedure for the purification of BDO

Oil bath temperature [° C]	Pressure [mbar]	Duration [hours]
50	6	1
75	7	1
85	6	1

BDO was then distilled at 7 mbar / 120 °C (oil bath) / 93 °C (head). A small foreshot of several drops was taken, then the main fraction of BDO was then distilled onto dry molecular sieves (3 Å). The amount of BDO needed for the polymer synthesis was then taken under argon.

N,N'-di-*tert*-butylethylene diamine (TBEDA) was distilled under vacuum. Distillation was done at 6 mbar / 85 °C (oil bath) / 56-57 °C (head) onto dry molecular sieves into a Schlenk flask. The product was then removed from the distillation apparatus under argon flux and stored over molecular sieves and under argon atmosphere until use.

N,N'-diisopropylethylene diamine (IPEDA) was also distilled under vacuum after stirring over molecular sieves. Distillation was done at 20 mbar / 70 °C (oil bath) / 58 – 59 °C (head) onto dry molecular sieves. The product was then stored under argon atmosphere until use.

2-(*tert*-Butylamino)ethanol (TBAE) was predried in its melted state by stirring over molecular sieves under argon at 70 °C. Afterward, it was distilled under vacuum after melting. Distillation was done at 5 mbar / 75 °C (oil bath) / 50 °C (head). The distilled monomer was afterward dried in the solid form under high vacuum at room temperature.

## 1.2.2 General polymer synthesis procedure

Generally, synthesis was done using Schlenk-technique and completely dry monomers (< 50 ppm H<sub>2</sub>O; TBEDA/IPEDA/TBAE < 100 ppm H<sub>2</sub>O). First, 1 eq. predried macrodiol was weighed into the reaction vessel (100 mL 3-necked round bottom flask with stopcock and two glass plugs) with mg accuracy and dried at high vacuum and 90 °C for 60 min. 2 eq. freshly distilled diisocyanate were weighed in a transport vessel under argon, diluted with 10 mL dry DMF and added to the reaction through a funnel. Everything was then rinsed with 5 mL dry DMF, and three drops Sn(Oct)<sub>2</sub> were added as catalyst. The reaction was stirred under argon atmosphere at 60 °C for 3 hours. Next, 0.5 eq. of chain extender 1 were weighed into the transport vessel under argon, dissolved in/diluted with 10 mL dry DMF and added to the reaction through a funnel. Everything was then again rinsed with 5 mL dry DMF in portions, and the reaction was continued to be stirred under argon atmosphere at 60 °C for 3 hours. Subsequently, 0.5 eq. of chain extender 2 (TBEDA/IPEDA/TBAE) were weighed in a transport vessel under argon, diluted with 10 mL dry DMF and again added to the reaction through a funnel before everything was rinsed with 10 mL dry DMF in portions. The reaction was then kept stirring under argon atmosphere at either 60 °C or room temperature overnight, depending on the monomers used. After one night, the polymer solution was diluted with a small amount of dry DMF if there was a strong increase in viscosity and transferred to a separation funnel. Afterward, the reaction flask was rinsed with dry DMF to ensure a quantitative transfer of the product to the separation funnel.

The solution was slowly dripped into approx. 1.2 L stirred, dry Et<sub>2</sub>O, and the polymer precipitated. If flaky polymer fell out of solution, the product was filtered off using a glass funnel and filter paper; otherwise, the precipitation agent and solvent were decanted off, and the often sticky polymer was manually extracted with a spatula. To limit the loss of polymer with this method, the beaker was rinsed with dry THF into a rotavapor flask, and the solvent was then removed under vacuum.

### 1.2.2.1 Synthesis of pTHF-HMDI-BHET-TBEDA 50/50

Table 25: Reactants used in the synthesis of pTHF-HMDI-BHET-TBEDA 50/50

Name	M [g mol <sup>-1</sup> ]	Eq.	n [mmol]	m [g]	weigh-in [g]
pTHF	1000	1	5.34	5.3443*	5.3443*
HMDI	168.2	2	10.69	1.7978	1.7976
BHET (chain extender 1)	254.2	0.5	2.67	0.6794	0.6797
TBEDA (chain extender 2)	172.3	0.5	2.67	0.4604	0.4608
<b>Cat.:</b> Sn(Oct) <sub>2</sub>				3 drops	3 drops
<b>Solvent:</b> dry DMF					
<b>Prec. agent:</b> dry diethyl ether					

\* weigh-ins were adjusted to the amount of pTHF used

The reaction was conducted following the general synthesis procedure with stirring at room temperature during the second CE-addition step.

Precipitation was done with 1.4 L dry diethyl ether under stirring. The reaction vessel and separation funnel were rinsed with 100 mL dry DMF. The precipitated white polymer was separated via filtration, and the polymer sticking to the beaker was extracted using a spatula. The polymer was then dried under vacuum at room temperature.

**Yield:** 7.24 g (87.4 %)

**GPC (conv. calibration):** M<sub>n</sub> 53.4 kDa (PDI 3.4)

**<sup>1</sup>H-NMR** (400 MHz, CDCl<sub>3</sub>) δ 8.11 (s, 4H, BHET), 4.73 (s, 3H, urea), 4.70 (s, 4H, urethane), 4.46 (d, 8H, BHET), 4.05 (s, 8H, pTHF), 3.41 (s, 110H, pTHF), 3.13 (s, 16H, HMDI), 1.61 (s, 125H, pTHF), 1.48 (s, 16H, HMDI), 1.40 (s, 17H, TBEDA), 1.36 (s, 4H, ), 1.32 (s, 16H, TBEDA)

**ATR-IR** = 3320 cm<sup>-1</sup> ν(N-H, urethane), 2939 cm<sup>-1</sup> ν(C-H), 2858 cm<sup>-1</sup> ν(OC-H), 2802 cm<sup>-1</sup> ν(N-H), 1718 cm<sup>-1</sup> ν(C=O, ester; C=O⋯H-N, urethane, unordered), 1690 cm<sup>-1</sup> ν(C=O⋯H-N, urethane, ordered), 1633 cm<sup>-1</sup> ν(C=O⋯H-N, urea, ordered), 1371 cm<sup>-1</sup> δ(O-H), 1250 cm<sup>-1</sup> ν(C-O, ether; C-N), 1104 cm<sup>-1</sup> ν(C-C)

### 1.2.2.2 Synthesis of pTHF-HMDI-BHET-TBEDA 75/25

Table 26: Reactants used in the synthesis of pTHF-HMDI-BHET-TBEDA 75/25

Name	M [g mol <sup>-1</sup> ]	Eq.	n [mmol]	m [g]	weigh-in [g]
pTHF	1000	1	5.34	5.3431*	5.3431*
HMDI	168.2	2	10.69	1.7974	1.7970
BHET (chain extender 1)	254.2	0.75	4.01	1.0188	1.0183
TBEDA (chain extender 2)	172.3	0.25	1.34	0.2302	0.2317
<b>Cat.:</b> Sn(Oct) <sub>2</sub>				3 drops	3 drops
<b>Solvent:</b> dry DMF					
<b>Prec. agent:</b> dry diethyl ether					

\* weigh-ins were adjusted to the amount of pTHF used

The reaction was conducted following the general synthesis procedure with stirring at room temperature during the second CE-addition step.

Precipitation was done with 1 L dry diethyl ether under stirring. The reaction vessel and separation funnel were rinsed with two portions of 10 mL dry DMF each. The precipitated flaky white polymer was separated via filtration, and the polymer sticking to the beaker was extracted using a spatula. The polymer was then dried under vacuum at room temperature.

**Yield:** 7.41 g (88.3 %)

**GPC (conv. calibration):** M<sub>n</sub> 59.3 kDa (PDI 2.3)

**<sup>1</sup>H-NMR** (400 MHz, CDCl<sub>3</sub>) δ 8.11 (s, 12H), 4.90 (s, 7H), 4.70 (s, 10H), 4.46 (d, 24H), 4.05 (s, 18H), 3.41 (s, 210H), 3.14 (s, 40H), 1.61 (s, 235H), 1.48 (s, 32H), 1.40 (s, 16H), 1.36 (s, 4H), 1.32 (s, 36H)

**ATR-IR** = 3321 cm<sup>-1</sup> ν(N-H, urethane), 2937 cm<sup>-1</sup> ν(C-H), 2855 cm<sup>-1</sup> ν(OC-H), 2797 cm<sup>-1</sup> ν(N-H), 1720 cm<sup>-1</sup> ν(C=O, ester; C=O⋯H-N, urethane, unordered), 1684 cm<sup>-1</sup> ν(C=O⋯H-N, urethane, ordered), 1535 cm<sup>-1</sup> ν(C=O⋯H-N, urea, ordered), 1367 cm<sup>-1</sup> δ(O-H), 1261 cm<sup>-1</sup> ν(C-O, ether; C-N), 1103 cm<sup>-1</sup> ν(C-C)

### 1.2.2.3 Synthesis of pTHF-HMDI-BHET-TBEDA 25/75

Table 27: Reactants used in the synthesis of pTHF-HMDI-BHET-TBEDA 25/75

Name	M [g mol <sup>-1</sup> ]	Eq.	n [mmol]	m [g]	weigh-in [g]
pTHF	1000	1	5.31	5.3127*	5.3127*
HMDI	168.2	2	10.63	1.7872	1.7867
BHET (chain extender 1)	254.2	0.25	1.33	0.3377	0.3373
TBEDA (chain extender 2)	172.3	0.75	3.98	0.6866	0.6863
<b>Cat.:</b> Sn(Oct) <sub>2</sub>				3 drops	3 drops
<b>Solvent:</b> dry DMF					
<b>Prec. agent:</b> dry diethyl ether					

\* weigh-ins were adjusted to the amount of pTHF used

The reaction was conducted following the general synthesis procedure with stirring at room temperature during the second CE-addition step.

Precipitation was done with 1.1 L dry diethyl ether under stirring. The reaction vessel and separation funnel were rinsed with 20 mL dry DMF. The precipitated polymer which was sticking to the beaker was separated manually using a spatula. The polymer was then dried under vacuum at room temperature.

**Yield:** 3.38 g (41.6 %)

**GPC (conv. calibration):** M<sub>n</sub> 37.6 kDa (PDI 1.7)

**<sup>1</sup>H-NMR** (400 MHz, CDCl<sub>3</sub>) δ 8.11 (s, 4H), 4.84 (s, 10H), 4.70 (s, 7H), 4.46 (d, 10H), 4.06 (s, 16H), 3.41 (s, 155H), 3.16 (s, 38H), 1.62 (s, 190H), 1.48 (s, 30H), 1.40 (s, 26H), 1.36 (s, 9H), 1.32 (s, 21H)

**ATR-IR** = 3318 cm<sup>-1</sup> ν(N-H, urethane), 2937 cm<sup>-1</sup> ν(C-H), 2853 cm<sup>-1</sup> ν(OC-H), 2798 cm<sup>-1</sup> ν(N-H), 1717 cm<sup>-1</sup> ν(C=O, ester; C=O⋯H-N, urethane, unordered), 1687 cm<sup>-1</sup> ν(C=O⋯H-N, urethane, ordered), 1535 cm<sup>-1</sup> ν(C=O⋯H-N, urea, ordered), 1367 cm<sup>-1</sup> δ(O-H), 1250 cm<sup>-1</sup> ν(C-O, ether; C-N), 1105 cm<sup>-1</sup> ν(C-C)

### 1.2.2.4 Synthesis of pTHF-HMDI-BDO-TBEDA 50/50

Table 28: Reactants used in the synthesis of pTHF-HMDI-BDO-TBEDA 50/50

Name	M [g mol <sup>-1</sup> ]	Eq.	n [mmol]	m [g]	weigh-in [g]
pTHF	1000	1	5.00	5.0005*	5.0005*
HMDI	168.2	2	10.00	1.6822	1.6826
BDO (chain extender 1)	90.12	0.5	2.50	0.2253	0.2257
TBEDA (chain extender 2)	172.3	0.5	2.50	0.4308	0.4307
<b>Cat.:</b> Sn(Oct) <sub>2</sub>				3 drops	3 drops
<b>Solvent:</b> dry DMF					
<b>Prec. agent:</b> dry diethyl ether					

\* weigh-ins were adjusted to the amount of pTHF used

The reaction was conducted following the general synthesis procedure with stirring at room temperature during the second CE-addition step.

Precipitation was done with 1.2 L dry diethyl ether under stirring. The reaction vessel and separation funnel were rinsed with 20 mL dry DMF. The precipitated flaky white polymer was separated via filtration, and the polymer sticking to the beaker was extracted using a spatula. The polymer was then dried under vacuum at room temperature.

**Yield:** 5.37 g (73.2 %)

**GPC (conv. calibration):** M<sub>n</sub> 21.9 kDa (PDI 2.5)

**<sup>1</sup>H-NMR** (400 MHz, CDCl<sub>3</sub>) δ 4.83 (3H), 4.74 (3H), 4.05 (11H), 3.40 (92H), 3.15-3.13 (18H), 1.61 (106H), 1.48 (16H), 1.40 (8H), 1.36-1.32 (18H)

**ATR-IR** = 3320 cm<sup>-1</sup> v (N-H, urethane), 2939 cm<sup>-1</sup> v(C-H), 2857 cm<sup>-1</sup> v(OC-H), 2800 cm<sup>-1</sup> v(N-H), 1717 cm<sup>-1</sup> v(C=O, ester; C=O···H-N, urethane, unordered), 1685 cm<sup>-1</sup> v(C=O···H-N, urethane, ordered), 1632 cm<sup>-1</sup> v(C=O···H-N, urea unordered), 1536 cm<sup>-1</sup> v(C=O···H-N, urea, ordered), 1370 cm<sup>-1</sup> δ(O-H), 1250 cm<sup>-1</sup> v(C-O, ether; C-N), 1106 cm<sup>-1</sup> v(C-C)

### 1.2.2.5 Synthesis of pTHF-HMDI-EGLA-TBEDA 50/50

Table 29: Reactants used in the synthesis of pTHF-HMDI-EGLA-TBEDA 50/50

Name	M [g mol <sup>-1</sup> ]	Eq.	n [mmol]	m [g]	weigh-in [g]
pTHF	1000	1	4.95	4.9505*	4.9505*
HMDI	168.2	2	9.91	1.6653	1.6647
EGLA (chain extender 1)	134.1	0.5	2.48	0.3320	0.3314
TBEDA (chain extender 2)	172.3	0.5	2.48	0.4265	0.4257
<b>Cat.:</b> Sn(Oct) <sub>2</sub>				3 drops	3 drops
<b>Solvent:</b> dry DMF					
<b>Prec. agent:</b> dry diethyl ether					

\* weigh-ins were adjusted to the amount of pTHF used

The reaction was conducted following the general synthesis procedure with stirring at room temperature during the second CE-addition step. The chain extender EGLA was prepared parallel to the reaction and freshly distilled added.

Precipitation was done with 1.2 L dry diethyl ether under stirring. The reaction vessel and separation funnel were rinsed with 10 mL dry DMF. After decanting off the precipitation solution, the polymer, which was sticking to the beaker, was partially removed using a spatula; the residual polymer was transferred to a rotavapor flask using dry THF, which was then removed under vacuum. The final polymer was then dried under vacuum at room temperature.

**Yield:** 2.46 g (33.4 %)

**GPC (conv. calibration):** M<sub>n</sub> 38.5 kDa (PDI 1.5)

**<sup>1</sup>H-NMR** (400 MHz, CDCl<sub>3</sub>) δ 5.95 (bs, 2H, EGLA), 5.04 (m, EGLA)\*, 4.72 (m, 4H, urethane/urea)\*, 4.25 – 4.20 (m, 3H, EGLA), 4.05 (s, 7H, pTHF), 3.80 (bs, 1H, EGLA), 3.52 (m, 2H, EGLA), 3.41 (s, 84H, pTHF), 3.26 - 3.15 (16H, HMDI), 1.61 (s, 96H, pTHF), 1.47 (m, 16H, HMDI), 1.40 (s, 8H, TBEDA), 1.32 (m, 16H, TBEDA) (\*overlapping)

**ATR-IR** = 3324 cm<sup>-1</sup> v (N-H, urethane), 2937 cm<sup>-1</sup> v(C-H), 2857 cm<sup>-1</sup> v(OC-H), 2855 cm<sup>-1</sup> v(OC-H), 2797 cm<sup>-1</sup> v(N-H), 1719 cm<sup>-1</sup> v(C=O, ester; C=O···H-N, urethane, unordered), 1688 cm<sup>-1</sup> v(C=O···H-N, urethane, ordered), 1630 cm<sup>-1</sup> v(C=O···H-N, urea unordered), 1535 cm<sup>-1</sup> v(C=O···H-N, urea, ordered), 1366 cm<sup>-1</sup> δ(O-H), 1247 cm<sup>-1</sup> v(C-O, ether; C-N), 1104 cm<sup>-1</sup> v(C-C)

### 1.2.2.6 Synthesis of pHMC-HMDI-BHET-TBEDA 50/50

Table 30: Reactants used in the synthesis of pHMC-HMDI-BHET-TBEDA 50/50

Name	M [g mol <sup>-1</sup> ]	Eq.	n [mmol]	m [g]	weigh-in [g]
pHMC	1232	1	5.29	6.5198*	6.5198*
HMDI	168.20	2	10.58	1.7802	1.7819
BHET (chain extender 1)	254.24	0.5	2.65	0.6727	0.6717
TBEDA (chain extender 2)	172.31	0.5	2.65	0.4559	0.4562
<b>Cat.:</b> Sn(Oct) <sub>2</sub>				3 drops	3 drops
<b>Solvent:</b> dry DMF					
<b>Prec. agent:</b> dry diethyl ether					

\* weigh-ins were adjusted to the amount of pHMC used

The reaction was done following the general synthesis procedure with stirring at 60 °C overnight.

Precipitation was done with 1.2 L dry diethyl ether under stirring. The reaction vessel and separation funnel were rinsed with 10 mL dry DMF. The precipitated flaky white polymer was separated via filtration, and the polymer sticking to the beaker was extracted using a spatula. The polymer was then dried under vacuum at room temperature.

**Yield:** 9.20 g (97.6 %)

**GPC (conv. calibration):** M<sub>n</sub> 52.0 kDa (PDI 2.5)

**<sup>1</sup>H-NMR** (400 MHz, CDCl<sub>3</sub>) δ 8.11 (d, 4H), 8.01 (s, 3H), 4.85 (2H), 4.70 (4H), 4.85 (4H), 4.70 (2H), 4.41 (s, 4H), 4.41 (sH), 4.11 (t, 44H), 4.02 (s, 6H), 3.25 - 3.16 (20H), 1.67 (q, 86H), 1.52 - 1.27 (132H), 1.25 (s, 6H), 1.09 (17H)

**ATR-IR** = 3320 cm<sup>-1</sup> ν(N-H, urethane), 2938 cm<sup>-1</sup> ν(C-H), 2864 cm<sup>-1</sup> ν(OC-H), 1734 cm<sup>-1</sup> ν(C=O, ester; C=O···H-N, urethane, unordered), 1633 cm<sup>-1</sup> ν(C=O···H-N, urea unordered), 1530 cm<sup>-1</sup> ν(C=O···H-N, urea, ordered), 1366 cm<sup>-1</sup> δ(O-H), 1246 cm<sup>-1</sup> ν(C-N)



### 1.2.2.7 Synthesis of pHMC-H12MDI-BHET-TBEDA 50/50

Table 31: Reactants used in the synthesis of pHMC-H12MDI-BHET-TBEDA 50/50

Name	M [g mol <sup>-1</sup> ]	Eq.	n [mmol]	m [g]	weigh-in [g]
pHMC	1232	1	4.31	5.3075*	5.3075*
H12MDI	262.35	2	8.62	2.2604	2.2606
BHET (chain extender 1)	254.24	0.5	2.15	0.5476	0.5475
TBEDA (chain extender 2)	172.31	0.5	2.15	0.3712	0.3717
<b>Cat.:</b> Sn(Oct) <sub>2</sub>				3 drops	3 drops
<b>Solvent:</b> dry DMF					
<b>Prec. agent:</b> dry diethyl ether					

\* weigh-ins were adjusted to the amount of pHMC used

The reaction was done following the general synthesis procedure with stirring at 60 °C overnight.

Precipitation was done with 1.2 L dry diethyl ether under stirring; reaction vessel and separation funnel were rinsed with 5 mL dry DMF. After decanting off the precipitation solution, the polymer, which was sticking to the beaker, was partially removed using a spatula; the residual polymer was transferred to a rotavapor flask using dry THF, which was then removed under vacuum. The final polymer was then dried under vacuum at room temperature.

**Yield:** 8.59 g (98.9 %)

**GPC (conv. calibration):** M<sub>n</sub> 26.4 (PDI 1.8)

**<sup>1</sup>H-NMR** (400 MHz, CDCl<sub>3</sub>) δ 8.11 (4H), 4.87 (3H), 4.77 (3H), 4.51 (5H), 4.43 (5H), 4.29 (2H), 4.24 (2H), 4.19- 3.96 (74H), 3.88 – 3.68 (7H), 3.52 – 3.32 (4H), 3.30 – 3.15 (3H), 2.08 – 1.77 (13H), 1.67 (115H), 1.40 (92H), 1.25 (9H), 1.09 (22H)

**ATR-IR** = 3374 cm<sup>-1</sup> v(N-H, urethane), 2933 cm<sup>-1</sup> v(C-H), 2860 cm<sup>-1</sup> v(OC-H), 1733 cm<sup>-1</sup> v(C=O, ester; C=O···H-N, urethane, unordered), 1626 cm<sup>-1</sup> v(C=O···H-N, urea unordered), 1522 cm<sup>-1</sup> v(C=O···H-N, urea, ordered), 1244 cm<sup>-1</sup> v(C-N)

### 1.2.2.8 Synthesis of pCL2000-HMDI-BHET-TBEDA 50/50

Table 32: Reactants used in the synthesis of pCL2000-HMDI-BHET-TBEDA 50/50

Name	M [g mol <sup>-1</sup> ]	Eq.	n [mmol]	m [g]	weigh-in [g]
pCL2000	2148	1	3.42	7.3561*	7.3561*
HMDI	168.20	2	6.85	1.1520	1.1506
BHET (chain extender 1)	254.24	0.5	1.71	0.4353	0.4352
TBEDA (chain extender 2)	172.31	0.5	1.71	0.2950	0.2954
<b>Cat.:</b> Sn(Oct) <sub>2</sub>				3 drops	3 drops
<b>Solvent:</b> dry DMF					
<b>Prec. agent:</b> dry diethyl ether					

\* weigh-ins were adjusted to the amount of pCL2000 used

The reaction was done following the general synthesis procedure with less amount of dry DMF (5 mL for solving/diluting and 5 mL for rinsing) for both chain extender additions and with stirring at 60 °C overnight.

Precipitation was done with 1.2 L dry diethyl ether under stirring. After decanting off the precipitation solution, the polymer, which was sticking to the beaker, was partially removed using a spatula; the residual polymer was transferred to a rotavapor flask using dry THF, which was then removed under vacuum. The final polymer was then dried under vacuum at room temperature.

**Yield:** 8.58 g (92.9 %)

**GPC (conv. calibration):** M<sub>n</sub> 35.3 (PDI 1.6)

**<sup>1</sup>H-NMR** (400 MHz, CDCl<sub>3</sub>) δ 8.11 (4H), 4.86 (4H), 4.73 (4H), 4.52 (4H), 4.41 (4H), 4.05 (70H), 3.87 (9H), 3.16 (16H), 2.30 (70H), 1.65 (144H), 1.49 (16H), 1.38 (92H), 1.08 (4H)

**ATR-IR** = 3322 cm<sup>-1</sup> v(N-H, urethane), 2942 cm<sup>-1</sup> v(C-H), 2866 cm<sup>-1</sup> v(OC-H), 1722 cm<sup>-1</sup> v(C=O, ester; C=O···H-N, urethane, unordered), 1533 cm<sup>-1</sup> v(C=O···H-N, urea, ordered), 1406 cm<sup>-1</sup> δ(O-H), 1366 cm<sup>-1</sup> δ(O-H), 1239 cm<sup>-1</sup> v(C-N), 1163 cm<sup>-1</sup> v(C-O, ester)

### 1.2.2.9 Synthesis of pCL530-HMDI-BHET-TBEDA 50/50

Table 33: Reactants used in the synthesis of pCL530-HMDI-BHET-TBEDA 50/50

Name	M [g mol <sup>-1</sup> ]	Eq.	n [mmol]	m [g]	weigh-in [g]
pCL530	546	1	10.97	5.9901*	5.9901*
HMDI	168.20	2	21.94	3.6906	3.6905
BHET (chain extender 1)	254.24	0.5	5.49	1.3946	1.3938
TBEDA (chain extender 2)	172.31	0.5	5.49	0.9452	0.9441
<b>Cat.:</b> Sn(Oct) <sub>2</sub>				3 drops	3 drops
<b>Solvent:</b> dry DMF					
<b>Prec. agent:</b> dry diethyl ether					

\* weigh-ins were adjusted to the amount of pCL530 used

The reaction was done following the general synthesis procedure with stirring at room temperature overnight.

Precipitation was done with 1.2 L dry diethyl ether under stirring. The precipitated flaky white polymer was separated via filtration, and the polymer sticking to the beaker was extracted using a spatula. The polymer was then dried under vacuum at room temperature.

**Yield:** 12.01 g (99.9 %)

**GPC (conv. calibration):** M<sub>n</sub> 37.4 (PDI 1.7)

**<sup>1</sup>H-NMR** (400 MHz, CDCl<sub>3</sub>) δ 8.11 (4H), 4.87 (3H), 4.77 (3H), 4.51 (4H), 4.40 (4H), 4.22 (8H), 4.05 (16H), 3.68 (8H), 3.26 (4H), 3.15 (16H), 2.32 (16H), 1.64 (36H), 1.55 – 1.22 (68H)

**ATR-IR** = 3322 cm<sup>-1</sup> ν(N-H, urethane), 2937 cm<sup>-1</sup> ν(C-H), 2863 cm<sup>-1</sup> ν(OC-H), 1720 cm<sup>-1</sup> ν(C=O, ester; C=O⋯H-N, urethane, unordered), 1687 cm<sup>-1</sup> ν(C=O⋯H-N, urethane, ordered), 1533 cm<sup>-1</sup> ν(C=O⋯H-N, urea, ordered), 1450 cm<sup>-1</sup> δ(C-H), 1342 cm<sup>-1</sup> δ(O-H), 1239 cm<sup>-1</sup> ν(C-N), 1164 cm<sup>-1</sup> ν(C-O, ester), 1136 cm<sup>-1</sup> ν(C-O), 1103 cm<sup>-1</sup> ν(C-C)

### 1.2.2.10 Synthesis of pTHF-HMDI-BHPC-TBEDA 50/50

Table 34: Reactants used in the synthesis of pTHF-HMDI-BHPC-TBEDA 50/50

Name	M [g mol <sup>-1</sup> ]	Eq.	n [mmol]	m [g]	weigh-in [g]
pTHF	1000	1	5.1727	5.1727	5.1727
HMDI	168.20	2	10.345	1.7401*	1.7409*
BHPC (chain extender 1)	178.18	0.5	2.5864	0.4608*	0.4607*
TBEDA (chain extender 2)	172.31	0.5	2.5864	0.4457*	0.4448*
<b>Cat.:</b> Sn(Oct) <sub>2</sub>				3 drops	3 drops
<b>Solvent:</b> dry DMF					
<b>Prec. agent:</b> dry diethyl ether					

\* weigh-ins were adjusted to the amount of pTHF used

The reaction was conducted following the general synthesis procedure with stirring at room temperature during the second CE-addition step.

Precipitation was done with 1.2 L dry diethyl ether under stirring. The reaction vessel and separation funnel were rinsed with 15 mL dry DMF. The precipitated flaky white polymer was separated via filtration, and the polymer sticking to the beaker was extracted using a spatula. The polymer was then dried under vacuum at room temperature.

**Yield:** 6.83 g (87.4 %)

**GPC (conv. calibration):** M<sub>n</sub> 60.8 kDa (PDI 2.7)

**<sup>1</sup>H-NMR** (400 MHz, CDCl<sub>3</sub>) δ 4.84 (6 H, urethane/urea), 4.30 (t, 4H, BHPC), 4.05 (9H, HMDI), 3.74 (t, 4H, BHPC), 3.40 (s, 90H, pTHF), 3.26 – 3.14 (18H, HMDI), 1.92 (t, 4H, BHPC), 1.65 (101H, pTHF), 1.48 (bs, 15H, TBEDA), 1.40 (s, 12H, TBEDA), 1.32 (m, 18H)

**ATR-IR** = 3322 cm<sup>-1</sup> ν(N-H, urethane), 2937 cm<sup>-1</sup> ν(C-H), 2855 cm<sup>-1</sup> ν(OC-H), 2796 cm<sup>-1</sup> ν(OC-H), 1720 cm<sup>-1</sup> ν(C=O, ester; C=O⋯H-N, urethane, unordered), 1683 cm<sup>-1</sup> ν(C=O⋯H-N, urethane, ordered), 1631 cm<sup>-1</sup> δ(N-H), 1537 cm<sup>-1</sup> ν(C=O⋯H-N, urea, ordered), 1248 cm<sup>-1</sup> ν(C-O, ether; C-N), 1104 cm<sup>-1</sup> ν(C-C)

### 1.2.2.11 Synthesis of pTHF-HMDI-BHET-TBAE 50/50

Table 35: Reactants used in the synthesis of pTHF-HMDI-BHET-TBAE 50/50

Name	M [g mol <sup>-1</sup> ]	Eq.	n [mmol]	m [g]	weigh-in [g]
pTHF	1000	1	5.4370	5.4370	5.4370
HMDI	168.20	2	10.874	1.8290*	1.8302*
BHET (chain extender 1)	254.24	0.5	2.7185	0.6912*	0.6908*
TBAE (chain extender 2)	117.19	0.5	2.7185	0.3186*	0.3178*
<b>Cat.:</b> Sn(Oct) <sub>2</sub>				3 drops	3 drops
<b>Solvent:</b> dry DMF					
<b>Prec. agent:</b> dry diethyl ether					

\* weigh-ins were adjusted to the amount of pTHF used

The reaction was conducted following the general synthesis procedure with stirring at room temperature during the second CE-addition step.

Precipitation was done with 1.2 L dry diethyl ether under stirring. The reaction vessel and separation funnel were rinsed with 10 mL dry DMF. The precipitated flaky white polymer was separated via filtration. The polymer was then dried under vacuum at room temperature.

**Yield:** 5.23 g (63.2 %)

**GPC (conv. calibration):** M<sub>n</sub> 37.7 kDa (PDI 2.7)

**<sup>1</sup>H-NMR** (400 MHz, CDCl<sub>3</sub>) δ 8.10 (s, 4H), 4.91 (s, 3H), 4.73 (s, 4H), 4.46 (d, 9H), 4.05 (s, 9H), 3.58 (t, 2H), 3.40 (s, 95H), 3.15 (s, 16H), 2.95 (s, 2H), 1.61 (s, 105H), 1.48 (s, 15H), 1.38 (s, 8H), 1.32 (s, 15H)

**ATR-IR** = 3321 cm<sup>-1</sup> ν(N-H, urethane), 2940 cm<sup>-1</sup> ν(C-H), 2859 cm<sup>-1</sup> ν(OC-H), 2803 cm<sup>-1</sup> ν(OC-H), 1720 cm<sup>-1</sup> ν(C=O, ester; C=O···H-N, urethane, unordered), 1688 cm<sup>-1</sup> ν(C=O···H-N, urethane, ordered), 1535 cm<sup>-1</sup> ν(C=O···H-N, urea, ordered), 1371 cm<sup>-1</sup> δ(O-H), 1250 cm<sup>-1</sup> ν(C-O, ether; C-N), 1103 cm<sup>-1</sup> ν(C-C)

## 1.2.2.12 Synthesis of pTHF-HMDI-BHET-IPEDA 50/50

Table 36: Reactants used in the synthesis of pTHF-HMDI-BHET-IPEDA 50/50

Name	M [g mol <sup>-1</sup> ]	Eq.	n [mmol]	m [g]	weigh-in [g]
pTHF	1000	1	5.0382	5.0382	5.0382
HMDI	168.20	2	10.076	1.6949*	1.6938*
BHET (chain extender 1)	254.24	0.5	2.5191	0.6405*	0.6408*
IPEDA (chain extender 2)	144.26	0.5	0.3634	0.3634*	0.3659*
<b>Cat.:</b> Sn(Oct) <sub>2</sub>				3 drops	3 drops
<b>Solvent:</b> dry DMF					
<b>Prec. agent:</b> dry diethyl ether					

\* weigh-ins were adjusted to the amount of pTHF used

The reaction was conducted following the general synthesis procedure with stirring at room temperature during the second CE-addition step.

Precipitation was done with 1.2 L dry diethyl ether under stirring. The reaction vessel and separation funnel were rinsed with 10 mL dry DMF. The precipitated flaky white polymer was separated via filtration. The polymer was then dried under vacuum at room temperature.

**Yield:** 7.14 g (92.3 %)

**GPC (conv. calibration):** M<sub>n</sub> 48.8 kDa (PDI 1.8)

**<sup>1</sup>H-NMR** (400 MHz, CDCl<sub>3</sub>) δ 8.10 (s, 4H), 4.85 (s, 2H), 4.74 (s, 3H), 4.45 (d, 8H), 3.40 (s, 110H), 3.15 (s, 18H), 1.61 (s, 120H), 1.48 (s, 18H), 1.32 (s, 20H), 1.12 (d, 9H), 1.07 (t, 3H)

**ATR-IR** = 3321 cm<sup>-1</sup> ν(N-H, urethane), 2938 cm<sup>-1</sup> ν(C-H), 2857 cm<sup>-1</sup> ν(OC-H), 2800 cm<sup>-1</sup> ν(OC-H), 1720 cm<sup>-1</sup> ν(C=O, ester; C=O⋯H-N, urethane, unordered), 1688 cm<sup>-1</sup> ν(C=O⋯H-N, urethane, ordered), 1625 cm<sup>-1</sup> ν(C=O⋯H-N, urea unordered), 1535 cm<sup>-1</sup> ν(C=O⋯H-N, urea, ordered), 1370 cm<sup>-1</sup> δ(O-H), 1250 cm<sup>-1</sup> ν(C-O, ether; C-N), 1103 cm<sup>-1</sup> ν(C-C)

### 1.2.2.13 Synthesis of pTHF-HMDI-BHET (reference material)

Table 37: Reactants used in the synthesis of pTHF-HMDI-BHET

Name	M [g mol <sup>-1</sup> ]	Eq.	n [mmol]	m [g]	weigh-in [g]
pTHF	1000	1	5.02	5.0177*	5.0177
HMDI	168.2	2	10.04	1.6880	1.6888
BHET	254.2	1	5.02	1.2757	1.2756
<b>Cat.:</b> Sn(Oct) <sub>2</sub>				3 drops	3 drops
<b>Solvent:</b> dry DMF					
<b>Prec. agent:</b> dry methanol					

\* weigh-ins were adjusted to the amount of pTHF used

The reaction was conducted following the general synthesis procedure, with the variation to only include one chain extender and stirring overnight at 60 °C.

Precipitation of the highly viscous polymer solution was done with 1.2 L dry MeOH under stirring. The flaky, white polymer was then extracted via filtration and dried in a drying oven at 40 °C / 40 mbar.

**Yield:** 6.55 g (82.1 %)

**GPC (conv. calibration):** M<sub>n</sub> 45.1 kDa (PDI 1.6)

**<sup>1</sup>H-NMR** (400 MHz, CDCl<sub>3</sub>) δ 8.10 (s, 4H), 4.74 (s, 4H), 4.46 (d, 7H), 4.05 (s, 4H), 3.41 (s, 50H), 3.15 (s, 8H), 1.61 (s, 50H), 1.48 (s, 6H), 1.32 (s, 8H)

**ATR-IR** = 3321 cm<sup>-1</sup> ν(N-H, urethane), 2938 cm<sup>-1</sup> ν(C-H), 2856 cm<sup>-1</sup> ν(OC-H), 2798 cm<sup>-1</sup> ν(OC-H), 1714 cm<sup>-1</sup> ν(C=O, ester; C=O⋯H-N, urethane, unordered), 1683 cm<sup>-1</sup> ν(C=O), 1535 cm<sup>-1</sup> ν(C=O⋯H-N) 1369 cm<sup>-1</sup> δ(O-H), 1262 cm<sup>-1</sup> ν(C-O, ether),, 1103 cm<sup>-1</sup> ν(C-C), 1060 cm<sup>-1</sup> ν(C-O)

## 2. Polymer analysis

### 2.1 Chemical constitution and polymer composition

The chemical constitution of the polymers was analyzed with  $^1\text{H-NMR}$  and ATR-IR. For  $^1\text{H-NMR}$  approx. 3-5 mg polymer were dissolved in deuterated chloroform. To aid the often difficult dissolving process, the samples were warmed up to 40-45 °C and put into an ultrasonic bath until fully dissolved (approx. 30 min). ATR-IR measurements were done with the remains of polymer films from tensile testing. These were under the same conditions as prescribed in the mechanical properties section and measured in the dry state.

### 2.2 Molecular weight via GPC

All prepared polymers were tested using a gel permeation chromatography system (GPC) with dry THF (spiked with Butylhydroxytoluol (BHT) as flowrate marker) as eluent with conventional calibration. In order to do this, samples of the polymers and the reference standard Pellethane were prepared by dissolving the polymer in THF. The desired final concentration of the polymer depends on the expected molecular weight and should be in the range of 2-3 mg mL<sup>-1</sup> for such polymers. This was done by weighing approx. 8-12 mg with mg accuracy and dissolving in the appropriate amount of THF in a test tube to get the desired concentration. Due to strong hydrogen bonding, many of the analyzed TPUUs are difficult to solve at room temperature; therefore, the samples were either heated with a heat gun and shaken or suspended into a 60 °C water bath until the polymer was completely in solution. If these methods were deemed unsuccessful, 1,1,1,3,3,3-hexafluoroisopropanol (HFIP) can be used to break hydrogen bonds between polymer chains by using a maximum of around 10/90 % v/v HFIP/THF. With all methods, the possible loss of volatile solvent must be accounted for in order not to distort the final polymer concentration. This can be done either by weighing or marking of the solvent level. The polymer solution was then filtered into a GPC vial through a syringe filter and measured.



## 2.3 Thermal properties

Thermal properties were analyzed using DSC and TGA measurements, which were conducted by Thomas Koch. For this, the polymers were dried for several days under high vacuum at room temperature. For each measurement, samples of approx. 10 mg were weighed into alumina crucibles and measured following the heat cycles described in Table 38 for DSC measurements and Table 39 for TGA measurements. Curve evaluations were done with the program "Proteus Thermal Analysis".

Table 38: Heat ramp used in DSC measurements

<b>Thermal step</b>	
Cool down to -90 °C	
Isothermal at -90 °C for 5 minutes	
Heat up to 150 °C with 10 °C/min	Temperature cycle 1
Hold for 2 minutes	
Cool down to -90 °C with -10 °C/min	
Isothermal at -90 °C for 5 minutes	
Heat up to 150 °C with 10 °C/min	Temperature cycle 2
Hold for 2 minutes	

Table 39: Heat ramp used in TGA measurements

<b>Thermal step</b>	
Ramp 10 °C/min to 150 °C	
Isothermal for 1.00 min	
Ramp 5 °C/min to 30 °C	Temperature cycle 1
Isothermal for 2.00 min	
Ramp 10 °C/min to 500 °C	
Isothermal for 1.00 min	Temperature cycle 2
Ramp 10.00 °C/min to 500.00 °C	

## 2.4 Mechanical properties

For the tensile tests, polymer films were prepared following a standard solution casting method using polymer solutions with a concentration of  $0.1 \text{ g mL}^{-1}$  polymer in 1,1,1,3,3,3-hexafluoroisopropanol (HFIP). This was done by dissolving 0.5 g polymer in 5 mL solvent under stirring at  $40 - 50 \text{ }^{\circ}\text{C}$  until the polymer was fully dissolved. These viscous polymer solutions were then poured into Teflon molds (dimensions:  $60 \times 40 \times 2 \text{ mm}$ ), which were kept under reverse funnels to prevent contamination during the drying of the films. The volatile solvent evaporated overnight under ambient conditions leaving the desired polymer films.

Conditioning of films was done by cutting each film in half and storing one half in porcelain dishes submerged in deionized water for different time periods (one day = 24 hours, seven days and 28 days) at different temperatures (room temperature,  $37 \text{ }^{\circ}\text{C}$ ,  $60 \text{ }^{\circ}\text{C}$ ). The second half was stored under dry conditions to be able to compare overall film quality.

Tensile tests were done with thin film specimens punched out from the film halves after drying on a universal testing machine. (For further details see “Materials and methods”). The results of the tensile tests can be seen in Table 40.

Table 40: Results of the tensile tests of each film (half) with the preconditioning parameters specified by the duration and whether it was stored under dry conditions ("dry") or preconditioned in deionized water ("wet")

Film	Young's modulus [MPa]	Ultimate tensile strength [MPa]	Elongation at break [%]
<b>pTHF-HMDI-BHET-TBEDA 50/50 preconditioned at room temperature</b>			
1D dry	17.0 ± 0.5	17.0 ± 2.3	1441 ± 209
1D wet	16.5 ± 1.4	16.5 ± 3.9	1361 ± 240
7D dry	15.0 ± 1.8	5.36 ± 0.17	919 ± 62
7D wet	17.6 ± 1.0	9.00 ± 0.57	1195 ± 121
28D dry	16.0 ± 1.5	3.84 ± 0.26	338 ± 56
28D wet	22.0 ± 2.5	23.4 ± 8.5	1304 ± 264
<b>pTHF-HMDI-BHET-TBEDA 50/50 preconditioned at 37°C</b>			
1D dry	14.6 ± 2.5	3.61 ± 0.38	325 ± 67
1D wet	17.0 ± 1.2	8.09 ± 0.75	1038 ± 191
7D dry	17.1 ± 1.6	8.45 ± 1.03	1376 ± 85
7D wet	22.9 ± 1.7	18.5 ± 4.2	1191 ± 206
28D dry	17.0 ± 1.6	4.43 ± 0.30	419 ± 94
28D wet	19.4 ± 1.8	3.76 ± 0.08	134 ± 25
<b>pTHF-HMDI-BHET-TBEDA 75/25 preconditioned at room temperature</b>			
1D dry	25.2 ± 0.87	25.2 ± 4.2	1208 ± 304
1D wet	24.9 ± 3.5	24.9 ± 3.6	1160 ± 316
7D dry	23.7 ± 3.1	14.6 ± 0.60	1447 ± 84
7D wet	26.0 ± 1.8	21.7 ± 0.92	1604 ± 151
28D dry	26.4 ± 1.9	4.99 ± 0.16	129 ± 19
28D wet	28.0 ± 0.82	5.87 ± 0.18	186 ± 31
<b>pTHF-HMDI-BHET-TBEDA 25/75 preconditioned at room temperature</b>			
1D dry	10.0 ± 0.92	6.66 ± 0.73	1467 ± 70
1D wet	9.08 ± 0.52	6.66 ± 0.86	1519 ± 100
7D dry	2.58 ± 0.53	0.82 ± 0.09	97 ± 23
7D wet	3.69 ± 1.5	3.53 ± 0.39	1213 ± 130
28D dry	3.97 ± 0.65	1.02 ± 0.03	74 ± 10
28D wet	6.23 ± 0.46	2.11 ± 0.12	388 ± 89

Film	Young's modulus [MPa]	Ultimate tensile strength [MPa]	Elongation at break [%]
<b>pTHF-HMDI-BDO-TBEDA 50/50 preconditioned at room temperature</b>			
1D dry	23.8 ± 7.1	4.49 ± 1.04	547 ± 105
1D wet	30.6 ± 3.1	10.5 ± 1.22	1289 ± 166
7D dry	15.5 ± 1.1	3.69 ± 0.20	395 ± 113
7D wet	19.8 ± 4.6	14.7 ± 1.18	1531 ± 147
28D dry	27.4 ± 5.1	4.70 ± 0.27	288 ± 37
28D wet	32.6 ± 3.6	18.1 ± 1.6	1345 ± 28
<b>pTHF-HMDI-EGLA-TBEDA 50/50 preconditioned at room temperature</b>			
28D dry	8.39 ± 2.0	0.62 ± 0.12	14 ± 3.8
28D wet	9.92 ± 0.48	0.82 ± 0.08	20 ± 5.3
<b>pTHF-HMDI-BHPC-TBEDA 50/50 preconditioned at room temperature</b>			
1D dry	26.2 ± 0.63	1.90 ± 0.09	55 ± 6.3
1D wet	23.5 ± 5.7	2.62 ± 0.10	229 ± 35
7D dry	27.2 ± 4.2	2.15 ± 0.13	105 ± 9.75
7D wet	24.6 ± 5.5	3.75 ± 0.84	961 ± 180
28D dry	28.4 ± 0.3	2.30 ± 0.06	96 ± 19
28D wet	32.5 ± 5.4	15.0 ± 2.8	1724 ± 123
<b>pTHF-HMDI-BHPC-TBEDA 50/50 preconditioned at 37°C</b>			
1D dry	24.0 ± 2.7	2.23 ± 0.13	160 ± 21
1D wet	28.3 ± 4.4	6.29 ± 1.10	1385 ± 179
7D dry	26.8 ± 2.6	2.66 ± 0.13	436 ± 101
7D wet	31.3 ± 3.0	18.3 ± 2.8	1833 ± 225
28D dry	33.1 ± 3.4	2.90 ± 0.31	479 ± 53
28D wet	34.5 ± 5.3	21.1 ± 2.1	1593 ± 104
<b>pHMC-HMDI-BHET-TBEDA 50/50 preconditioned at room temperature</b>			
1D dry	18.1 ± 2.2	19.0 ± 1.0	975 ± 66
1D wet	30.7 ± 6.4	21.8 ± 6.6	890 ± 223
7D dry	18.6 ± 0.77	22.9 ± 1.5	1010 ± 25
7D wet	32.6 ± 2.2	28.3 ± 1.8	921 ± 49
28D dry	28.0 ± 2.2	17.4 ± 1.6	891 ± 90
28D wet	50.2 ± 3.9	31.7 ± 2.6	1000 ± 85

Film	Young's modulus [MPa]	Ultimate tensile strength [MPa]	Elongation at break [%]
<b>pHMC-H12MDI-BHET-TBEDA 50/50 preconditioned at room temperature</b>			
1D dry	265.8 ± 108.6	13.2 ± 1.4	134 ± 88
1D wet	347.0 ± 99.5	20.4 ± 0.2	46 ± 14
7D dry	200.0 ± 39.4	16.1 ± 1.0	33 ± 8.5
7D wet	197.8 ± 39.4	21.5 ± 0.7	23 ± 4.7
28D dry	212.3 ± 88.4	15.0 ± 2.1	169 ± 157
28D wet	242.5 ± 29.7	18.3 ± 1.5	122 ± 98
<b>pCL2000-HMDI-BHET-TBEDA 50/50 preconditioned at room temperature</b>			
1D dry	77.0 ± 15.1	18.0 ± 2.1	1268 ± 110
1D wet	78.1 ± 14.7	24.3 ± 3.8	1258 ± 85
7D dry	62.6 ± 15.4	14.0 ± 1.8	1188 ± 100
7D wet	110.1 ± 9.8	22.8 ± 3.0	1295 ± 94
28D dry	89.3 ± 13.0	17.2 ± 0.9	1240 ± 103
28D wet	97.6 ± 11.4	31.1 ± 1.6	1543 ± 128
<b>pCL530-HMDI-BHET-TBEDA 50/50 preconditioned at room temperature</b>			
1D dry	25.1 ± 0.78	3.00 ± 0.09	38 ± 6.8
1D wet	34.1 ± 3.4	4.36 ± 0.19	67 ± 2.6
7D dry	29.6 ± 1.8	4.24 ± 0.15	95 ± 4.7
7D wet	33.0 ± 3.4	4.90 ± 0.29	263 ± 26
28D dry	35.1 ± 2.6	4.36 ± 0.14	89 ± 2.8
28D wet	45.8 ± 0.61	6.62 ± 0.61	643 ± 107
<b>pTHF-HMDI-BHET-IPEDA 50/50 preconditioned at room temperature</b>			
1D dry	14.0 ± 1.3	9.53 ± 0.55	1483 ± 30
1D wet	14.0 ± 1.6	9.49 ± 1.58	1275 ± 227
7D dry	12.4 ± 1.7	8.89 ± 1.01	1437 ± 97
7D wet	13.0 ± 0.73	9.90 ± 1.02	1424 ± 93
28D dry	15.7 ± 0.96	10.6 ± 0.1	1493 ± 17
28D wet	14.3 ± 0.62	11.0 ± 0.5	1501 ± 88

Film	Young's modulus [MPa]	Ultimate tensile strength [MPa]	Elongation at break [%]
<b>pTHF-HMDI-BHET-IPEDA 50/50 preconditioned at 37°C</b>			
1D dry	15.3 ± 0.75	9.58 ± 1.89	1288 ± 323
1D wet	13.8 ± 0.72	10.0 ± 1.36	1356 ± 170
7D dry	11.5 ± 1.6	9.22 ± 1.48	1447 ± 107
7D wet	12.8 ± 1.2	9.22 ± 1.26	1264 ± 171
28D dry	14.0 ± 0.72	12.5 ± 0.4	1687 ± 20
28D wet	12.6 ± 1.7	13.8 ± 1.3	1615 ± 114
<b>pTHF-HMDI-BHET-IPEDA 50/50 preconditioned at 60°C</b>			
1D dry	12.4 ± 0.75	9.16 ± 1.05	1353 ± 155
1D wet	15.6 ± 0.55	14.0 ± 1.0	1421 ± 120
7D dry	14.9 ± 1.3	9.80 ± 1.40	1274 ± 138
7D wet	12.4 ± 2.2	24.2 ± 1.9	1389 ± 36
28D dry	12.5 ± 1.4	10.9 ± 0.9	1542 ± 89
28D wet	13.3 ± 0.72	27.7 ± 3.9	1397 ± 142
<b>pTHF-HMDI-BHET-TBAE 50/50 preconditioned at room temperature</b>			
1D dry	28.3 ± 2.4	5.89 ± 0.66	355 ± 130
1D wet	28.4 ± 2.1	12.1 ± 1.08	1158 ± 51
7D dry	16.7 ± 1.2	2.36 ± 0.19	40 ± 3.4
7D wet	22.6 ± 3.2	4.38 ± 0.46	161 ± 14
28D dry	22.1 ± 2.4	3.51 ± 0.18	67 ± 5.1
28D wet	30.7 ± 1.1	7.12 ± 0.94	437 ± 206
<b>pTHF-HMDI-BHET-TBAE 50/50 preconditioned at 37°C</b>			
1D dry	17.3 ± 3.3	2.35 ± 0.78	42 ± 17
1D wet	27.0 ± 1.9	5.73 ± 0.26	223 ± 45
7D dry	27.0 ± 2.8	6.84 ± 0.99	557 ± 289
7D wet	26.2 ± 2.4	12.3 ± 5.5	764 ± 388
28D dry	30.5 ± 2.8	7.47 ± 1.14	698 ± 245
28D wet	36.3 ± 1.4	26.2 ± 1.3	1258 ± 36

<b>Film</b>	<b>Young's modulus [MPa]</b>	<b>Ultimate tensile strength [MPa]</b>	<b>Elongation at break [%]</b>
<b>pTHF-HMDI-BHET preconditioned at room temperature</b>			
1D dry	33.7 ± 5.2	6.36 ± 0.95	240 ± 112
1D wet	32.4 ± 7.2	6.89 ± 0.93	291 ± 155
7D dry	33.5 ± 1.1	7.82 ± 0.40	451 ± 97
7D wet	34.7 ± 1.4	7.28 ± 1.02	343 ± 222
28D dry	34.8 ± 4.8	5.99 ± 0.21	124 ± 48
28D wet	38.2 ± 1.9	6.27 ± 0.24	101 ± 40
<b>Reference Pellethane preconditioned at room temperature</b>			
1D dry	16.3 ± 1.1	33.9 ± 0.7	1762 ± 86
1D wet	16.4 ± 1.1	34.7 ± 6.1	1695 ± 181
7D dry	15.3 ± 0.41	29.8 ± 4.8	1655 ± 137
7D wet	14.8 ± 1.0	34.0 ± 4.0	1664 ± 117
28D dry	17.6 ± 2.0	31.7 ± 4.2	1657 ± 166
28D wet	18.9 ± 1.7	32.1 ± 0.9	1785 ± 91

## 2.5 Degradation behavior

For the degradation study, one polymer film was prepared with the same method used for films for tensile testing purposes. From this film, round samples with a diameter of 5 mm were punched out, weighed and preconditioned in PBS buffer with four times buffer capacity for 28 days at 37 °C. Afterward, the samples were removed from the solutions, dried and transferred to test tubes in again PBS buffer solution with four times buffer capacity. The samples were then put under degradation conditions at 90 °C using an autoclave to ensure constant conditions. After specific time periods, samples were removed from the autoclave in triplicates. After cooling to room temperature, the solution was decanted off, the samples washed in the test tube with distilled water to remove buffer salts and afterward transferred into vials in which they were dried under high vacuum at room temperature.

Afterward, the residual mass of all samples was calculated using Equation 10.

$$\text{residual mass} = \frac{m_0}{m_{\text{degr}}} \cdot 100 \% \quad (10)$$

residual mass [%]	percentage of mass remaining after degradation
$m_0$ [mg]	initial mass of the dry sample
$m_{\text{degr}}$ [mg]	dry mass after degradation

The results of these calculations can be seen in Table 41.



Table 41: Results of the degradation study

Degradation time [days]	$m_0$ [mg]	$m_{\text{degr}}$ [mg]	residual mass [%]	average residual mass [%]
2	2.51	1.31	52.2	64.5 ± 15.5
	2.88	2.36	82.0	
	4.82	2.86	59.3	
4	2.82	0.75	26.6	21.6 ± 9.93
	2.29	0.64	27.9	
	3.36	0.34	10.1	
6*	1.89	0.32	16.9	11.9 ± 7.10
	2.9	0.20	6.90	
8*	2.67	0.48	18.0	13.1 ± 6.84
	2.89	0.24	8.30	
10	3.26	0.41	12.6	13.8 ± 6.57
	2.8	0.22	7.86	
	2.64	0.55	20.8	

\* the third measurement was removed as a statistical outlier

## Materials and Methods

All **reagents and solvents** were purchased and used in appropriate quality for organic synthesis. Purification was done using methods following Armarego et al.<sup>166</sup> if needed. All reagents were dried before use in synthesis, with the exception of the solvent DMF, which was purchased in anhydrous grade. Water contents were checked via Karl Fischer titration before application.

**Karl Fischer titrations (KFT)** were done using an Envirotech CA-21 moisture meter with the anode solution “Aquamicron AX Karl Fischer Reagent for Coulometric Moisture Meter” containing methanol, propylene carbonate, 2,2'-iminodiethanol, sulfodioxide and iodine. As a cathode solution, the reagent “Aquamicron CXU Karl Fischer Reagent for Coulometric Moisture Meter” was used, which contains methanol, ethane-1,2-diol and choline chloride. In order to measure the water content, an appropriate amount of reagent (0.1 – 0.3 mL) was weighed in a syringe with mg accuracy and injected into the device. Liquid reagents could be measured without further preparation steps; for solid reagents, solutions in dry solvents were prepared, and the water content of the solid reagent was calculated from the difference in water content between solution and pure dry solvent (determined separately from blank measurements).

**Thin layer chromatography (TLC)** was done on silica-coated aluminum foils (silica 60 F254) produced by the company Merck.

**Column chromatography** was done using silica gel 60 from VWR. In the case of MPLC (medium pressure liquid chromatography), the separation system Buechi Sepacore Flash System was used. This system is built from the following parts: Buechi pump module C-605, Buechi control unit C-620, Buechi UV-Photometer C-635, Buechi fraction collector C-660 and a polyethylene column.

The **titrations** for OH-value determination were done with a potentiometric titration system from the company Metrohm. The titration was done fully automatic with the dosage unit 736 GP Titrino under stirring (using 703 Ti Stand with stirring function) and monitored with a pH-electrode 6.0229.010 (operating parameters: pH 0-14, temperature 0-70 °C, sat. solution of LiCl in EtOH). For OH-titrations, solutions with 0.5 M KOH in methanol are used (determination of the titer against benzoic acid).

**NMR-spectra** (<sup>1</sup>H and <sup>13</sup>C) were measured with and Bruker Advance spectrometer at 400 MHz (<sup>1</sup>H-spectra) and 101 MHz (<sup>13</sup>C-spectra). If this spectrometer was not available, a Bruker DPX-200 Fourier transform spectrometer at 200 MHz for <sup>1</sup>H-spectra was used. <sup>31</sup>P-NMR spectra (for molecular weight determination with quantitative <sup>31</sup>P-NMR spectroscopy) were recorded

with a Bruker Advance spectrometer at 243 MHz. All NMR signals are denoted in ppm, describing their shift to tetramethylsilane ( $\delta = 0$  ppm) and are referenced to the signal of the used deuterated NMR-solvent. Fine structures of the signals showing coupling with other NMR-active cores are described using the following notation:

s = singlet, d = doublet (dd = doublet of a doublet), t = triplet, q = quadruplet, m = multiplet, bs = broad singlet

Recorded spectra are analyzed with the software “MestReNova v12.0.4-22023” from Mestrelab Research S.L.

**Gel permeation chromatography (GPC)/size exclusion chromatography (SEC)** was used to determine molecular weights and polydispersities of synthesized polymers. As a measurement system, a Malvern VISCOTEK TDA system containing a ViscotekTDA 305-021 RI+Viscodetector, a UV Detector Module 2550 for TDA 305 and a VISCOTEK SEC-MALS 9 light scattering detector was used. Separation was done with three series-connected PSS SDC columns with particle sizes 100 Å, 1000 Å and 100000 Å and the eluent dry THF (stabilized with 250 ppm butylated hydroxytoluene (BHT) to hinder the formation of radicals) with a flow rate of 0.8 mL min<sup>-1</sup> at isothermal conditions at 35 °C. Conventional calibration is done following a calibration curve from the measurements of 11 narrow polystyrene standards produced by PSS. For triple detection measurements, the dn/dc values are determined by injecting the same sample five times with different injection volumina (80, 90, 100, 110, 120 µL) and customizing the triple detection file created with one narrow ( $M_w$  105 kDa) and one broad ( $M_w$  245 kDa) PS-standard from Malvern. Elugrams are analyzed with the software OmniSEC V5.12.461 from Malvern to calculate the number and weight average molecular weight ( $M_n$  and  $M_w$ ) and the polydispersity  $\bar{M}_w/\bar{M}_n$ .

Samples are prepared by dissolving an appropriate amount of polymer in THF-solutions spiked with 0.5 mg mL<sup>-1</sup> BHT as a flowrate marker to achieve a final concentration of 1-3 mg mL<sup>-1</sup>. After dissolving (possibly aided with the warming of the sample or ultrasonic treatment), the solutions are filtered using a syringe filter (200 nm PTFE) directly into GPC vials and measuring thereafter. If the polymer cannot be dissolved otherwise, this can be aided by breaking the hydrogen bonds of the polymer with hexafluoroisopropanol (HFIP) first before adding spiked THF. The final ratio should not be higher than 10/90 HFIP/THF.

**Solution casting** of polymer films for tensile testing was done by dissolving 0.5 g dry polymer in 5 mL dry hexafluoro isopropanol under stirring (concentration 0.1 g mL<sup>-1</sup>) under stirring. Dissolving was started at room temperature and if slowly warmed up to a maximum of 45 °C until the polymer was fully dissolved. The viscous solutions are then poured into Teflon molds (dimensions: 60 x 40 x 2 mm) and put underneath reversed funnels at ambient conditions. As

soon as possible, the films are removed from the mold without damaging them and subjected to a final drying step under vacuum at room temperature. Storage of the films is done in desiccators until use.

**Tensile testing** was done with a *Zwick Z050* universal testing machine (Zwick GmbH & Co. KG, Ulm, Germany) with a 100 N load cell and a crosshead speed of 50 mm min<sup>-1</sup>. Each tested polymer film was cut in half before subjecting it to different storage conditions, and it was tried to measure each half in quadruplets (if possible). For the tensile tests following ISO 527-1, the test specimen with a shape according to ISO 527-1 type 5B were punched out of the solution cast films and width was measured using a slide caliper and thickness with micrometer screw (thickness around 120 – 180 μm). Also, to combat the problem of samples sliding out of the clamps during measurements, adhesive tape is applied to the non-measured parts of each sample in the clamps.

**Attenuated total reflection infrared (ATR-IR) spectra** were measured on a Perkin Elmer Spectrum 65 with a Golden Gate MKII design in ATR-mode. The range of the measurements was between 4000 and 600 cm<sup>-1</sup> with a resolution of 4 cm<sup>-1</sup> and 20 scans for each spectrum. Results were analyzed with the software “Spectrum” by Perkin Elmer (version 10.03.07.0112). As samples, the solution cast films with/without preconditioning were used.

**Preconditioning/incubation of polymers** was done with one half of polymer films prepared via the solution casting method. The film halves were stored in porcelain dishes in deionized water (weighed down to ensure complete submergence) for different time periods (24 hours = 1 day, seven days, 28 days) and at different temperatures (room temperature, 37 °C = body temperature and 60 °C). The durations and temperatures of each preconditioning process are described for each measurement of such films.

**Degradation studies** are done with samples punched out of standard polymer films prepared by solution casting. These round-shaped samples (diameter 5 mm, thickness approx. 150 μm, weight 2-4 mg) are preconditioned at 37 °C in PBS buffer with four times buffer capacity for 28 days before being transferred to test tubes to degrade in PBS buffer with four times buffer capacity at 90 °C. Samples are measured in triplicates, each other day for ten days due to the fast degradation. After decanting off the PBS buffer solution, the samples are washed with deionized water to remove buffer salts and transferred before being dried and afterward weighed to determine weight loss.

## Abbreviations

Abbreviation	Meaning
2AB	2-amino-1-butanol
ATR-IR	attenuated total reflection infrared spectroscopy
BAEA	N-butylaminoethanol
BDI	tetramethylene diisocyanate
BDO	1,4-butanediol
BHET	bis(2-hydroxyethyl) terephthalate
BHPC	bis(3-hydroxypropyl) carbonate
BHT	butylhydroxytoluol
BIMC	bis(isocyanatemethyl)cyclohexane
CER	chain extender ratio
DIT	2,2'-dithiobisethanol
DMF	dimethylformamide
DSC	differential scanning calorimetry
EAE	N-ethylaminoethanol
EEDA	N,N'-diethylethylenediamine
EG	ethylene glycol
EGLA	lactic acid ethylene glycol ester
ePTFE	expanded poly(tetrafluoro ethylene)
GPC	gel permeation chromatography
H12MDI	4,4'-diisocyanato dicyclohexylmethane
HFIP	hexafluoro isopropanol
HMDI	hexamethylene diisocyanate
HPN	hydroxypivalic acid neopentyl glycol ester
HUB	hindered urea bond
IPAE	N-(isopropylamino)ethanol
IPDI	isophorone diisocyanate
IPEDA	N,N'-diisopropylethylenediamine
KFT	Karl-Fischer-titration
LDI	lysine diisocyanate
MDEA	2,2-(methylimino) diethanol
MDI	methylene diphenyl diisocyanate
MDI	4,4'-methylene diphenyl diisocyanate
NMR spectroscopy	nuclear magnetic resonance spectroscopy
PCI	percutaneous coronary intervention

<b>Abbreviation</b>	<b>Meaning</b>
pCL	poly(caprolactone)diol
PET	poly(ethylene terephthalate)
pHMC	poly(hexamethylene carbonate)diol
pTHF	poly(tetrahydrofuran)
PU	polyurethane
TBAE	tert-butyl aminoethanol
TBEDA	N,N'-di-tert-butylethylenediamine
TDI	toluene diisocyanate
TGA	thermogravimetric analysis
THF	tetrahydrofuran
TMDI	2,2,4-trimethylene diisocyanate
TMDP	2-chloro-4,4,5,5-tetramethyl-1,2,3-dioxaphospholane
TMPCA	ditetramethylpiperidine sebacate
TMP-OH	2,2,6,6-tetramethyl-4-piperidinol
TPUU	thermoplastic poly(urethane/urea) elastomer
UTS	ultimate tensile strength
WHO	World Health Organization

## References

- (1) Junqueira, L. C. U.; Carneiro, J.: *Histologie*; 6. ed.; Manfed Gratzl: Springer Medizin Verlag Heidelberg, 2005.
- (2) Arnold, G.; Beier, H. M.; Hermann, M.; Kretschmann, H.-J.; Kühnel, W.; Rollhäuser, H.; Schiebler, T. H.; Schmidt, W.; Winckler, J.; van der Zypen, E.: *Lehrbuch der gesamten Anatomie des Menschen*; 2. ed.; T. H. Schiebler; W. Schmidt: Springer-Verlag Berlin Heidelberg, 1981.
- (3) Ulfing, N.: *Kurzlehrbuch Histologie*; 2. ed.; Georg Thieme Verlag: Rostock, 2005.
- (4) Lloyd-Jones Donald, M.; Leip Eric, P.; Larson Martin, G.; D'Agostino Ralph, B.; Beiser, A.; Wilson Peter, W. F.; Wolf Philip, A.; Levy, D. Prediction of Lifetime Risk for Cardiovascular Disease by Risk Factor Burden at 50 Years of Age. *Circulation* **2006**, *113*, 791-798.
- (5) *Herz-Kreislauf-Erkrankungen in Österreich: Angina Pectoris, Myokardinfarkt, ischämischer Schlaganfall, periphere arterielle Verschlusskrankheit. Epidemiologie und Prävention.*: Wien, 2014.
- (6) Choi, D.; Hwang, K. C.; Lee, K. Y.; Kim, Y. H. Ischemic heart diseases: current treatments and future. *J Control Release* **2009**, *140*, 194-202.
- (7) Lonn, E.; Bosch, J.; Teo Koon, K.; Pais, P.; Xavier, D.; Yusuf, S. The Polypill in the Prevention of Cardiovascular Diseases. *Circulation* **2010**, *122*, 2078-2088.
- (8) Andreotti, F.; Rocca, B.; Husted, S.; Ajjan, R. A.; ten Berg, J.; Cattaneo, M.; Collet, J. P.; De Caterina, R.; Fox, K. A.; Halvorsen, S.; Huber, K.; Hylek, E. M.; Lip, G. Y.; Montalescot, G.; Morais, J.; Patrono, C.; Verheugt, F. W.; Wallentin, L.; Weiss, T. W.; Storey, R. F. Antithrombotic therapy in the elderly: expert position paper of the European Society of Cardiology Working Group on Thrombosis. *Eur Heart J* **2015**, *36*, 3238-3249.
- (9) Grüntzig, A. R.; Senning, A.; Siegenthaler, W. E. Nonoperative dilatation of coronary-artery stenosis: percutaneous transluminal coronary angioplasty. *The New England Journal of Medicine* **1979**, *301*, 7.
- (10) Scheller, B.; Hehrlein, C.; Bocksch, W.; Rutsch, W.; Haghi, D.; Dietz, U. D.; Böhm, M.; Speck, U. Treatment of Coronary In-Stent Restenosis with a Paclitaxel-Coated Balloon Catheter. *The New England Journal of Medicine* **2006**, 2113-2124.
- (11) Scheller, B.; Levenson, B.; Joner, M.; Zahn, R.; Klauss, V.; Naber, C.; Schächinger, V.; Elsässer, A. Medikamente freisetzende Koronarstents und mit Medikamenten beschichtete Ballonkatheter. *Der Kardiologe* **2011**, *5*, 411-435.
- (12) Lei, L.; Guo, S.-R.; Chen, W.-L.; Rong, H.-J.; Lu, F. Stents as a platform for drug delivery. *Expert Opinion on Drug Delivery* **2011**, *8*, 813-831.
- (13) Garrett, H. E.; Dennis, E. W.; DeBakey, M. E. Aortocoronary Bypass With Saphenous Vein Graft: Seven-Year Follow-Up. *JAMA* **1973**, *223*, 792-794.
- (14) Seifalian, A. M.; Tiwari, A.; Hamilton, G.; Salacinski, H. J. Improving the clinical patency of prosthetic vascular and coronary bypass grafts: the role of seeding and tissue engineering. *Artif Organs* **2002**, *26*, 307-320.
- (15) Veith, F. J.; Moss, C. M.; Sprayregen, S.; Montefusco, C. Preoperative saphenous venography in arterial reconstructive surgery of the lower extremity. *Surgery* **1979**, *85*, 253-256.
- (16) Langer, R.; Vacanti, J. P. Tissue Engineering. *Science* **1993**, *260*, 920-926.
- (17) Shinsuke, O.; Fumiko, Y.; Ung-il, C. Tissue Engineering of bone and cartilage. *Nature* **2009**, *IBMS BoneKEy* *6*, 405-419.
- (18) O'Brien, F. J. Biomaterials & scaffolds for tissue engineering. *materialstoday* **2011**, *14*, 88-95.
- (19) Sarkar, S.; Salacinski, H. J.; Hamilton, G.; Seifalian, A. M. The Mechanical Properties of Infringuinal Vascular Bypass Grafts: Their Role in Influencing Patency. *European Journal of Vascular and Endovascular Surgery* **2006**, *31*, 627-636.



- (20) Gauvin, R.; Guillemette, M.; Galbraith, T.; Bourget, J.-M.; Larouche, D.; Marcoux, H.; Aubé, D.; Hayward, C.; Auger, F. A.; Germain, L. Mechanical properties of tissue-engineered vascular constructs produced using arterial or venous cells. *Tissue Eng Part A* **2011**, *17*, 2049-2059.
- (21) Zdrachala, R. J.; Zdrachala, I. J. Biomedical Applications of Polyurethanes: A Review of Past Promises, Present Realities, and a Vibrant Future. *Journal of Biomaterials Applications* **1999**, *14*, 67-90.
- (22) Seidi, A.; Ramalingam, M.; Elloumi-Hannachi, I.; Ostrovidov, S.; Khademhosseini, A. Gradient biomaterials for soft-to-hard interface tissue engineering. *Acta Biomaterialia* **2011**, *7*, 1441-1451.
- (23) Enayati, M.; Puchhammer, S.; Iturri, J.; Grasl, C.; Kaun, C.; Baudis, S.; Walter, I.; Schima, H.; Liska, R.; Wojta, J.; Toca-Herrera, J. L.; Podesser, B. K.; Bergmeister, H. Assessment of a long-term in vitro model to characterize the mechanical behavior and macrophage-mediated degradation of a novel, degradable, electrospun poly-urethane vascular graft. *Journal of the Mechanical Behavior of Biomedical Materials* **2020**, *112*, 104077.
- (24) Zhao, L.; Lee, V. K.; Yoo, S. S.; Dai, G.; Intes, X. *Biomaterials* **2012**, *33*, 5325-5332.
- (25) Cui, X.; Boland, T. *Biomaterials* **2009**, *30*, 6221-6227.
- (26) Elomaa, L.; Yang, Y. P. Additive Manufacturing of Vascular Grafts and Vascularized Tissue Constructs. *Tissue Eng Part B Rev* **2017**, *23*, 436-450.
- (27) Hasan, A.; Memic, A.; Annabi, N.; Hossain, M.; Paul, A.; Dokmeci, M. R.; Dehghani, F.; Khademhosseini, A. Electrospun scaffolds for tissue engineering of vascular grafts. *Acta Biomater* **2014**, *10*, 11-25.
- (28) Sell, S. A.; McClure, M. J.; Garg, K.; Wolfe, P. S.; Bowlin, G. L. *Adv. Drug Deliv. Rev.* **2009**, *61*, 1007-1019.
- (29) Baudis, S. Development and Processing of Materials for Vascular Tissue Regeneration. Technische Universität Wien, 2010.
- (30) Wang, X.; Ding, B.; Li, B. Biomimetic electrospun nanofibrous structures for tissue engineering. *Materials Today* **2013**, *16*, 229-241.
- (31) Abdulghani, S.; Mitchell, G. R. Biomaterials for In Situ Tissue Regeneration: A Review. *Biomolecules* **2019**, *9*.
- (32) Huynh, T.; Abraham, G.; Murray, J.; Brockbank, K.; Hagen, P. O.; Sullivan, S. Remodeling of an acellular collagen graft into a physiologically responsive neovessel. *Nat Biotechnol* **1999**, *17*, 1083-1086.
- (33) Koens, M. J.; Faraj, K. A.; Wisman, R. G.; van der Vliet, J. A.; Krasznai, A. G.; Cuijpers, V. M.; Jansen, J. A.; Daamen, W. F.; van Kuppevelt, T. H. Controlled fabrication of triple layered and molecularly defined collagen/elastin vascular grafts resembling the native blood vessel. *Acta Biomater* **2010**, *6*, 4666-4674.
- (34) Detta, N.; Errico, C.; Dinucci, D.; Puppi, D.; Clarke, D. A.; Reilly, G. C.; Chiellini, F. Novel electrospun polyurethane/gelatin composite meshes for vascular grafts. *J Mater Sci Mater Med* **2010**, *21*, 1761-1769.
- (35) Marelli, B.; Alessandrino, A.; Farè, S.; Freddi, G.; Mantovani, D.; Tanzi, M. C. Compliant electrospun silk fibroin tubes for small vessel bypass grafting. *Acta Biomater* **2010**, *6*, 4019-4026.
- (36) Zhang, Y.; Li, X. S.; Guex, A. G.; Liu, S. S.; Müller, E.; Malini, R. I.; Zhao, H. J.; Rottmar, M.; Maniura-Weber, K.; Rossi, R. M.; Spano, F. A compliant and biomimetic three-layered vascular graft for small blood vessels. *Biofabrication* **2017**, *9*, 025010.
- (37) Mi, H. Y.; Jiang, Y.; Jing, X.; Enriquez, E.; Li, H.; Li, Q.; Turng, L. S. Fabrication of triple-layered vascular grafts composed of silk fibers, polyacrylamide hydrogel, and polyurethane nanofibers with biomimetic mechanical properties. *Mater Sci Eng C Mater Biol Appl* **2019**, *98*, 241-249.
- (38) McClure, M. J.; Simpson, D. G.; Bowlin, G. L. Tri-layered vascular grafts composed of polycaprolactone, elastin, collagen, and silk: Optimization of graft properties. *Journal of the Mechanical Behavior of Biomedical Materials* **2012**, *10*, 48-61.



- (39) Filipe Elyse, C.; Santos, M.; Hung, J.; Lee Bob, S. L.; Yang, N.; Chan Alex, H. P.; Ng Martin, K. C.; Rnjak-Kovacina, J.; Wise Steven, G. Rapid Endothelialization of Off-the-Shelf Small Diameter Silk Vascular Grafts. *JACC: Basic to Translational Science* **2018**, *3*, 38-53.
- (40) Matsuda, T.; Miwa, H. A hybrid vascular model biomimicking the hierarchic structure of arterial wall: neointimal stability and neoarterial regeneration process under arterial circulation. *J Thorac Cardiovasc Surg* **1995**, *110*, 988-997.
- (41) Aflori, M.; Drobotu, M.; Dimitriu, D. G.; Stoica, I.; Simionescu, B.; Harabagiu, V. Collagen immobilization on polyethylene terephthalate surface after helium plasma treatment. *Materials Science and Engineering: B* **2013**, *178*, 1303-1310.
- (42) Al Meslmani, B.; Mahmoud, G.; Strehlow, B.; Mohr, E.; Leichtweiß, T.; Bakowsky, U. Development of thrombus-resistant and cell compatible crimped polyethylene terephthalate cardiovascular grafts using surface co-immobilized heparin and collagen. *Materials Science and Engineering: C* **2014**, *43*, 538-546.
- (43) Sell, S. A.; McClure, M. J.; Barnes, C. P.; Knapp, D. C.; Walpoth, B. H.; Simpson, D. G.; Bowlin, G. L. Electrospun polydioxanone–elastin blends: potential for bioresorbable vascular grafts. *Biomedical Materials* **2006**, *1*, 72-80.
- (44) Wong, C. S.; Liu, X.; Xu, Z.; Lin, T.; Wang, X. Elastin and collagen enhances electrospun aligned polyurethane as scaffolds for vascular graft. *Journal of Materials Science: Materials in Medicine* **2013**, *24*, 1865-1874.
- (45) Devalliere, J.; Chen, Y.; Dooley, K.; Yarmush, M. L.; Uygun, B. E. Improving functional re-endothelialization of acellular liver scaffold using REDV cell-binding domain. *Acta Biomaterialia* **2018**, *78*, 151-164.
- (46) Al Kayal, T.; Losi, P.; Pierozzi, S.; Soldani, G. A New Method for Fibrin-Based Electrospun/Sprayed Scaffold Fabrication. *Scientific Reports* **2020**, *10*, 5111.
- (47) Yang, L.; Li, X.; Wu, Y.; Du, P.; Sun, L.; Yu, Z.; Song, S.; Yin, J.; Ma, X.; Jing, C.; Zhao, J.; Chen, H.; Dong, Y.; Zhang, Q.; Zhao, L. Preparation of PU/Fibrin Vascular Scaffold with Good Biomechanical Properties and Evaluation of Its Performance in vitro and in vivo. *Int J Nanomedicine* **2020**, *15*, 8697-8715.
- (48) Yang, L.; Li, X.; Wang, D.; Mu, S.; Lv, W.; Hao, Y.; Lu, X.; Zhang, G.; Nan, W.; Chen, H.; Xie, L.; Zhang, Y.; Dong, Y.; Zhang, Q.; Zhao, L. Improved mechanical properties by modifying fibrin scaffold with PCL and its biocompatibility evaluation. *Journal of Biomaterials Science, Polymer Edition* **2020**, *31*, 658-678.
- (49) Zhao, L.; Li, X.; Yang, L.; Sun, L.; Mu, S.; Zong, H.; Li, Q.; Wang, F.; Song, S.; Yang, C.; Zhao, C.; Chen, H.; Zhang, R.; Wang, S.; Dong, Y.; Zhang, Q. Evaluation of remodeling and regeneration of electrospun PCL/fibrin vascular grafts in vivo. *Materials Science and Engineering: C* **2021**, *118*, 111441.
- (50) Catelas, I.: 2.17 Fibrin☆. In *Comprehensive Biomaterials II*; Ducheyne, P., Ed.; Elsevier: Oxford, 2017; pp 381-411.
- (51) He, Z.; Ma, X.; Wang, Y.; Liu, G.; Yang, D.; Li, Q.; Li, N. Decellularized Fibrin Gel-Covered Canine Carotid Artery: A Completely Biological Composite Scaffold for Tissue-Engineered Small-Caliber Vascular Graft. *Journal of Biomaterials and Tissue Engineering* **2018**, *8*, 336-346.
- (52) Kasoju, N.; Bora, U. Silk Fibroin in Tissue Engineering. *Advanced Healthcare Materials* **2012**, *1*, 393-412.
- (53) Vepari, C.; Kaplan, D. L. Silk as a biomaterial. *Progress in Polymer Science* **2007**, *32*, 991-1007.
- (54) Zhou, J.; Cao, C.; Ma, X.; Lin, J. Electrospinning of silk fibroin and collagen for vascular tissue engineering. *International Journal of Biological Macromolecules* **2010**, *47*, 514-519.
- (55) Wang, S.; Zhang, Y.; Wang, H.; Yin, G.; Dong, Z. Fabrication and Properties of the Electrospun Poly(lactide)/Silk Fibroin-Gelatin Composite Tubular Scaffold. *Biomacromolecules* **2009**, *10*, 2240-2244.

- (56) Wang, S.; Zhang, Y.; Yin, G.; Wang, H.; Dong, Z. Electrospun polylactide/silk fibroin–gelatin composite tubular scaffolds for small-diameter tissue engineering blood vessels. *Journal of Applied Polymer Science* **2009**, *113*, 2675-2682.
- (57) Enomoto, S.; Sumi, M.; Kajimoto, K.; Nakazawa, Y.; Takahashi, R.; Takabayashi, C.; Asakura, T.; Sata, M. Long-term patency of small-diameter vascular graft made from fibroin, a silk-based biodegradable material. *Journal of Vascular Surgery* **2010**, *51*, 155-164.
- (58) Aussel, A.; Thébaud, N. B.; Bérard, X.; Brizzi, V.; Delmond, S.; Bareille, R.; Siadous, R.; James, C.; Ripoché, J.; Durand, M.; Montembault, A.; Burdin, B.; Letourneur, D.; L'Heureux, N.; David, L.; Bordenave, L. Chitosan-based hydrogels for developing a small-diameter vascular graft: in vitro and in vivo evaluation. *Biomedical Materials* **2017**, *12*, 065003.
- (59) Wang, Y.; He, C.; Feng, Y.; Yang, Y.; Wei, Z.; Zhao, W.; Zhao, C. A chitosan modified asymmetric small-diameter vascular graft with anti-thrombotic and anti-bacterial functions for vascular tissue engineering. *Journal of Materials Chemistry B* **2020**, *8*, 568-577.
- (60) Zhang, J.; Wang, D.; Jiang, X.; He, L.; Fu, L.; Zhao, Y.; Wang, Y.; Mo, H.; Shen, J. Multistructured vascular patches constructed via layer-by-layer self-assembly of heparin and chitosan for vascular tissue engineering applications. *Chemical Engineering Journal* **2019**, *370*, 1057-1067.
- (61) Subramaniam, R.; Mani, M. P.; Jaganathan, S. K. Fabrication and Testing of Electrospun Polyurethane Blended with Chitosan Nanoparticles for Vascular Graft Applications. *Cardiovascular Engineering and Technology* **2018**, *9*, 503-513.
- (62) Kim, I. L.; Mauck, R. L.; Burdick, J. A. Hydrogel design for cartilage tissue engineering: A case study with hyaluronic acid. *Biomaterials* **2011**, *32*, 8771-8782.
- (63) Ozawa, F.; Ino, K.; Takahashi, Y.; Shiku, H.; Matsue, T. Electrodeposition of alginate gels for construction of vascular-like structures. *Journal of Bioscience and Bioengineering* **2013**, *115*, 459-461.
- (64) Sarker, B.; Rompf, J.; Silva, R.; Lang, N.; Detsch, R.; Kaschta, J.; Fabry, B.; Boccaccini, A. R. Alginate-based hydrogels with improved adhesive properties for cell encapsulation. *International Journal of Biological Macromolecules* **2015**, *78*, 72-78.
- (65) Park, M.; Lee, D.; Hyun, J. Nanocellulose-alginate hydrogel for cell encapsulation. *Carbohydrate Polymers* **2015**, *116*, 223-228.
- (66) Strand, B. L.; Coron, A. E.; Skjak-Braek, G. Current and Future Perspectives on Alginate Encapsulated Pancreatic Islet. *STEM CELLS Translational Medicine* **2017**, *6*, 1053-1058.
- (67) Azevedo, M. A.; Bourbon, A. I.; Vicente, A. A.; Cerqueira, M. A. Alginate/chitosan nanoparticles for encapsulation and controlled release of vitamin B2. *International Journal of Biological Macromolecules* **2014**, *71*, 141-146.
- (68) Klinkert, P.; Schepers, A.; Burger, D. H. C.; Bockel, J. H. v.; Breslau, P. J. Vein versus polytetrafluoroethylene in above-knee femoropopliteal bypass grafting: Five-year results of a randomized controlled trial. *Journal of Vascular Surgery* **2003**, *37*, 149-155.
- (69) Ma, Z.; Kotaki, M.; Yong, T.; He, W.; Ramakrishna, S. Surface engineering of electrospun polyethylene terephthalate (PET) nanofibers towards development of a new material for blood vessel engineering. *Biomaterials* **2005**, *26*, 2527-2536.
- (70) Giol, E. D.; Van Vlierberghe, S.; Unger, R. E.; Schaubroeck, D.; Ottevaere, H.; Thienpont, H.; Kirkpatrick, C. J.; Dubrue, P. Endothelialization and Anticoagulation Potential of Surface-Modified PET Intended for Vascular Applications. *Macromolecular Bioscience* **2018**, *18*, 1800125.
- (71) Pu, F. R.; Williams, R. L.; Markkula, T. K.; Hunt, J. A. Expression of leukocyte-endothelial cell adhesion molecules on monocyte adhesion to human endothelial cells on plasma treated PET and PTFE in vitro. *Biomaterials* **2002**, *23*, 4705-4718.
- (72) Walluscheck, K. P.; Steinhoff, G.; Kelm, S.; Haverich, A. Improved endothelial cell attachment on ePTFE vascular grafts pretreated with synthetic RGD-containing peptides. *Eur J Vasc Endovasc Surg* **1996**, *12*, 321-330.

- (73) Táborská, J.; Riedelová, Z.; Brynda, E.; Májek, P.; Riedel, T. Endothelialization of an ePTFE vessel prosthesis modified with an antithrombogenic fibrin/heparin coating enriched with bound growth factors. *RSC Advances* **2021**, *11*, 5903-5913.
- (74) Catto, V.; Farè, S.; Freddi, G.; Tanzi, M. C. Vascular Tissue Engineering: Recent Advances in Small Diameter Blood Vessel Regeneration. *ISRN Vascular Medicine* **2014**, *2014*, 923030.
- (75) Xue, L.; Greisler, H. P. Biomaterials in the development and future of vascular grafts. *J Vasc Surg* **2003**, *37*, 472-480.
- (76) Klinkert, P.; Schepers, A.; Burger, D. H. C.; van Bockel, J. H.; Breslau, P. J. Vein versus polytetrafluoroethylene in above-knee femoropopliteal bypass grafting: Five-year results of a randomized controlled trial. *Journal of Vascular Surgery* **2003**, *37*, 149-155.
- (77) Zhang, F.; King, M. W. Biodegradable Polymers as the Pivotal Player in the Design of Tissue Engineering Scaffolds. *Advanced Healthcare Materials* **2020**, *9*, 1901358.
- (78) Talacua, H.; Smits, A. I. P. M.; Muylaert, D. E. P.; van Rijswijk, J. W.; Vink, A.; Verhaar, M. C.; Driessen-Mol, A.; van Herwerden, L. A.; Bouten, C. V. C.; Kluin, J.; Baaijens, F. P. T. In Situ Tissue Engineering of Functional Small-Diameter Blood Vessels by Host Circulating Cells Only. *Tissue Engineering Part A* **2015**, *21*, 2583-2594.
- (79) Li, S.; Sengupta, D.; Chien, S. Vascular tissue engineering: from in vitro to in situ. *WIREs Systems Biology and Medicine* **2014**, *6*, 61-76.
- (80) Jiang, T.; Zhang, G. Q.; Li, H.; Xun, J. N. Preparation of Electrospun Poly( $\epsilon$ -caprolactone)/Poly(trimethylene carbonate) Blend Scaffold for In Situ Vascular Tissue Engineering. *Advanced Materials Research* **2013**, *629*, 60-63.
- (81) Matsumura, G.; Isayama, N.; Matsuda, S.; Taki, K.; Sakamoto, Y.; Ikada, Y.; Yamazaki, K. Long-term results of cell-free biodegradable scaffolds for in situ tissue engineering of pulmonary artery in a canine model. *Biomaterials* **2013**, *34*, 6422-6428.
- (82) Murdock, M. H.; Badylak, S. F. Biomaterials-based In Situ Tissue Engineering. *Curr Opin Biomed Eng* **2017**, *1*, 4-7.
- (83) Sengupta, D.; Waldman, S. D.; Li, S. From In Vitro to In Situ Tissue Engineering. *Annals of Biomedical Engineering* **2014**, *42*, 1537-1545.
- (84) Chu, C. C. Hydrolytic degradation of polyglycolic acid: Tensile strength and crystallinity study. *Journal of Applied Polymer Science* **1981**, *26*, 1727-1734.
- (85) Shum, A. W. T.; Mak, A. F. T. Morphological and biomechanical characterization of poly(glycolic acid) scaffolds after in vitro degradation. *Polymer Degradation and Stability* **2003**, *81*, 141-149.
- (86) Niklason, L. E.; Gao, J.; Abbott, W. M.; Hirschi, K. K.; Houser, S.; Marini, R.; Langer, R. Functional arteries grown in vitro. *Science* **1999**, *284*, 489-493.
- (87) Harrane, A.; Leroy, A.; Nouailhas, H.; Garric, X.; Coudane, J.; Nottelet, B. PLA-based biodegradable and tunable soft elastomers for biomedical applications. *Biomedical Materials* **2011**, *6*, 065006.
- (88) Gonzalez, M. F.; Ruseckaite, R. A.; Cuadrado, T. R. Structural changes of polylactic-acid (PLA) microspheres under hydrolytic degradation. *Journal of Applied Polymer Science* **1999**, *71*, 1223-1230.
- (89) Huang, R.; Gao, X.; Wang, J.; Chen, H.; Tong, C.; Tan, Y.; Tan, Z. Triple-Layer Vascular Grafts Fabricated by Combined E-Jet 3D Printing and Electrospinning. *Ann Biomed Eng* **2018**, *46*, 1254-1266.
- (90) Li, C.; Wang, F.; Chen, P.; Zhang, Z.; Guidoin, R.; Wang, L. Preventing collapsing of vascular scaffolds: The mechanical behavior of PLA/PCL composite structure prostheses during in vitro degradation. *Journal of the Mechanical Behavior of Biomedical Materials* **2017**, *75*, 455-462.
- (91) Hu, X.; Shen, H.; Yang, F.; Bei, J.; Wang, S. Preparation and cell affinity of microtubular orientation-structured PLGA(70/30) blood vessel scaffold. *Biomaterials* **2008**, *29*, 3128-3136.
- (92) Mo, X.; Weber, H. J.; Ramakrishna, S. PCL-PGLA composite tubular scaffold preparation and biocompatibility investigation. *Int J Artif Organs* **2006**, *29*, 790-799.

- (93) Bergmeister, H.; Seyidova, N.; Schreiber, C.; Strobl, M.; Grasl, C.; Walter, I.; Messner, B.; Baudis, S.; Fröhlich, S.; Marchetti-Deschmann, M.; Griesser, M.; di Franco, M.; Krssak, M.; Liska, R.; Schima, H. Biodegradable, thermoplastic polyurethane grafts for small diameter vascular replacements. *Acta Biomaterialia* **2015**, *11*, 104-113.
- (94) Seidler, K. Development of biodegradable thermoplastic polyurethane elastomers for electrospinning of vascular grafts. Technische Universität Wien, 2012.
- (95) Guo, F.; Wang, N.; Wang, L.; Hou, L.; Ma, L.; Liu, J.; Chen, Y.; Fan, B.; Zhao, Y. An electrospun strong PCL/PU composite vascular graft with mechanical anisotropy and cyclic stability. *Journal of Materials Chemistry A* **2015**, *3*, 4782-4787.
- (96) Potzmann, P. New building blocks for thermoplastic polyurethane elastomers for vascular tissue engineering. Technische Universität Wien, 2011.
- (97) Tiwari, A.; Salacinski, H.; Seifalian, A. M.; Hamilton, G. New prostheses for use in bypass grafts with special emphasis on polyurethanes. *Cardiovascular Surgery* **2002**, *10*, 191-197.
- (98) Prisacariu, C.: *Polyurethane Elastomers, From Morphology to Mechanical Aspects*; SpringerWienNewYork: Springer-Verlag, Wien, 2011.
- (99) He, Y.; Xie, D.; Zhang, X. The structure, microphase-separated morphology, and property of polyurethanes and polyureas. *Journal of Materials Science* **2014**, *49*, 7339-7352.
- (100) Versteegen, R. M.; Sijbesma, R. P.; Meijer, E. W. Synthesis and Characterization of Segmented Copoly(ether urea)s with Uniform Hard Segments. *Macromolecules* **2005**, *38*, 3176-3184.
- (101) Eceiza, A.; Martin, M. D.; de la Caba, K.; Kortaberria, G.; Gabilondo, N.; Corcuera, M. A.; Mondragon, I. Thermoplastic polyurethane elastomers based on polycarbonate diols with different soft segment molecular weight and chemical structure: Mechanical and thermal properties. *Polymer Engineering & Science* **2008**, *48*, 297-306.
- (102) Buckley, C. P.; Prisacariu, C.; Martin, C. Elasticity and inelasticity of thermoplastic polyurethane elastomers: Sensitivity to chemical and physical structure. *Polymer* **2010**, *51*, 3213-3224.
- (103) Yilgor, I.; Yilgor, E. Structure-Morphology-Property Behavior of Segmented Thermoplastic Polyurethanes and Polyureas Prepared without Chain Extenders. *Polymer Reviews* **2007**, *47*, 487-510.
- (104) Malik, J.; Goldslager, B. A.; Clarson, S. J. Thermally controlled molecular disassembly of a crosslinked polymer network by the incorporation of sterically hindered urea linkages. *Journal of Applied Polymer Science* **2002**, *85*, 856-864.
- (105) Zechel, S.; Geitner, R.; Abend, M.; Siegmann, M.; Enke, M.; Kuhl, N.; Klein, M.; Vitz, J.; Gräfe, S.; Dietzek, B.; Schmitt, M.; Popp, J.; Schubert, U. S.; Hager, M. D. Intrinsic self-healing polymers with a high E-modulus based on dynamic reversible urea bonds. *NPG Asia Materials* **2017**, *9*, e420-e420.
- (106) Zhang, Q.; Wang, S.; Rao, B.; Chen, X.; Ma, L.; Cui, C.; Zhong, Q.; Li, Z.; Cheng, Y.; Zhang, Y. Hindered urea bonds for dynamic polymers: An overview. *Reactive and Functional Polymers* **2021**, *159*, 104807.
- (107) Jia, Y.; Ying, H.; Zhang, Y.; He, H.; Cheng, J. Reconfigurable Poly(urea-urethane) Thermoset Based on Hindered Urea Bonds with Triple-Shape-Memory Performance. *Macromolecular Chemistry and Physics* **2019**, *220*, 1900148.
- (108) Wang, S.; Yang, Y.; Ying, H.; Jing, X.; Wang, B.; Zhang, Y.; Cheng, J. Recyclable, Self-Healable, and Highly Malleable Poly(urethane-urea)s with Improved Thermal and Mechanical Performances. *ACS Applied Materials & Interfaces* **2020**, *12*, 35403-35414.
- (109) Ying, H.; Yen, J.; Wang, R.; Lai, Y.; Hsu, J.-L.-A.; Hu, Y.; Cheng, J. Degradable and biocompatible hydrogels bearing a hindered urea bond. *Biomaterials Science* **2017**, *5*, 2398-2402.
- (110) Ehrmann, K. Development of Thermoplastic Elastomers for Cardiovascular Tissue Regeneration. Technische Universität Wien, 2020.
- (111) Ying, H.; Zhang, Y.; Cheng, J. Dynamic urea bond for the design of reversible and self-healing polymers. *Nature communications* **2014**, *5*, 3218.



- (112) Ehrmann, K. Development of Thermoplastic Elastomers for Cardiovascular Tissue Regeneration. Technische Universität Wien, 2020.
- (113) Li, J.; Chen, Z.; Yang, X. State of the Art of Small-Diameter Vessel-Polyurethane Substitutes. *Macromolecular Bioscience* **2019**, *19*, 1800482.
- (114) Woźniak, P.; Bil, M.; Ryszkowska, J.; Wychowański, P.; Wróbel, E.; Ratajska, A.; Hoser, G.; Przybylski, J.; Kurzydłowski, K. J.; Lewandowska-Szumieł, M. Candidate bone-tissue-engineered product based on human-bone-derived cells and polyurethane scaffold. *Acta Biomaterialia* **2010**, *6*, 2484-2493.
- (115) Chen, Q.; Liang, S.; Thouas, G. A. Elastomeric biomaterials for tissue engineering. *Progress in Polymer Science* **2013**, *38*, 584-671.
- (116) Kim, H.-D.; Lee, T.-J.; Huh, J.-H.; Lee, D.-J. Preparation and properties of segmented thermoplastic polyurethane elastomers with two different soft segments. *Journal of Applied Polymer Science* **1999**, *73*, 345-352.
- (117) Martin, D. J.; Meijs, G. F.; Renwick, G. M.; McCarthy, S. J.; Gunatillake, P. A. The effect of average soft segment length on morphology and properties of a series of polyurethane elastomers. I. Characterization of the series. *Journal of Applied Polymer Science* **1996**, *62*, 1377-1386.
- (118) Asensio, M.; Costa, V.; Nohales, A.; Bianchi, O.; Gómez, C. Tunable Structure and Properties of Segmented Thermoplastic Polyurethanes as a Function of Flexible Segment. *Polymers* **2019**, *11*, 1910.
- (119) Tatai, L.; Moore, T. G.; Adhikari, R.; Malherbe, F.; Jayasekara, R.; Griffiths, I.; Gunatillake, P. A. Thermoplastic biodegradable polyurethanes: The effect of chain extender structure on properties and in-vitro degradation. *Biomaterials* **2007**, *28*, 5407-5417.
- (120) Seidler, K.; Ehrmann, K.; Steinbauer, P.; Rohatschek, A.; Andriotis, O. G.; Dworak, C.; Koch, T.; Bergmeister, H.; Grasl, C.; Schima, H.; J. Thurner, P.; Liska, R.; Baudis, S. A structural reconsideration: Linear aliphatic or alicyclic hard segments for biodegradable thermoplastic polyurethanes? *Journal of Polymer Science Part A: Polymer Chemistry*, *0*.
- (121) Avaz Seven, S.; Oguz, O.; Menciloglu, Y. Z.; Atilgan, C. Tuning Interaction Parameters of Thermoplastic Polyurethanes in a Binary Solvent To Achieve Precise Control over Microphase Separation. *Journal of Chemical Information and Modeling* **2019**, *59*, 1946-1956.
- (122) Martin, D. J.; Meijs, G. F.; Gunatillake, P. A.; Yozghatlian, S. P.; Renwick, G. M. The influence of composition ratio on the morphology of biomedical polyurethanes. *Journal of Applied Polymer Science* **1999**, *71*, 937-952.
- (123) Prisacariu, C.; Scortanu, E.; Agapie, B.; Prisacariu, V. A.; Coseri, S. Inelastic response of copolyurethane elastomers with varying soft segment molecular weights and preparation procedure. *Polymer International* **2013**, *62*, 1600-1607.
- (124) Bagdi, K.; Molnár, K.; Kállay, M.; Schön, P.; Vancsó, J. G.; Pukánszky, B. Quantitative estimation of the strength of specific interactions in polyurethane elastomers, and their effect on structure and properties. *European Polymer Journal* **2012**, *48*, 1854-1865.
- (125) Prisacariu, C.; Scortanu, E.; Agapie, B. Effect of the hydrogen bonding on the inelasticity of thermoplastic polyurethane elastomers. *Journal of Industrial and Engineering Chemistry* **2013**, *19*, 113-119.
- (126) Gorna, K.; Polowinski, S.; Gogolewski, S. Synthesis and characterization of biodegradable poly( $\epsilon$ -caprolactone urethane)s. I. Effect of the polyol molecular weight, catalyst, and chain extender on the molecular and physical characteristics. *Journal of Polymer Science Part A: Polymer Chemistry* **2002**, *40*, 156-170.
- (127) Brugmans, M. C. P.; Söntjens, S. H. M.; Cox, M. A. J.; Nandakumar, A.; Bosman, A. W.; Mes, T.; Janssen, H. M.; Bouten, C. V. C.; Baaijens, F. P. T.; Driessen-Mol, A. Hydrolytic and oxidative degradation of electrospun supramolecular biomaterials: In vitro degradation pathways. *Acta Biomaterialia* **2015**, *27*, 21-31.
- (128) Santerre, J. P.; Woodhouse, K.; Laroche, G.; Labow, R. S. Understanding the biodegradation of polyurethanes: From classical implants to tissue engineering materials. *Biomaterials* **2005**, *26*, 7457-7470.

- (129) Hakkarainen, M.; Höglund, A.; Odelius, K.; Albertsson, A.-C. Tuning the Release Rate of Acidic Degradation Products through Macromolecular Design of Caprolactone-Based Copolymers. *Journal of the American Chemical Society* **2007**, *129*, 6308-6312.
- (130) Guan, J.; Sacks, M. S.; Beckman, E. J.; Wagner, W. R. Synthesis, characterization, and cytocompatibility of elastomeric, biodegradable poly(ester-urethane)ureas based on poly(caprolactone) and putrescine. *Journal of biomedical materials research* **2002**, *61*, 493-503.
- (131) Asplund, J. O. B.; Bowden, T.; Mathisen, T.; Hilborn, J. Synthesis of Highly Elastic Biodegradable Poly(urethane urea). *Biomacromolecules* **2007**, *8*, 905-911.
- (132) Ehrmann, K.; Potzmann, P.; Dworak, C.; Bergmeister, H.; Eilenberg, M.; Grasl, C.; Koch, T.; Schima, H.; Liska, R.; Baudis, S. Hard Block Degradable Polycarbonate Urethanes: Promising Biomaterials for Electrospun Vascular Prostheses. *Biomacromolecules* **2020**, *21*, 376-387.
- (133) Jiang, X.; Li, J.; Ding, M.; Tan, H.; Ling, Q.; Zhong, Y.; Fu, Q. Synthesis and degradation of nontoxic biodegradable waterborne polyurethanes elastomer with poly( $\epsilon$ -caprolactone) and poly(ethylene glycol) as soft segment. *European Polymer Journal* **2007**, *43*, 1838-1846.
- (134) Wang, W.; Ping, P.; Yu, H.; Chen, X.; Jing, X. Synthesis and characterization of a novel biodegradable, thermoplastic polyurethane elastomer. *Journal of Polymer Science Part A: Polymer Chemistry* **2006**, *44*, 5505-5512.
- (135) Ochiai, B.; Amemiya, H.; Yamazaki, H.; Endo, T. Synthesis and properties of poly(carbonate-urethane) consisting of alternating carbonate and urethane moieties. *Journal of Polymer Science Part A: Polymer Chemistry* **2006**, *44*, 2802-2808.
- (136) Maafi, E. M.; Malek, F.; Tighzert, L. Synthesis and characterization of new polyurethane based on polycaprolactone. *Journal of Applied Polymer Science* **2010**, *115*, 3651-3658.
- (137) Zhang, C.; Wen, X.; Vyavahare, N. R.; Boland, T. Synthesis and characterization of biodegradable elastomeric polyurethane scaffolds fabricated by the inkjet technique. *Biomaterials* **2008**, *29*, 3781-3791.
- (138) Martin, C.; Winet, H.; Bao, J. Y. Acidity near eroding polylactide-polyglycolide in vitro and in vivo in rabbit tibial bone chambers. *Biomaterials* **1996**, *17*, 2373-2380.
- (139) Agrawal, C. M.; Athanasiou, K. A. Technique to control pH in vicinity of biodegrading PLA-PGA implants. *Journal of biomedical materials research* **1997**, *38*, 105-114.
- (140) Netzel-Arnett, S.; Fields, G. B.; Birkedal-Hansen, H.; Van Wart, H. E.; Fields, G. Sequence specificities of human fibroblast and neutrophil collagenases. *Journal of Biological Chemistry* **1991**, *266*, 6747-6755.
- (141) de Paz, M. V.; Zamora, F.; Begines, B.; Ferris, C.; Galbis, J. A. Glutathione-mediated biodegradable polyurethanes derived from L-arabinitol. *Biomacromolecules* **2010**, *11*, 269-276.
- (142) Kim, H. D.; Huh, J. H.; Kim, E. Y.; Park, C. C. Comparison of properties of thermoplastic polyurethane elastomers with two different soft segments. *Journal of Applied Polymer Science* **1998**, *69*, 1349-1355.
- (143) Mirhosseini, M. M.; Haddadi-Asl, V.; Jouibari, I. S. How the soft segment arrangement influences the microphase separation kinetics and mechanical properties of polyurethane block polymers. *Materials Research Express* **2019**, *6*, 085311.
- (144) Bil, M.; Ryszkowska, J.; Kurzydłowski, K. J. Effect of polyurethane composition and the fabrication process on scaffold properties. *Journal of Materials Science* **2009**, *44*, 1469-1476.
- (145) Zhang, C.; Zhang, N.; Wen, X. Improving the elasticity and cytophilicity of biodegradable polyurethane by changing chain extender. *J Biomed Mater Res B Appl Biomater* **2006**, *79*, 335-344.
- (146) Cohn, D.; Salomon, A. H. Designing biodegradable multiblock PCL/PLA thermoplastic elastomers. *Biomaterials* **2005**, *26*, 2297-2305.
- (147) Sánchez-Adsuar, M. S. Influence of the composition on the crystallinity and adhesion properties of thermoplastic polyurethane elastomers. *International Journal of Adhesion and Adhesives* **2000**, *20*, 291-298.
- (148) Schoental, R. Carcinogenic and Chronic Effects of 4,4'-Diaminodiphenylmethane, an Epoxyresin Hardener. *Nature* **1968**, *219*, 1162-1163.

- (149) Cardy, R. H. Carcinogenicity and Chronic Toxicity of 2,4-Toluenediamine in F344 Rats. *JNCI: Journal of the National Cancer Institute* **1979**, *62*, 1107-1116.
- (150) Cohn, D.; Hotohely-Salomon, A. Biodegradable multiblock PEO/PLA thermoplastic elastomers: molecular design and properties. *Polymer* **2005**, *46*, 2068-2075.
- (151) da Silva, G. R.; da Silva-Cunha, A.; Behar-Cohen, F.; Ayres, E.; Oréface, R. L. Biodegradation of polyurethanes and nanocomposites to non-cytotoxic degradation products. *Polymer Degradation and Stability* **2010**, *95*, 491-499.
- (152) Courtney, T.; Sacks, M. S.; Stankus, J.; Guan, J.; Wagner, W. R. Design and analysis of tissue engineering scaffolds that mimic soft tissue mechanical anisotropy. *Biomaterials* **2006**, *27*, 3631-3638.
- (153) Soletti, L.; Hong, Y.; Guan, J.; Stankus, J. J.; El-Kurdi, M. S.; Wagner, W. R.; Vorp, D. A. A bilayered elastomeric scaffold for tissue engineering of small diameter vascular grafts. *Acta Biomaterialia* **2010**, *6*, 110-122.
- (154) van Minnen, B.; Leeuwen, M. B. M. v.; Stegenga, B.; Zuidema, J.; Hissink, C. E.; van Kooten, T. G.; Bos, R. R. M. Short-term in vitro and in vivo biocompatibility of a biodegradable polyurethane foam based on 1,4-butanediisocyanate. *Journal of Materials Science: Materials in Medicine* **2005**, *16*, 221-227.
- (155) Lendlein, A.; Neuenchwander, P.; Suter, U. W. Tissue-compatible multiblock copolymers for medical applications, controllable in degradation rate and mechanical properties. *Macromolecular Chemistry and Physics* **1998**, *199*, 2785-2796.
- (156) Skarja, G. A.; Woodhouse, K. A. In vitro degradation and erosion of degradable, segmented polyurethanes containing an amino acid-based chain extender. *J Biomater Sci Polym Ed* **2001**, *12*, 851-873.
- (157) Marcos-Fernández, A.; Abraham, G. A.; Valentín, J. L.; Román, J. S. Synthesis and characterization of biodegradable non-toxic poly(ester-urethane-urea)s based on poly( $\epsilon$ -caprolactone) and amino acid derivatives. *Polymer* **2006**, *47*, 785-798.
- (158) Guo, Q.; Knight, P. T.; Mather, P. T. Tailored drug release from biodegradable stent coatings based on hybrid polyurethanes. *Journal of Controlled Release* **2009**, *137*, 224-233.
- (159) Benrashid, E.; McCoy, C. C.; Youngwirth, L. M.; Kim, J.; Manson, R. J.; Otto, J. C.; Lawson, J. H. Tissue engineered vascular grafts: Origins, development, and current strategies for clinical application. *Methods* **2016**, 13-19.
- (160) Baudis, S.; Ligon, S. C.; Seidler, K.; Weigel, G.; Grasl, C.; Bergmeister, H.; Schima, H.; Liska, R. Hard-block degradable thermoplastic urethane-elastomers for electrospun vascular prostheses. *Journal of Polymer Science Part A: Polymer Chemistry* **2012**, *50*, 1272-1280.
- (161) Baudis, S.; Ligon, S. C.; Seidler, K.; Weigel, G.; Grasl, C.; Bergmeister, H.; Schima, H.; Liska, R. Hard-Block Degradable Thermoplastic Urethane-Elastomers for Electrospun Vascular Prostheses. *JOURNAL OF POLYMER SCIENCE PART A: POLYMER CHEMISTRY* **2012**, *50*, 1272-1280.
- (162) Fischer, K. Neues Verfahren zur maßanalytischen Bestimmung des Wassergehaltes von Flüssigkeiten und festen Körpern. *Angewandte Chemie* **1935**, *48*, 394-396.
- (163) DIN 53240-1 Bestimmung der Hydroxylzahl - Teil 1: Verfahren ohne Katalysator. Deutsches Institut für Normierung, 2013.
- (164) Meng, X.; Crestini, C.; Ben, H.; Hao, N.; Pu, Y.; Ragauskas, A. J.; Argyropoulos, D. S. Determination of hydroxyl groups in biorefinery resources via quantitative  $^{31}\text{P}$  NMR spectroscopy. *Nature Protocols* **2019**, *14*, 2627-2647.
- (165) Grasl, C.; Bergmeister, H.; Stoiber, M.; Schima, H.; Weigel, G. Electrospun polyurethane vascular grafts: in vitro mechanical behavior and endothelial adhesion molecule expression. *J Biomed Mater Res A* **2010**, *93*, 716-723.
- (166) Armarego, W. L. F.; Chai, C.: *Purification of Laboratory Chemicals*; Elsevier Science, 2013.

# Appendix

## DSC measurement curves

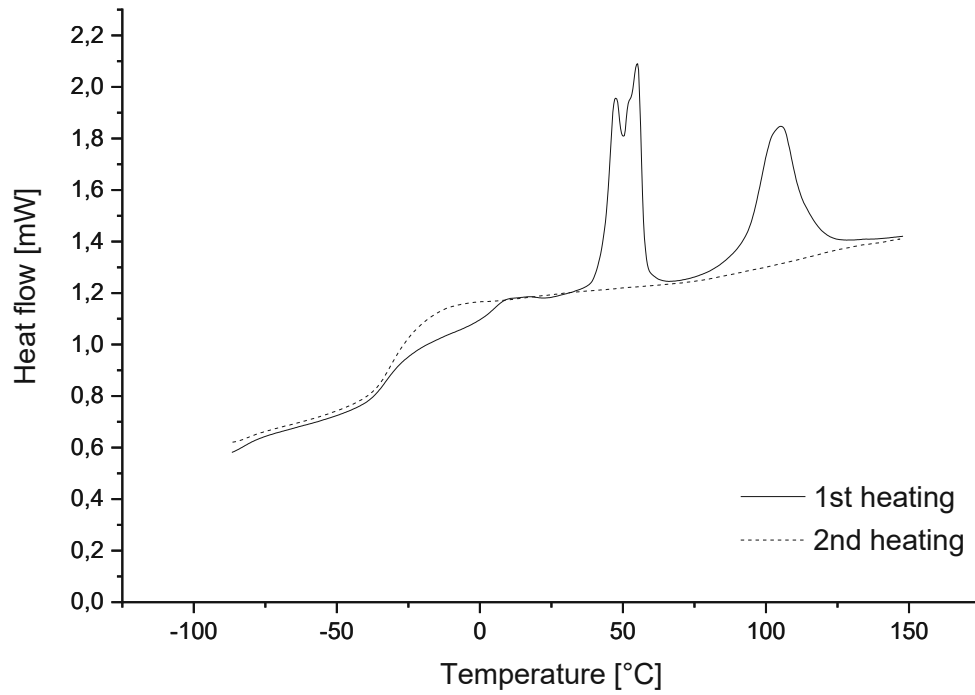


Figure 51: Heat flow of 1st and 2nd heating during DSC of pHMC/HMDI (exo down)

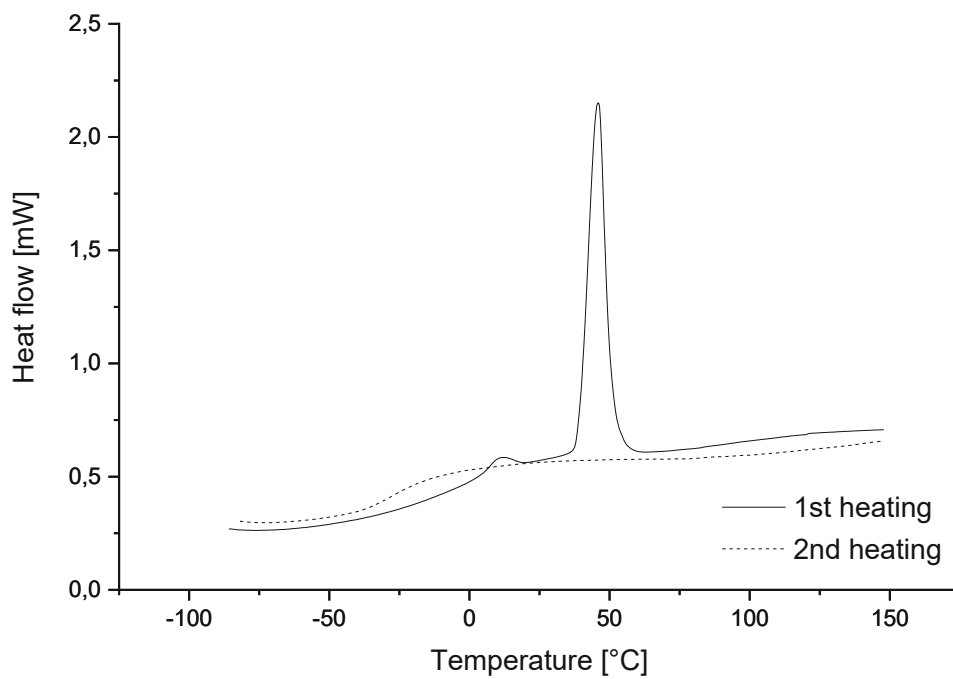


Figure 52: Heat flow of 1st and 2nd heating during DSC of pHMC/H12MDI (exo down)



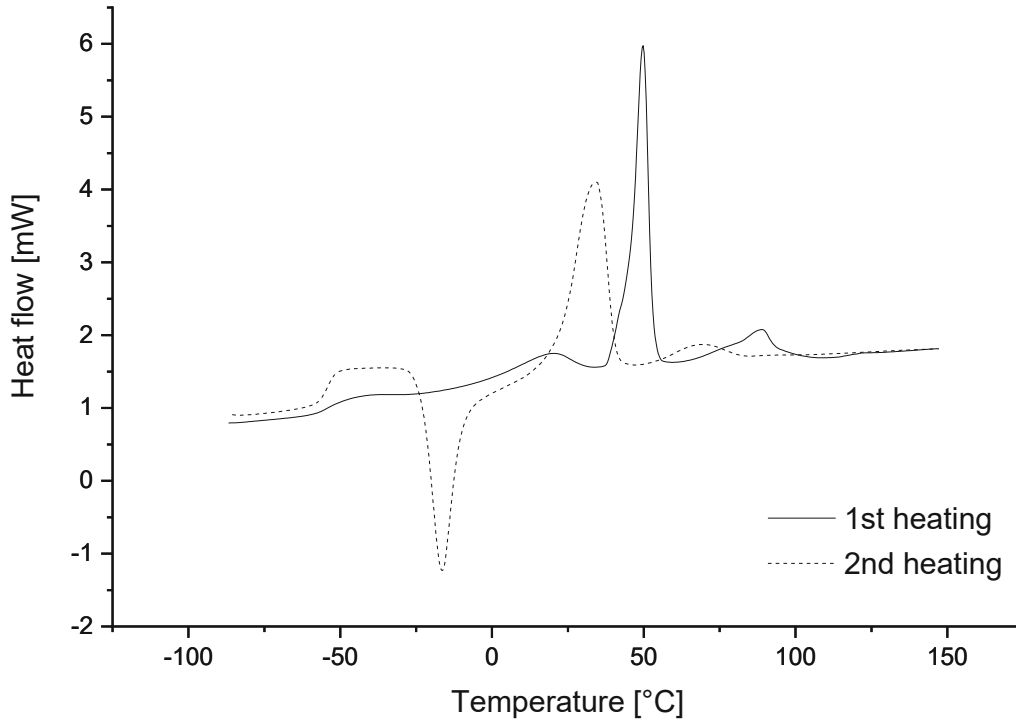


Figure 53: Heat flow of 1st and 2nd heating during DSC of pCL2000 (exo down)

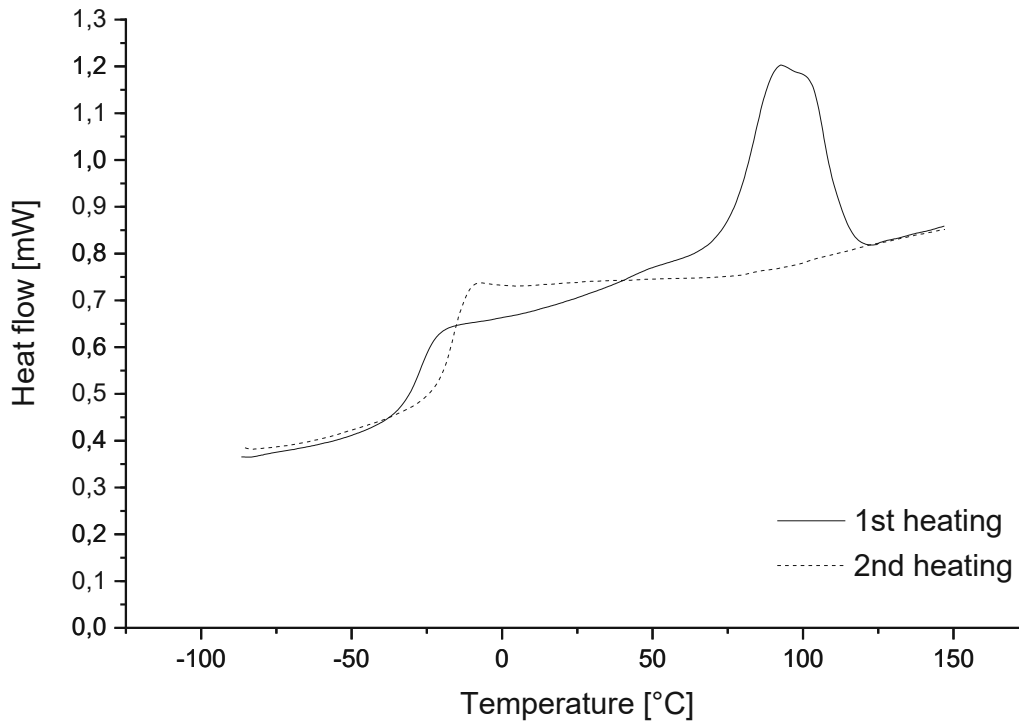


Figure 54: Heat flow of 1st and 2nd heating during DSC of pCL530 (exo down)

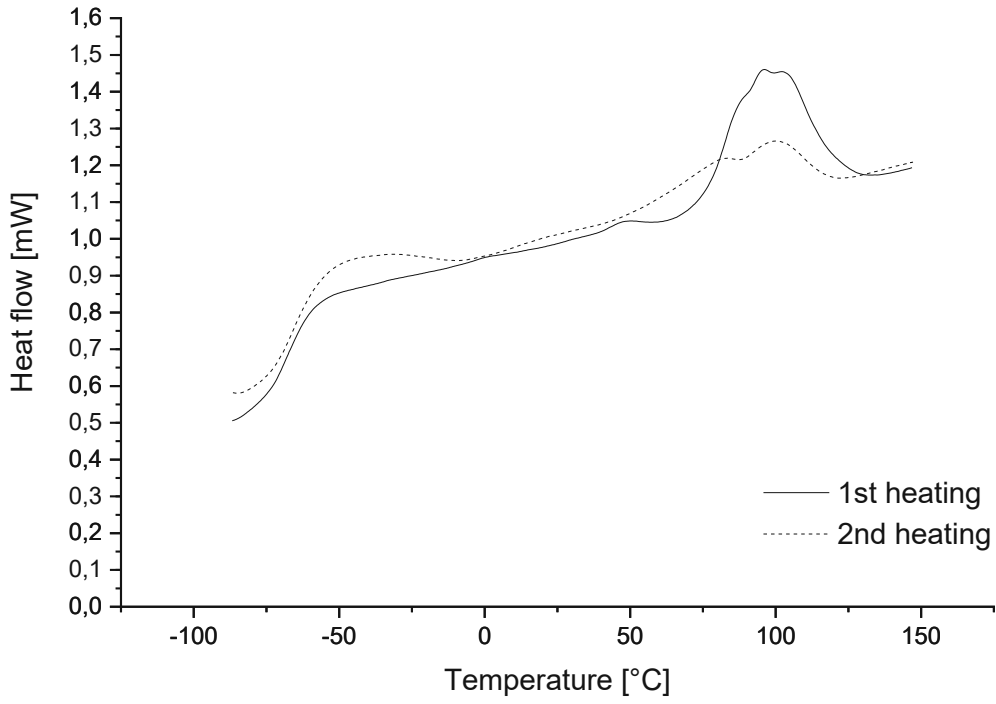


Figure 55: Heat flow of 1st and 2nd heating during DSC of BDO/TBEDA (exo down)

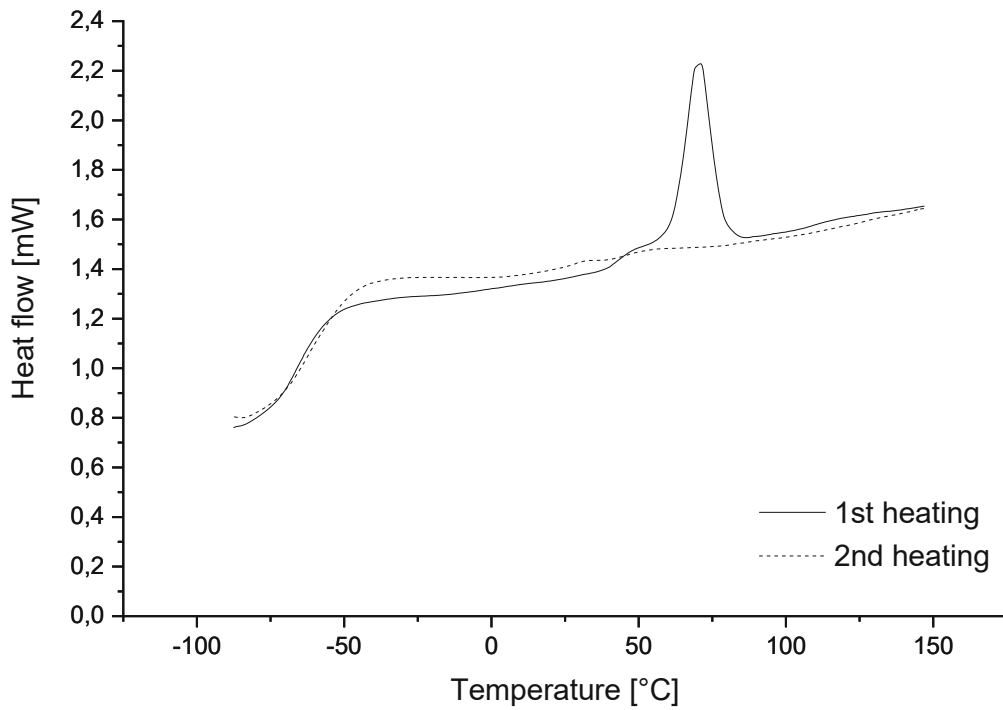


Figure 56: Heat flow of 1st and 2nd heating during DSC of BHPC/TBEDA (exo down)

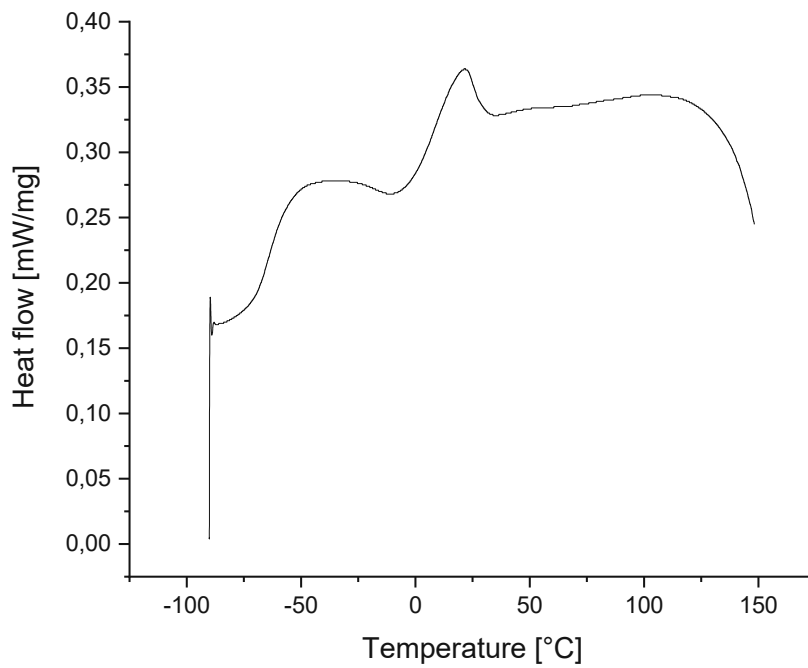


Figure 57: Heat flow of the 1st heating during DSC of ECLA/TBEDA (exo down)

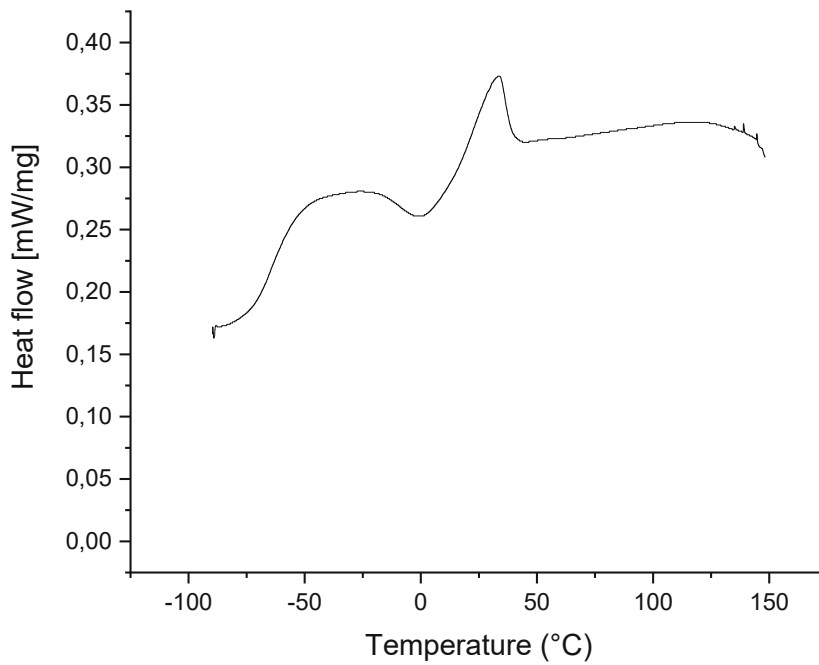


Figure 58: Heat flow of the 1st heating during DSC of HPN/TBEDA (exo down)

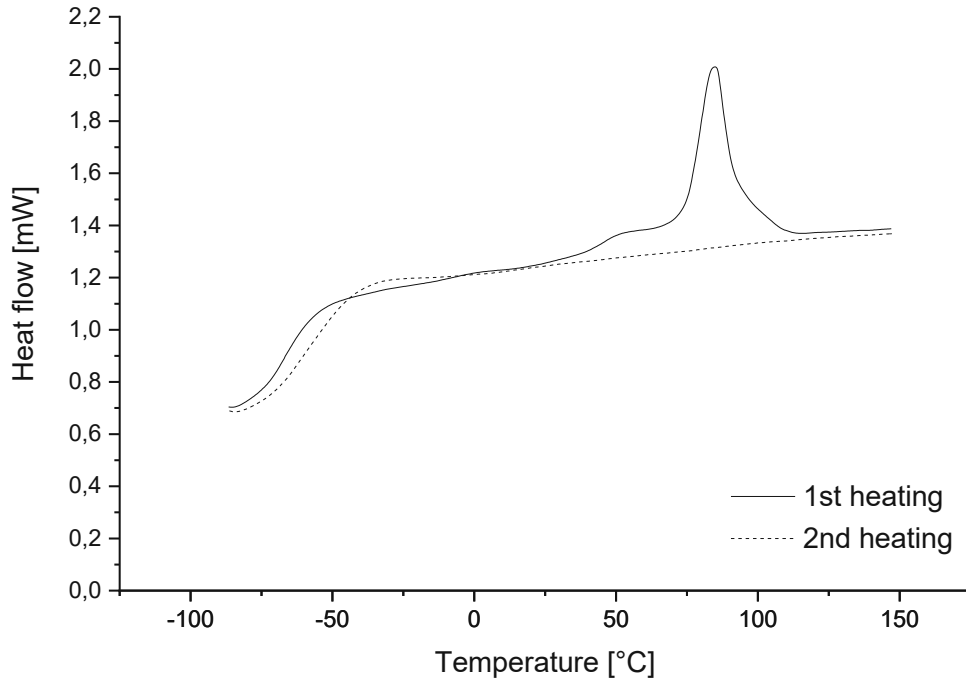


Figure 59: Heat flow of 1st and 2nd heating during DSC of BHET/IPEDA (exo down)

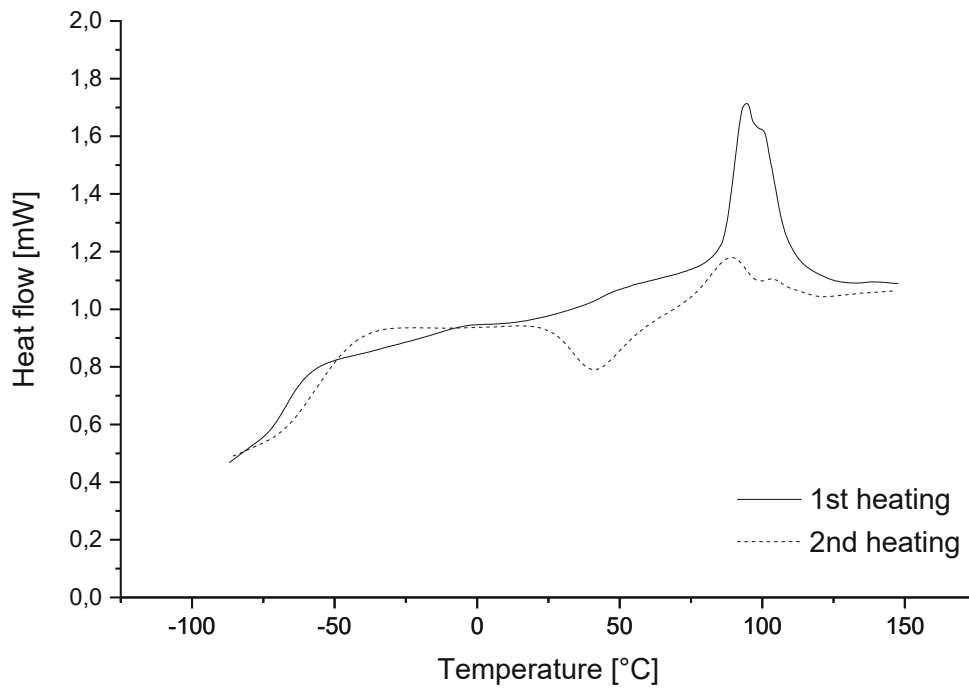


Figure 60: Heat flow of 1st and 2nd heating during DSC of BHET/TBAE (exo down)

## Film reproducibility

One problem which has to be addressed is the reproducibility of film quality with the solution casting method. With the design of the systematic study with preconditioning periods of one day, seven days and 28 days in which films of polymers from the same synthesis (and therefore the same molecular weight and polydispersity) were compared, one half of the film was always tested after dry storage to recognize deviations coming from differences in film quality. Such differences were encountered with varying extents for the different polymers. As an example, the comparison of three film halves of the polymer BHET/TBEDA, which were all stored under dry conditions can be seen in Figure 61.

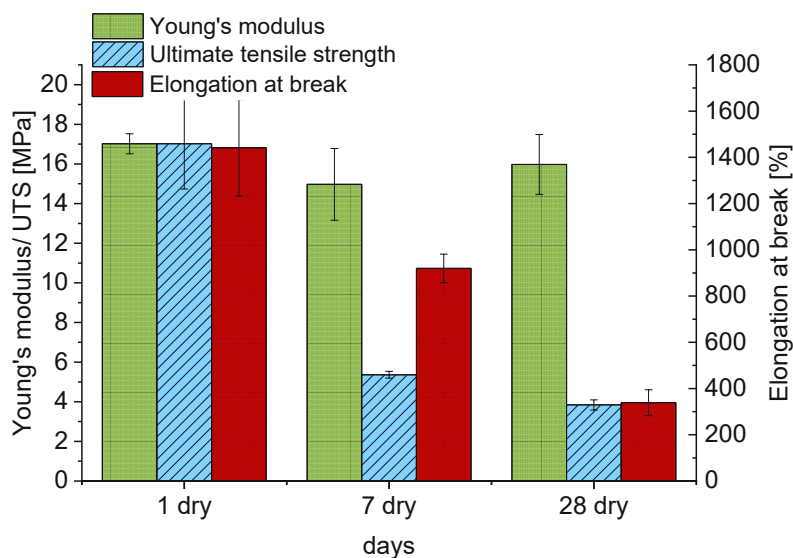


Figure 61: Comparison of three film halves of the TPUU BHET/TBEDA prepared by the same method and stored under dry conditions

Although films with high deviations towards inferior quality stemming from possible problems during the solution casting process were mainly avoided with a simple optical control, the changes in mechanical properties between the film halves, which were stored under dry conditions, often stayed significant. A definitive reason for this behavior could not be found; however possible explanations could be the different age of the polymers or films, which is an already described phenomenon<sup>110</sup>, as well as problems with the dry storage of the films leading to undesired self-reinforcing with minuscule amounts of water over longer periods of time. While bulk materials usually showed no such behavior under dry storage conditions, polymer films have a considerably higher surface to bulk ratio and are more susceptible to such unwanted self-reinforcing (or degradation) effects already under minimally wet conditions like

moisture in the air entering the storage container. Such behavior would result in a seemingly weaker self-reinforcing effect by pushing the mechanical properties of dry film halves towards better, partially self-reinforced mechanical properties. While this does not lower the mechanical properties achievable by the material, it, on the one hand, falsely indicates better mechanical properties for dry materials than their actual values; on the other hand, the degree of self-reinforcing is lowered between the different states by shifting the baseline upwards. Both of these behaviors are no problem for real-life applications, though; the properties of completely dry polymers are not really usable anyhow, since contact with moisture from the air is in most application cases unavoidable, and in tissue engineering, the environment is even moister. Also, even with variations in film quality, the relative comparison between film halves of the same film still allows judging if a positive (or negative) change takes place. After identifying polymer compositions with wanted mechanical properties, further studies could be used to analyze these more in-depth, which was not done in the scope of this work, which main focus was to give an overview of whether the self-reinforcing effect can be applied to more different TPUUs with different monomers.

## Additional tensile tests

### Chain extender 1 with steric hindrance

For polymers with a change in chain extender 1 to a monomer with steric hindrance (EGLA and HPN), two polymers were synthesized. The first TPUU with chain extender 1 being hydroxypivalic acid neopentyl glycol ester (HPN) leading to a polymer with the composition **pTHF-HMDI-HPN-TBEDA 1:2:0.5:0.5**, was not usable, as it is impossible to prepare solid films for measurements. The steric hindrance in this new chain extender combined with the steric hindrance of the (*tert*)-butyl groups of TBEDA probably hinder the formation of hard blocks in the final polymer. Even though the final polymer is a waxy solid after reaction workup, the mechanical properties were so poor that the preparation of test specimens for tensile testing was impossible. After solution casting, the films could not be removed from the mold without completely destroying it regardless of drying time or care during handling.

The second thermoplastic polyurethane/urea polymer elastomer with a chain extender with steric hindrance showed similar problems. For this polymer with a composition of **pTHF:HMDI:EGLA:TBEDA 1:2:0.5:0.5**, only a single film could be prepared without destroying it during the removal from the mold. This film was then preconditioned for 28 days.

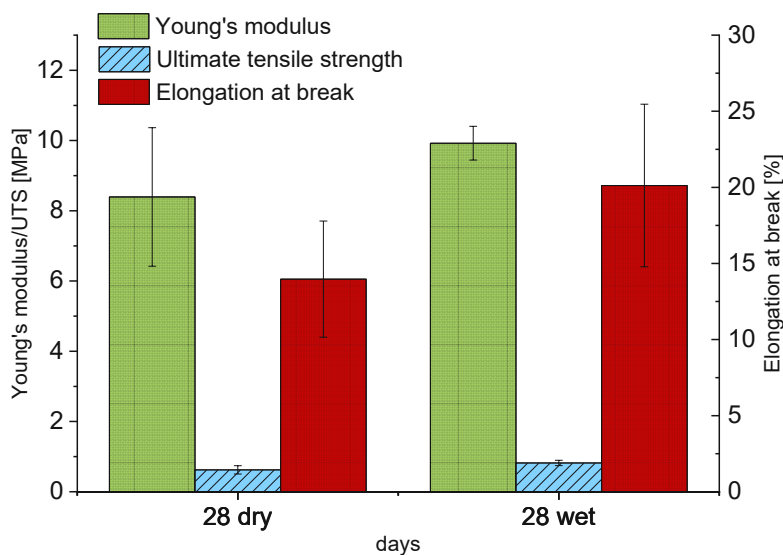


Figure 62: Results of the tensile tests for EGLA/TBEDA 50/50 after incubating for 28 days

While the Young's modulus of this polymer is in a similar range to other TPUUs with around 8 – 10 MPa for both the dry and preconditioned half (Figure 62), the ultimate tensile strength is extremely low at around 0.7 MPa. Preconditioning showed an increase in this material property; however, the increase is very low and not statistically significant. Also, even after

conditioning, the UTS remained in such a low range that an application of this material is impossible for any use.

The same can then also be said about the elongation at break. Even though it increased slightly (and not statistically significantly), it is extremely low in the dry stored film half and stays extremely low (for such material) even after conditioning.

Although it is quite disappointing that both polymers with a sterically hindered first chain extender showed no usability, this teaches an essential lesson in the role of this monomer in the final thermoplastic polyurethane/urea elastomer. While the second chain extender, which brings the hindered urea bonds in the polymer, is needed to allow self-reinforcement, the first chain extender plays an equally important role. If this chain extender does not support the formation of good hard blocks, the self-reinforcement is still possible, but the basic material properties from which it starts are so low that even a self-reinforced material still stays subpar to other non-self-reinforcing materials.

#### pTHF-HMDI-BHET-IPEDA 50/50 at room temperature and 37 °C

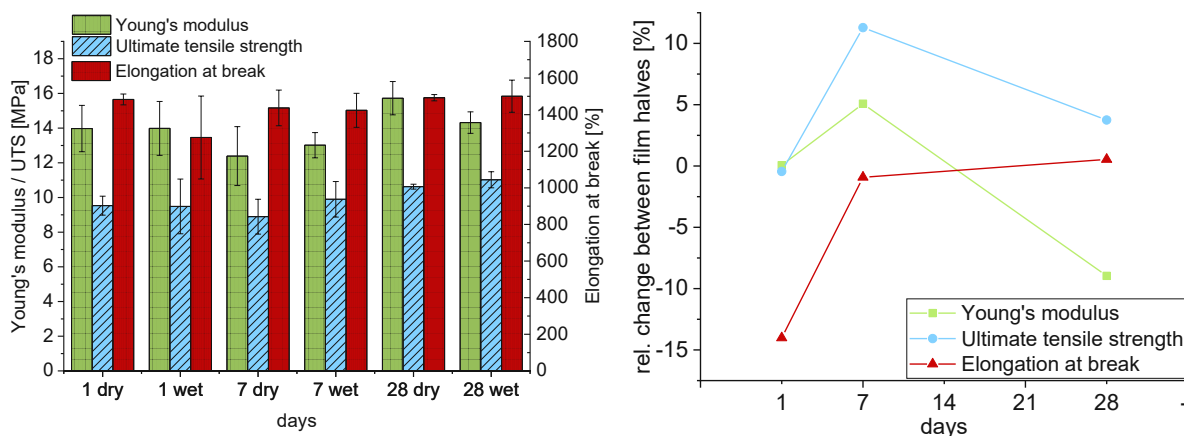


Figure 63: Results of the tensile tests for BHET/IPEDA 50/50 after different incubation periods at room temperature (absolute and relative values)

The results of the tensile tests for the polymer **pTHF-HMDI-BHET-IPEDA 50/50** at room temperature can be seen in Figure 63. For the two parameters, Young's modulus and UTS, the TPUU shows no difference between the film halves, regardless of preconditioning times at room temperature. Also, both parameters are quite constant over different films. The elongation at break also does not vary between film halves, and the differences between different films are also quite negligible.



For the measurements of BHET/IPEDA 50/50 with incubation at 37 °C, the results are similar (Figure 64). The Young's moduli showed no significant differences between films as well as film halves, as these are always within standard deviation. For the UTS, the films with a preconditioning period of one day and seven days showed no changes; for the film with a preconditioning period of 28 days, a slight, but not statistically significant increase is visible. Maybe even longer preconditioning times could be helpful to determine if self-reinforcing with this TPUU is possible at 37 °C if given enough time. Alternatively, higher temperatures could aid bond-reversibility with this substituent of low steric hindrance.

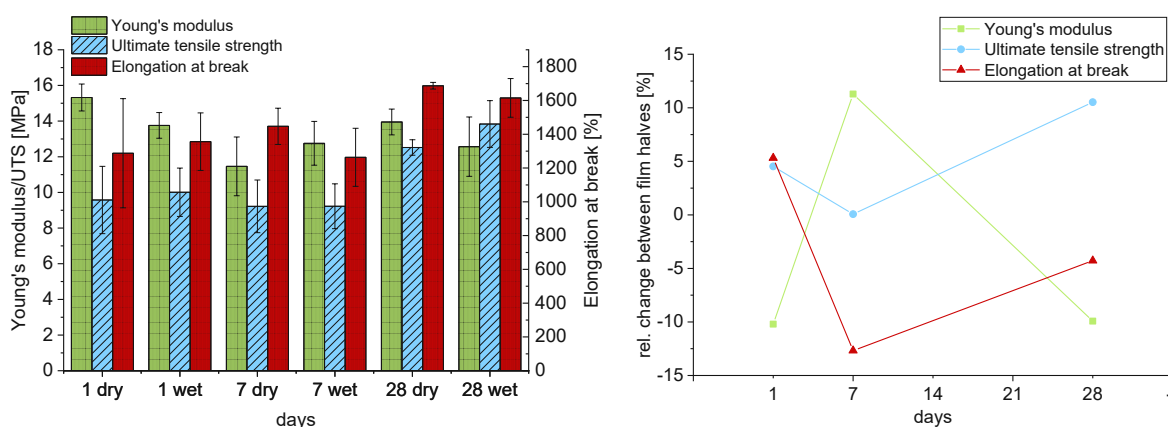


Figure 64: Results of the tensile tests for BHET/IPEDA 50/50 after different incubation periods at 37 °C (absolute and relative values); the dry stored halves were kept at room temperature

The elongation at break between film halves showed no significant changes regardless of incubation time. It should be noted, though, that the elongation at break is exceptionally high, ranging between roughly 1300 - 1700 %.